Interactions in Weyl semimetals of type I

Master's Thesis

Fabrizio Detassis

Supervisors:

dr. Lars Fritz
Simonas Grubinskas, MSc.

Institute for Theoretical Physics
Utrecht University
June 2016

Universiteit Utrecht

Abstract

The discovery of graphene opened the way to an intriguing field in condensed matter: that of Dirac materials (DM). In these materials, electrons have a linear dispersion relation, making them a solid-state analoguos of relativistic massless particles. The possible realization of DM in three dimensions has drawed a lot of attention, since these systems are much more stable than their 2D cousins, e.g. graphene. In my research I focus on three dimensional DM and investigate their properties once an additional interaction term is added to the Hamiltonian. This latter has the effect of tilting the characteristic Weyl cones in the momentum space and breaks isotropy. We will investigate whether this symmetry breaking finds a signature in observables that can be measured: to this end we will compute both the optical conductivity and the polarization function in the framework of linear response theory.
Finally we will study the role of electron-electron interactions within the system: using a renormalization group approach we will investigate whether the tilting term influences the system parameter's flow and compare our result with the literature.

Contents

Chapter 1

Introduction

1.1 A breakthrough into material science

In the last decade, material science has seen the birth of a rising star, graphene. The material was isolated for the first time in a laboratory in 2004, [24], and since then the interest of large part of the scientific community (physicists, chemists, engineers, ...) has been focused on it. The reasons are various, ranging from its peculiar electronic properties to the possible applications [1], and the material has been widely investigated both theoretically, [9, 20] and experimentally. The first theoretical studies of graphene can be traced back to 1947, when Wallace studied the properties of a layer of graphite [32], that is indeed graphene. Almost fourty years later a high energy physicist, Gordon Semenoff, pointed out that such a condensed-matter system could realize an analog of a 2D massless Dirac fermion, [27]. In those years there was a big attention to topological quantum states: the quantum Hall effect (QHE) was just discovered and physicists were looking for relativistic (2+1)-dimensional systems of fermions, but a realistic physical setting was lacking. Graphene was the perfect candidate to realize a solid state analogue of 2D massless Dirac fermions and provided the possibility for studying phenomena that were allowed only for high-energy physics processes. Physicists had to wait more than 20 years before having their theories confirmed, but in the end graphene was succesfully isolated.
This partially explains the huge success of graphene. A parallel development was the discovery by Kane and Mele of the quantum spin Hall effect (QSHE), a phenomenon that emerges in topological insulator when the energy gap is provided by a spin-orbit like interaction, for which time-reversal symmetry is not broken [17]. Graphene-like structures are in fact very good candidates to show the aforementioned topological properties.

The huge success of graphene and its properties are not due to it's only chemical component, ^{12}C, but rather to how the carbon atoms are arranged in the lattice: in a honeycomb structure, see Fig. 1.1. In the inner structure is hidden the key to graphene's peculiar band structure, shown in Fig. 1.2. The band structure is characterized by band-touching points, which are referred to as Dirac points, and the corresponding materials are called Dirac materials.
Shortly after the isolation of graphene the condensed-matter community started to explore further variations on the field of Dirac materials and to contemplate the possibility of a 3D analogue to graphene, that is a 3D Dirac material, also referred to as a Dirac semimetal (DSM). In the present work I focus on these latter systems and investigate their electronic properties as well as their response functions.

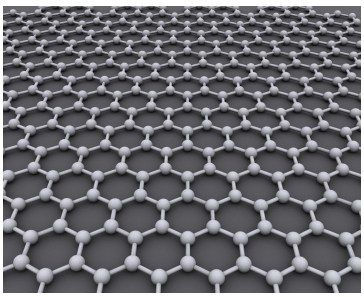

Figure 1.1: *Honeycomb lattice structure.*

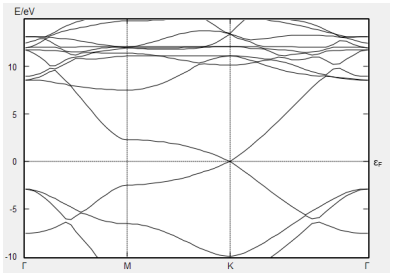

Figure 1.2: *Band structure of graphene.*

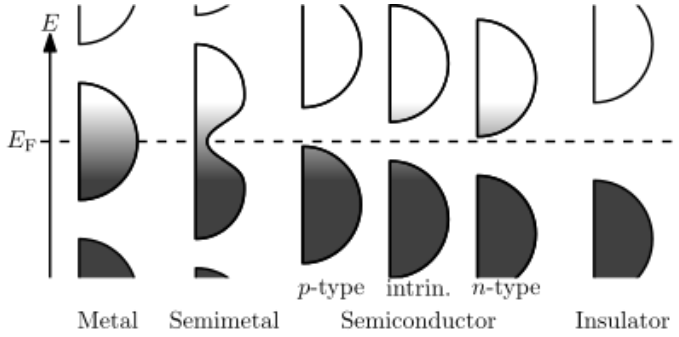

Figure 1.3: *Filling of the band structure for different types of materials. Taken from [33]*

1.2 Insulators, metals and semimetals

In solid-state physics a huge role is played by the study of the electronic band structure, or simply band structure. This is where the analysis of a novel type of material, or model, starts. The physicist would first write down the possible Hamiltonian for the system under consideration, starting from symmetry reasonings and trying to guess what are the interactions that is necessary to include; once the Hamiltonian for the system is found, it is then diagonalized.
From the Schroedinger equation

$$H_{\mathbf{k}}\,\psi(\mathbf{k}) = E_{\mathbf{k}}\,\psi(\mathbf{k})$$

we know that the eigenvalues of the Hamiltonian constitue the energies that are allowed for the electrons moving in the system. According to one of the fundamental principle in physics, that of energy minimization, the electrons will tend to occupy the energy with lower energies. At zero temperature the only states occupied will be those having an energy lower than the Fermi energy, E_F, while by increasing the temperature excitations to higher energy states will be allowed. In Fig. 1.3 is synthetized a classification of the materials based on their band structure.ads By looking at a band structure even the untrained eye will notice that there exist gaps, separations between different bands: this are a consequence of quantum mechanics and the reason is precisely the same of the quantization of the energy spectrum in the hydrogen atom.
The gaps showing up in a band structure are very important: they characterize the electronic behaviour of the material that are thus classified accordingly, see Fig. 1.3. The classification plays a mayor role, just think of the different employments between insulators and semiconductors and the extraordinary revolution that the industry of these latter brought. But why is a band gap so important? The consequence of a band gap is naively that for electrons to go from the lower to the upper band, they have to "jump" the gap, that is have an energy at least equal to the energy gap. This defines an energy measure specific of a certain material and therefore the practical applications it can be employed for.

We shall now focus on semimetals, which are the topic of my work. These have rather exotic band structure: there is no gap between bands but the density of states is zero at the Fermi energy. They are not metals nor insulators. It is clear that the most interesting features of these materials show up at zero doping, $\mu = 0$, and for very low temperatures - or equivalently at scales of energy much bigger compared to thermal energy, $E \gg k_B T$. In fact if these two conditions are not satisfyed, then one ends up with a metal-like system.

The study of semimetals has seen a huge increase in the last years after the isolation of graphene and the kick-off of a big industry, that of layered materials. Starting with the lattice structure of graphene - the honeycomb - one can play around and replace the carbon atoms with different atoms or even molecules, exploiting the two-band electronic structure. For the more it is now possible to stack different layer of graphene or alike materials to build a 3D structure. Theoretical investigation in this sector is very lively and promise not only to unveil new features but eventually reach and possibly replace the semiconductors industry.

1.3 From Dirac points to Weyl points

A DSM is characterized by the presence of one or more Dirac points: these are regions of the Brillouin zone where valence and conduction bands touch. Near the Dirac point it is possible to describe the system via

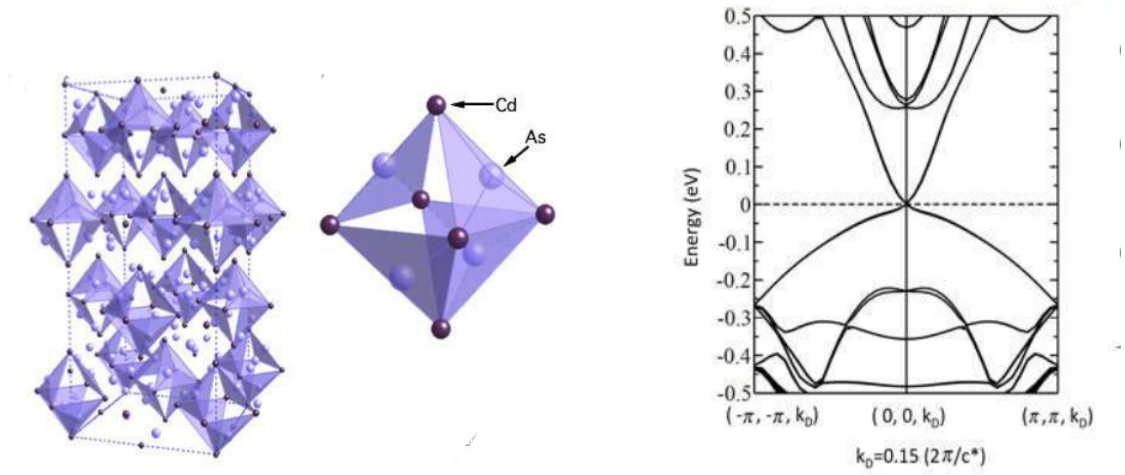

Figure 1.4: Cd_3As_2*: lattice structure (left) and corresponding band structure (right). Taken from [23].*

an effective low-energy Hamiltonian,

$$\mathcal{H}(\mathbf{k}) = v_F \tau_z \otimes (\mathbf{k} \cdot \sigma) \tag{1.1}$$

where v_F represents the velocity at which electrons move, the Fermi velocity, and $\sigma = (\sigma_x, \sigma_y, \sigma_z)$ is the vector comprising the three Pauli matrices. τ_z has the same matrix structure of σ_z. The electron described by eq. (1.1) has a linear dispersion relation in the three directions.
The system results two-fold degenerate, there are two identical cones one on top of the other. This is a consequence of the pseudospin symmetry of the system, represented by τ_z; since there is no coupling between opposite pseudospins, we can regard to all purposes the system as being composed of two different kind of electrons, independent of each other.
If a symmetry is broken, for instance inversion symmetry (IS) by means of a chemical potential or time-reversal symmetry (TRS) by applying a magnetic field, then the two cones split in momentum space and are addressed to as *Weyl cones*, [6, 8].
As one may guess, the reason for their name is that near to Weyl points the system can be described by a low-energy 2×2 Hamiltonian which is precisely the one introduced by Weyl to describe massless Dirac particles carrying charge. Because Weyl cones result from splitting the Dirac Hamiltonian, they always come in pair and with opposite chirality. For this reason WSM are considered very good physical system for the observation of the so-called chiral anomalies.
It is important to remark than the two Weyl cones do not interact with each other, being for all purposes independent; the only trace of the original Dirac cone lies within the fact that electrons belonging to different cones carry opposite chirality.

One may argue that as for the case of graphene, the Weyl nodes are very little protected and even a small perturbation would lead to a gap opening and the loss of the semimetallic structure. However if this is well understood in 2D, it is easy to convince yourself that it doesn't hold in 3D. The reason being that any perturbation we introduce in our system has to couple to one of the Pauli matrices or to the identity matrix: in 3D this results in a mere shift of the Weyl node in the momentum space, therefore preserving the linear dispersion relation. WSM are much more protected to external perturbation than graphene and this has its roots in the topological properties of the material.

A big effort has been put in the last years towards an experimental realization of 3D DSMs and such materials have been found in Cd_3As_2 (see Fig. 1.4) and Na_3Bi. Several WSM have been discovered, such as TaAs and NbAs, which show broken I symmetry and $YbMnBi_2$ for a WSM with broken TR symmetry.

1.4 Our case study

Until now our attention focused on WSM arising from eq. (1.1). Here we are interested in a generalization of Dirac materials that comes about when an additional term is added to the Hamiltonian. We suppose our

system to be described at low energy by the effective Hamiltonian.

$$H(\mathbf{k},\mathbf{d}) = v_F\left(\tau_z \otimes (\mathbf{k}\cdot\sigma) + w\mathbf{d}\cdot\mathbf{k}\mathbb{I}_4\right) \tag{1.2}$$
$$= v_F \begin{pmatrix} \mathbf{k}\cdot\sigma + w\mathbf{d}\cdot\mathbf{k} & 0 \\ 0 & -\mathbf{k}\cdot\sigma + w\mathbf{d}\cdot\mathbf{k} \end{pmatrix}$$

where v_F, the Fermi velocity, is the velocity at which electrons move within the material, $\mathbf{d}$ is a unit vector and w is an adimensional parameter which will be referred to as **tilting parameter**. In order to study what the effects of the novel term are, we diagonalize the Hamiltonian and find its eigenvalues,

$$\lambda_\pm = w\mathbf{d}\cdot\mathbf{k} \pm v_F|\mathbf{k}|$$

Each of them has multiplicity 2, therefore there are two Dirac cones one on top of the other. A very important feature is that these two cones **do not interact** with each other, as can be read from the zero off-diagonal component of eq. (1.2). This means that we can treat electrons belonging to different cones as independent of each other.

The additional term has the effect of tilting the Dirac cones in the direction pointed by $\mathbf{d}$, as can be seen in Fig. 1.5. It is clear that the additional term breaks isotropy in the momentum space, introducing an asymmetry in the tilting direction. In order to explore further how this novel term affects the features of

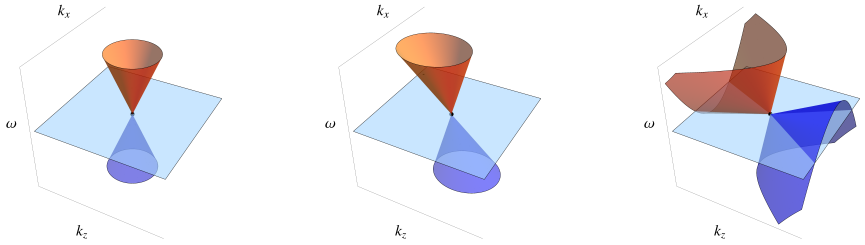

(a) $w = 0$ ***untilted*** ***(b)*** $w = 0.5$ ***tilted*** ***(c)*** $w = 1.2$ ***overtilted***

Figure 1.5: *Dispersion relation for different values of the tilting parameter w for $\mathbf{d} = (0, 0, 1)$.*

our system, we look at how the Fermi surface gets reshaped by it at different values of energy. In Fig. 1.6 is plotted the Fermi surface correspondent to positive, negative and zero energies for different values of the tilting parameter w. We see that for $0 < |w| < 1$, the Fermi surface at non-zero energies turns into an ellipse, the center of which moves along the direction pointed by $\mathbf{d}$. The Fermi surface still shrinks to a point for zero energy and particle-hole symmetry is broken, although the system preserves a point symmetry correspondent to the Dirac point.
When $|w| > 1$ the Fermi surface becomes an hyberbola for non-zero energies which becomes degenerate at zero energy; also in this case the system retains a point symmetry. The analysis suggests two observations,

1. The system retains a point symmetry around the Dirac point

2. We shall distinguish between two types of WSM,

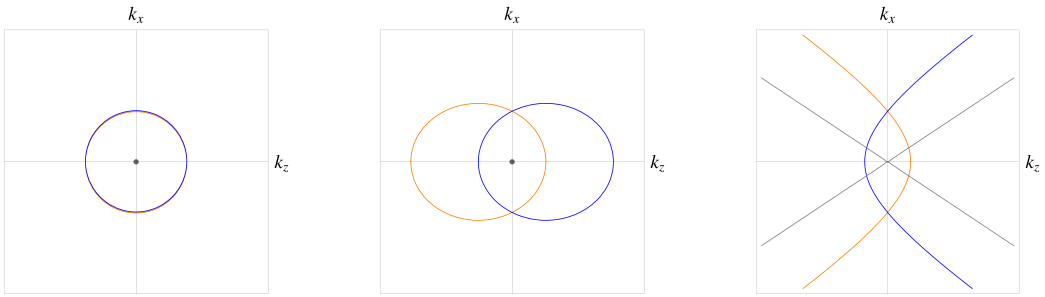

Figure 1.6: *Fermi surface for $w = 0,\ 0.5,\ 1.2$ (left to right) at different energies: $\omega = 0, \pm E$ in orange, blue and grey respectively*

(i) WSM of **type I**, for which the density of states is zero at zero energy, $\rho(\omega = 0) = 0$;

(ii) WSM of **type II**, for which the density of states is finite at zero energy, $\rho(\omega = 0) \neq 0$.

1.5 Outline of the research

My research is organized as follow: in Chapter 2 we introduce the framework of linear response theory and the Kubo formula for Dirac fields is derived. This will constitue the theoretical framework which will be used to derive all the response functions. The chapter is devoted to the calculation of the optical conductivity for two different systems: we start with the case of massive Dirac fermions to get acquainted with the formalism and then move on to the case of interest, that is 3D Dirac materials with tilted Dirac cones, eq. (1.2).
In Chapter 3 we will focus on the calculation of the polarization function for such systems: we will start with the 2D case, that of graphene, and then turn to the case of interest. The polarization function for electron-doped WSM will also be derived and this will allow for an interpretation of the result from the point of view of transitions.
In Chapter 4 we will study the effect of the interactions by means of the renormalization group theory: we will set up an RG scheme that will allows us to study the effect of the interactions on the system's parameter, the RG equations latter will be derived and their flow will be investigated.

The results that are presented in the next chapters are completely analytic: this involves, every now and then, lengthy calculations. In order for the derivations to be more compact and for the reader to understand the method, rather that the calculations, part of these latter is sometimes skipped and an apposite section with the full derivation is to be found in the Appendix, to which the reader will be properly redirected. The results of Chapter 3, although very recent, are not new and have already been obtained by different authors. The present work, however, includes a full derivation of the results, that is often omitted in the papers and is to be interpreted in this sense. Chapter 4 constitues probably the novel and most interesting part of the work.
A final remark: the approach to this work was thought to be hands-on and with this philosophy has been carried on; what follows consitue the starting point for understanding the physics behind systems described by eq. (1.2) and is to be interpreted in this sense. It will often happen that a detailed theoretical framework is dropped in favor of a result and the analysis that comes out of it.

Chapter 2

The linear response approach and the conductivity

2.1 Introduction

The theory of linear response constitues one of the most powerful tools when it comes to the computation of observables, both in classical and quantum mechanics. We will here employ it to investigate the electromagnetic (EM) response functions of our system. The assumption on which the theory is founded is that if we perturb the system with a small EM field, it will be possible to describe its behavior by considering only the terms that depends linearly in the field, thus disregarding higher order corrections. The reasoning is similar to that of a Taylor expansion.
In the Chapter we will first generalize the Kubo formula for conductivity to the case of relativistic Dirac fermion fields. By means of this formula, we will see that it is possible to interpret the conductivity and the related quantities in terms of Feynman diagrams. Once we have an operational formula, we will start with an exercise: computing the optical conductivity for a massive Dirac field. The calculation will be done in a fully covariant notation, however we will later drop the notation in favour of the Hamiltonian language, which will be employed also in the next Chapters. In this framework we will compute the conductivity for Weyl semimetals with an additional "tilting" term and look for a signature of the symmetry breaking by evaluating the observable in different directions. Finally some graphs will be shown and we will conclude by analysing them in the theoretical picture of electron transitions.

2.2 Kubo formula for conductivity

We will here derive the Kubo formula for the conductivity that will be employed later in most of our calculations. We suppose our system to be composed of a set of charged particles that has been subjected at some time to an EM signal. The system will respond to the perturbation through a redistribution of charge, $\rho(x) = \langle\rho(x)\rangle$ and a current flow, $\mathbf{j}(x) = \langle\mathbf{j}(x)\rangle$ that we represent as a 4-vector $j^\mu = (\rho, \mathbf{j})$. We suppose the external EM perturbation to be small enough so that we can treat the problem with the tool of linear response theory, that is we assume

$$j = K[A] + \mathcal{O}(A^2)$$

where the second order correction results small enough to be negligible. First of all we define the **EM linear response kernel** $K_{\mu\nu}(x, x')$

$$j^\mu(x) = \int_{t'<t} dx'\; K^{\mu\nu}(x, x')\, A_\nu(x') \tag{2.1}$$

where the restriction on the integration domain follows from causality.
From this relation we get how to compute the kernel,

$$K^{\mu\nu}(x, x') = \frac{\delta}{\delta A_\nu(x')}\langle j^\mu(x)\rangle \quad . \tag{2.2}$$

For convenience we perform a Wick rotation and work in Euclidean space-time, see Appendix A for details. The current is read directly from the Lagrangian after minimal coupling: $(\partial_\mu)_E \to (\partial_\mu)_E - ieA_\mu$

$$\mathcal{L} = \bar\psi(i\not\partial_E - m)\psi \qquad \to \qquad \bar\psi(i\not\partial_E - m)\psi + e\,\bar\psi\gamma^\mu A_\mu\psi$$

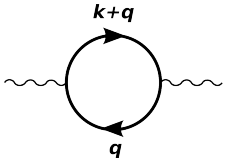

Figure 2.1: *Bubble diagram corresponding to eq.* (2.6).

from which we get $j^\mu = e\,\bar\psi\gamma^\mu\psi$. By means of the path integral formalism, we gets

$$\begin{aligned} K^{\mu\nu}(x,x') &= \frac{\delta}{\delta A_\nu(x')}\langle j_\mu(x)\rangle_0 \\ &= \frac{\delta}{\delta A_\nu(x')}\,\frac{1}{Z}\int \mathcal{D}\bar\psi\mathcal{D}\psi\; e\bar\psi(x)\gamma^\mu\psi(x)\, e^{\int d^4x[\bar\psi(i\partial\!\!\!/_E - m)\psi + j^\mu A_\mu]}\Big|_{A=0} \\ &= \big\langle j^\mu(x)\big\rangle_0\big\langle j^\nu(x')\big\rangle_0 + e\left\langle \frac{\delta j^\mu(x)}{\delta A_\nu(x')}\right\rangle_0 + e^2\left\langle \bar\psi(x)\gamma^\mu\psi(x)\,\bar\psi(x')\gamma^\nu\psi(x')\right\rangle_0 \quad . \end{aligned}$$

Notice that the first term is an average performed at equilibrium and in our case is zero since at equilibrium there is no current within the system; the second term is referred to as the diamagnetic term and is zero in the case of Dirac fields. We use Wick theorem:

$$\left\langle \bar\psi(x)\gamma^\mu\psi(x)\,\bar\psi(x')\gamma^\nu\psi(x')\right\rangle_0 = \Big[\mathrm{Tr}\,\gamma^\mu G_E(x,x)\mathrm{Tr}\gamma^\nu G_E(x',x') - \mathrm{Tr}\,\gamma^\mu G_E(x,x')\gamma^\nu G_E(x',x)\Big] \tag{2.3}$$

the first term corresponds to a disconnected diagram describing vacuum fluctuations that we shall drop. We find the relation that links the propagator in Euclidean space-time to the conductivity.
Summarizing what just written, in our case

$$K^{\mu\nu}(x,x') = -e^2\mathrm{Tr}\,\gamma^\mu G_E(x,x')\gamma^\nu G_E(x',x) \quad . \tag{2.4}$$

It is convenient to go to Fourier space. Recall that

$$G(\tau,\mathbf{x};\tau',\mathbf{x}') = \frac{1}{\beta}\sum_m\int\frac{d^3k}{(2\pi)^3}\; G(i\omega_m,\mathbf{k})\, e^{-i\omega_m(\tau-\tau')}\, e^{i\mathbf{k}\cdot(\mathbf{x}-\mathbf{x}')} \quad .$$

where ω_m denotes Matsubara frequencies, see Appendix A. Then

$$K^{\mu\nu}(x,x') = -e^2\mathrm{Tr}\,\gamma^\mu G_E(x,x')\gamma^\nu G_E(x',x) \tag{2.5}$$

$$\downarrow$$

$$K^{\mu\nu}(i\omega_m,\mathbf{k}) = -e^2\frac{1}{\beta}\sum_n\int\frac{d^3q}{(2\pi)^3}\;\mathrm{Tr}\,\gamma^\mu G(i\omega_m+i\omega_n,\mathbf{k}+\mathbf{q})\,\gamma^\nu G(i\omega_n,\mathbf{q}) \quad . \tag{2.6}$$

We can represent the equation by means of the Feynman diagram shown in Fig. 2.1. At this point we still don't know how to relate the kernel $K^{\mu\nu}$ to the conductivity of our system.
The link follows from the assumption that an EM field induces in the system a current, and the conductivity is the linear response "coefficient". Mathematically,

$$j^\alpha(x) = \int d^4x'\sigma^{\alpha\beta}(x,x')E^\beta(x') \tag{2.7}$$

that is equivalent to say that

$$\sigma^{\alpha\beta}(x,x') = \frac{\delta j^\alpha(x)}{\delta E^\beta(x')} \quad . \tag{2.8}$$

We work in Euclidean space-time, In this framework,

$$E^\alpha(t,\mathbf{x}) = -\frac{\partial A^\alpha(t,\mathbf{x})}{\partial t} \qquad \to \qquad E^\alpha(\tau,\mathbf{x}) = -i\,\frac{\partial A^\alpha(\tau,\mathbf{x})}{\partial\tau}$$

which in the space of momenta and Matsubara frequencies reads

$$E^\alpha(i\omega_m,\mathbf{k}) = -\omega_m A^\alpha(i\omega_m,\mathbf{k}) \quad .$$

Generalizing the linear response expression in Fourier space one gets

$$\begin{aligned} j^\mu(i\omega_m,\mathbf{k}) &= \sigma^{\mu\nu}(i\omega_m,\mathbf{k})E_\nu(i\omega_m,\mathbf{k}) \\ &= -\omega_m\sigma^{\mu\nu}(i\omega_m,\mathbf{k})A_\nu(i\omega_m,\mathbf{k}) \quad . \end{aligned}$$

Hence,

$$\begin{aligned} \sigma^{\mu\nu}(i\omega_m,\mathbf{k}) &= \frac{1}{i(i\omega_m)}\frac{\delta j^\mu(i\omega_m,\mathbf{k})}{\delta A_\nu(i\omega_m,\mathbf{k})} \\ &= \frac{1}{i(i\omega_m)}K^{\mu\nu}(i\omega_m,\mathbf{k}) \end{aligned}$$

We want our result to depend on real time, hence we perform so-called analytic continuation: this corresponds to substitue $i\omega_m \to \omega + i\delta$ and then take the limit for $\delta \to 0$.

$$\sigma^{\mu\nu}(\omega^+,\mathbf{k}) = \frac{1}{i}\left[\frac{K^{\mu\nu}(i\omega_m,\mathbf{k})}{i\omega_m}\right]_{i\omega_m\to\omega^+} \quad . \tag{2.9}$$

We see that the real part of the conductivity is given by the formula

$$\mathrm{Re}\,\sigma^{\mu\nu}(\omega,\mathbf{k}) = \frac{1}{\omega}\mathrm{Im}\,K^{\mu\nu}(\omega^+,\mathbf{k}) \quad . \tag{2.10}$$

2.3 Conductivity of a massive Dirac fermion

In order to get a bit acquainted with the computation of the conductivity, we start with an exercise: we compute the conductivity for a free massive Dirac fermion which is described by the Lagrangian

$$\mathcal{L} = \bar{\psi}\left(i\partial\!\!\!/ - m\right)\psi$$

For details about the notation convention as well as the Green's function we are going to use, see Appendix A. We start evaluating the EM kernel, as defined in eq. (2.6)

$$K^{\mu\nu}(i\omega_n,\mathbf{k}) = -e^2\frac{1}{\beta}\sum_m\int\frac{d^3q}{(2\pi)^3}\,\mathrm{Tr}\gamma^\mu G^0(i\omega_m+i\omega_n,\mathbf{k}+\mathbf{q})\gamma^\nu G^0(i\omega_m,\mathbf{q}) \tag{2.11}$$

where

$$G^0(i\omega_m,\mathbf{q}) = \frac{-\gamma_\tau^0\omega_m + \gamma\cdot\mathbf{q} - m}{-(i\omega_m)^2 + \mathbf{q}^2 + m^2}$$

The notation G^0 stands for the non-interacting Green's function, as opposed as the interacting cases that will be presented later on. In order to solve the former integral, it is useful to introduce the **spectral function**, defined as in eq. (A.8), which results in eq. (A.9)

$$A(\omega,\mathbf{k}) = \pi\frac{\not{k} - m}{\sqrt{\mathbf{k}^2+m^2}}\left[\delta(\sqrt{\mathbf{k}^2+m^2}+\omega) - \delta(\sqrt{\mathbf{k}^2+m^2}-\omega)\right]$$

This is the **spectral function for massive Dirac fields**. By means of it we can rewrite eq. (2.11) as

$$\begin{aligned} K^{\mu\nu}(i\omega_n,\mathbf{k}) &= -e^2\frac{1}{\beta}\sum_m\int\frac{d^3q}{(2\pi)^3}\,\mathrm{Tr}\gamma^\mu G^0(i\omega_m+i\omega_n,\mathbf{k}+\mathbf{q})\gamma^\nu G^0(i\omega_m,\mathbf{q}) \\ &= -e^2\frac{1}{\beta}\sum_m\int\frac{d^3q}{(2\pi)^3}\int\frac{d\omega'}{2\pi}\int\frac{d\omega''}{2\pi}\,\mathrm{Tr}\gamma^\mu\frac{A(\omega',\mathbf{k}+\mathbf{q})}{i\omega_m+i\omega_n-\omega'}\gamma^\nu\frac{A(\omega'',\mathbf{q})}{i\omega_m-\omega''} \end{aligned} \tag{2.12}$$

In order to sum over the Matsubara frequencies we rewrite the denominator,

$$\frac{1}{i\omega_m+i\omega_n-\omega'}\frac{1}{i\omega_m-\omega''} = \frac{1}{i\omega_n-\omega'+\omega''}\left(\frac{1}{i\omega_m-\omega''} - \frac{1}{i\omega_m+i\omega_n-\omega'}\right)$$

Recall that

$$\frac{1}{\beta}\sum_m\frac{1}{i\omega_m-\omega} = \mp\frac{1}{e^{\beta\omega}\mp 1} \tag{2.13}$$

depending on the statistics of the particles, bosonic (-) or fermionic (+). Here ω_m describes the Dirac field, that is fermionic, while ω_n refers to the bosonic gauge field, i.e. the external photon.
Thus,

$$\sum_m \frac{1}{i\omega_n - \omega' + \omega''}\left(\frac{1}{i\omega_m - \omega''} - \frac{1}{i\omega_m + i\omega_n - \omega'}\right) = \frac{1}{i\omega_n - \omega' + \omega''}\left(\frac{1}{e^{\beta\omega''}+1} - \frac{1}{e^{\beta(\omega' - i\omega_n)}+1}\right)$$
$$= \frac{n_F(\omega'') - n_F(\omega')}{i\omega_n - \omega' + \omega''}$$

Finally,

$$K^{\mu\nu}(i\omega_n, \mathbf{k}) = -e^2 \int \frac{d^3q}{(2\pi)^3} \int \frac{d\omega'}{2\pi} \int \frac{d\omega''}{2\pi} \frac{n_F(\omega'') - n_F(\omega')}{i\omega_n - \omega' + \omega''} \mathrm{Tr}\left[\gamma^\mu A(\omega', \mathbf{k}+\mathbf{q})\gamma^\nu A(\omega'', \mathbf{q})\right] \tag{2.14}$$

We now insert the expression just obtained for the spectral function and we trace out the gamma matrices, see Appendix A

$$K^{\mu\nu}(i\omega_n, \mathbf{k}) = -e^2 \int \frac{d^3q}{(2\pi)^3} \int \frac{d\omega'}{2\pi} \int \frac{d\omega''}{2\pi} \pi^2 \frac{n_F(\omega'') - n_F(\omega')}{i\omega_n - \omega' + \omega''} \frac{T^{\mu\nu}}{\sqrt{(\mathbf{k}+\mathbf{q})^2 + m^2}\sqrt{\mathbf{q}^2 + m^2}} \times$$
$$\times \left[\delta(\sqrt{(\mathbf{k}+\mathbf{q})^2 + m^2} + \omega') - \delta(\sqrt{(\mathbf{k}+\mathbf{q})^2 + m^2} - \omega')\right] \left[\delta(\sqrt{\mathbf{q}^2 + m^2} + \omega'') - \delta(\sqrt{\mathbf{q}^2 + m^2} - \omega'')\right] \tag{2.15}$$

where

$$T^{\mu\nu} = 4[\eta^{\mu\sigma}\eta^{\nu\rho} - \eta^{\mu\nu}\eta^{\sigma\rho} + \eta^{\mu\rho}\eta^{\sigma\nu}](k_\sigma + q_\sigma)q_\rho - 4\eta^{\mu\nu}m^2$$

By analytic continuation ($i\omega_n \to \omega + i\delta$) we find the imaginary part of the retarded linear response kernel to be

$$\mathrm{Im}\, K^{\mu\nu}(\omega^+, \mathbf{k}) = -e^2 \int \frac{d^3q}{(2\pi)^3} \int \frac{d\omega'}{2\pi} \frac{\pi^2}{2} [n_F(\omega') - n_F(\omega' - \omega)] \frac{T^{\mu\nu}}{\sqrt{(\mathbf{k}+\mathbf{q})^2 + m^2}\sqrt{\mathbf{q}^2 + m^2}} \times$$
$$\times \left[\delta(\sqrt{(\mathbf{k}+\mathbf{q})^2 + m^2} + \omega') - \delta(\sqrt{(\mathbf{k}+\mathbf{q})^2 + m^2} - \omega')\right] \times$$
$$\times \left[\delta(\sqrt{\mathbf{q}^2 + m^2} + \omega' - \omega) - \delta(\sqrt{\mathbf{q}^2 + m^2} - \omega' + \omega)\right] \tag{2.16}$$

where ω^+ indicates the retardation feature.

Longitudinal conductivity

We compute the longitudinal conductivity $\sigma_L \equiv \sum_i \sigma^{ii}/3$. It is convenient to introduce also a longitudinal linear response kernel, $K^L = \sum_i K^{ii}/3$. First of all we notice that

$$\sum_i T^{ii} = 12\omega'\omega'' - 4(\mathbf{k}+\mathbf{q})\cdot\mathbf{q} - 12m^2 \quad .$$

For the sake of simplicity we will name $\Omega_k = \sqrt{\mathbf{k}^2 + m^2}$.

$$\mathrm{Im}\, K^L(\omega^+, \mathbf{k}) = -\frac{e^2}{24\pi^2} \int d^3q \int d\omega' [n_F(\omega') - n_F(\omega' - \omega)] \frac{3\omega'^2 - 3\omega'\omega - 3m^2 - (\mathbf{k}+\mathbf{q})\cdot\mathbf{q}}{\Omega_{k+q}\Omega_q} \times$$
$$\times \left[\delta(\Omega_{k+q} + \omega') - \delta(\Omega_{k+q} - \omega')\right] \left[\delta(\Omega_q + \omega' - \omega) - \delta(\Omega_q - \omega' + \omega)\right] \quad .$$

We perform the integration over ω'

$$\begin{aligned}\operatorname{Im} K^L(\omega^+,\mathbf{k}) = \\ -\frac{e^2}{24\pi^2}\int d^3q\Bigg\{&[n_F(-\Omega_{k+q})-n_F(-\Omega_{k+q}-\omega)]\frac{3\Omega_{k+q}^2+3\Omega_{k+q}\omega-3m^2-(\mathbf{k}+\mathbf{q})\cdot\mathbf{q}}{\Omega_{k+q}\Omega_q}\times \\ &\times[\delta(\Omega_q-\Omega_{k+q}-\omega)-\delta(\Omega_q+\Omega_{k+q}+\omega)] \\ &-[n_F(\Omega_{k+q})-n_F(\Omega_{k+q}-\omega]\frac{3\Omega_{k+q}^2-3\Omega_{k+q}\omega-3m^2-(\mathbf{k}+\mathbf{q})\cdot\mathbf{q}}{\Omega_{k+q}\Omega_q}\times \\ &\times[\delta(\Omega_q+\Omega_{k+q}-\omega)-\delta(\Omega_q-\Omega_{k+q}+\omega)]\Bigg\} \quad .\end{aligned}$$

We will solve the integral for the case of an homogeneour external EM field, that is, we set $\mathbf{k}=0$. Now we have that $\Omega_{k+q}\to\Omega_q$ and switching to spherical coords we get

$$\begin{aligned}\operatorname{Im} K^L(\omega^+,\mathbf{k}) = -\frac{e^2}{6\pi}\int dq\, q^2 \\ \Bigg\{&[n_F(-\Omega_q)-n_F(-\Omega_q-\omega)]\frac{3\Omega_q^2+3\Omega_q\omega-3m^2-\mathbf{q}^2}{\Omega_q^2}[\delta(-\omega)-\delta(2\Omega_q+\omega)] \\ &-[n_F(\Omega_q)-n_F(\Omega_q-\omega)]\frac{3\Omega_q^2-3\Omega_q\omega-3m^2-\mathbf{q}^2}{\Omega_q^2}[\delta(2\Omega_q-\omega)-\delta(\omega)]\Bigg\}\end{aligned}$$

We look at the case for which $\omega\neq 0$: in this case the two terms involving $\delta(\omega)$ give zero contribution. These divergent terms at zero frequency are usually to be expected and correspond to the **Drude peak** of the conductivity. Although it might seem unphysical, it is natural to find such a diverging term in the calculation carried on so far. In the simple model for classical conductivity, the Drude model, impurities are added to the system. They play indeed a crucial role for if one considers a simple electron gas moving under the effect of an external electric field, it is natural to expect the particles to accelerate indefinetely. The same reason is precisely why we should expect a Drude peak at $\omega=0$.
Before integrating out the momentum, we make use of the property of the Dirac delta,

$$\delta(\Omega_q\pm\omega)=\delta(\sqrt{q^2+m^2}\pm\omega)$$

which has solutions that depend on the sign of ω, negative (+) or positive(-), provided that $|\omega|>m$. This means that there is an energy gap within system $\Delta E=2m$. Below this threeshold there occur no transitions between the valence and conduction band and therefore the conductivity is just zero.
If the solution exists, then we can rewrite the delta function as

$$\delta(\sqrt{q^2+m^2}\pm\omega)=\frac{\sqrt{q^2+m^2}}{2q}\delta\left(q\pm\sqrt{\frac{\omega^2}{4}-m^2}\right)$$

and see that there's always a solution for $q>0$. Performing the integration over the internal momentum q we get

$$\operatorname{Im} K^L(\omega^+,\mathbf{k}=0)=-\frac{\omega^2e^2}{12\pi}\left[\left[n_F\big(\frac{\omega}{2}\big)-n_F\big(-\frac{\omega}{2}\big)\right]\left(1+\frac{2m^2}{\omega^2}\right)\left(1-\frac{4m^2}{\omega^2}\right)^{1/2}+\delta(\omega)...\right] \tag{2.17}$$

from which we deduce the longitudinal conductivity for an homogeneous external field,

$$\begin{aligned}\operatorname{Re}\sigma(\omega)&=\frac{1}{\omega}\operatorname{Im} K(\omega^+) \\ &=-\frac{\omega\, e^2}{12\pi}\left[\left[n_F\big(\frac{\omega}{2}\big)-n_F\big(-\frac{\omega}{2}\big)\right]\left(1+\frac{2m^2}{\omega^2}\right)\left(1-\frac{4m^2}{\omega^2}\right)^{1/2}+\delta(\omega)...\right]\end{aligned}$$

We can expand the term within the brackets by means of a Taylor series,

$$f(x)=(1+2x^2)(1-4x^2)^{1/2}=1-6x^4+\mathcal{O}(x^5)$$

to get an expression for the longitudinal conductivity in the case $|\omega| \gg m$ up to second order in m/ω:

$$\sigma^L(\omega) = -\frac{\omega\, e^2}{12\pi}\left(1 - \frac{6m^4}{\omega^4}\right)\left[n_F\Big(\frac{\omega}{2}\Big) - n_F\Big(-\frac{\omega}{2}\Big)\right] \tag{2.18}$$

In the zero-temperature limit, or equivalently for $|\omega| \gg T$, the previous boils down to

$$\sigma^L(\omega) = \frac{|\omega|\, e^2}{12\pi}\left(1 - \frac{6m^4}{\omega^4}\right) \tag{2.19}$$

It is interesting to notice that the mass correction to the optical conductivity shows up only at the quartic order.

2.4 Conductivity for a massless Fermion field with tilting term

So far we've seen the simple case of massive Dirac fermions. We now dive into the world of Weyl Semimetals (WSM), where the particle of our system will be a massless Dirac fermion.
We consider a system described by the Hamiltonian given in eq. (1.2). We can recast it in a more convenient form for the calculations to come,

$$H(\mathbf{k},\mathbf{d}) = v_F \begin{pmatrix} h_+ & 0 \\ 0 & h_- \end{pmatrix} \qquad , \qquad h_\pm(\mathbf{k},\mathbf{d}) = w\mathbf{d}\cdot\mathbf{k} \pm \mathbf{k}\cdot\sigma \tag{2.20}$$

For the sake of simplicity, we shall drop the term v_F in the calculations and restore it only in the final results. There is no ambiguity in doing so and the expressions becomes much more readable. The Green's function is defined as

$$(i\omega_n - H(\mathbf{k},\mathbf{d}))G(i\omega_n,\mathbf{k},\mathbf{d}) = \mathbb{I}_4$$

which gives us the inverse of the Green's function,

$$G^{-1}(i\omega_n,\mathbf{k},\mathbf{d}) = \begin{pmatrix} i\omega_n - h_+ & 0 \\ 0 & i\omega_n - h_- \end{pmatrix}$$

Since G^{-1} is block diagonal, also its inverse has to be

$$G(i\omega_n,\mathbf{k},\mathbf{d}) = \begin{pmatrix} G_+ & 0 \\ 0 & G_- \end{pmatrix} \qquad , \qquad (i\omega_n - h_\pm(\mathbf{k},\mathbf{d}))\; G_\pm(i\omega_n,\mathbf{k},\mathbf{d}) = \mathbb{I}_2$$

which can be easily inverted,

$$\begin{aligned} (i\omega_n - h_\mp(\mathbf{k},\mathbf{d}))\,(i\omega_n - h_\pm(\mathbf{k},\mathbf{d}))\; G_\pm(i\omega_n,\mathbf{k},\mathbf{d}) &= (i\omega_n - h_\mp(\mathbf{k},\mathbf{d})) \\ \left((i\omega_n - w\mathbf{d}\cdot\mathbf{k})^2 - |\mathbf{k}|^2\right)\; G_\pm(i\omega_n,\mathbf{k},\mathbf{d}) &= (i\omega_n - h_\mp(\mathbf{k},\mathbf{d})) \end{aligned}$$

from which we get

$$G_\pm(i\omega_n,\mathbf{k},\mathbf{d}) = \frac{i\omega_n - w\mathbf{d}\cdot\mathbf{k} \pm \mathbf{k}\cdot\sigma}{(i\omega_n - w\mathbf{d}\cdot\mathbf{k})^2 - |\mathbf{k}|^2}$$

Finally the Green's function is given by

$$\begin{aligned} G(i\omega_n,\mathbf{k},\mathbf{d}) &= \frac{1}{(i\omega_n - w\mathbf{d}\cdot\mathbf{k})^2 - \mathbf{k}^2}\begin{pmatrix} i\omega_n + \mathbf{k}\cdot\sigma - w\mathbf{d}\cdot\mathbf{k} & 0 \\ 0 & i\omega_n - \mathbf{k}\cdot\sigma - w\mathbf{d}\cdot\mathbf{k} \end{pmatrix} \\ &= \frac{1}{(i\omega_n - w\mathbf{d}\cdot\mathbf{k})^2 - \mathbf{k}^2}\left[(i\omega_n - w\mathbf{d}\cdot\mathbf{k})\otimes\mathbb{I}_4 + \tau_z\otimes(\mathbf{k}\cdot\sigma)\right] \end{aligned} \tag{2.21}$$

At this point we just need the current vertices to compute the conductivity. These latter are given by

$$j^\mu = e\frac{\partial H}{\partial k_\mu} \quad \longrightarrow \quad j^i = e(\tau_z\otimes\sigma^i + wd_i)$$

We follow the same procedure seen above for the computation of the conductivity, thus we first focus on the imaginary part of the EM kernel and from that we derive the optical conductivity. The more technical steps can be found in the Appendix section.

$$K^{ij}(i\omega_n,\mathbf{k}) = -e^2\frac{1}{\beta}\sum_m \int \frac{d^3q}{(2\pi)^3}\,\mathrm{Tr}(\tau_z\otimes\sigma^i + wd_i)G(i\omega_m + i\omega_n,\mathbf{k}+\mathbf{q})(\tau_z\otimes\sigma^j + wd_j)G(i\omega_m,\mathbf{q}) \tag{2.22}$$

The spectral function is obtained by analytic continuation from the (Euclidean) Green's function and reads (see Appendix A)

$$A(\omega^+,\mathbf{q},\mathbf{d}) = \frac{\pi}{|\mathbf{q}|}\big[(\omega - w\mathbf{d}\cdot\mathbf{q}) + \tau_z\otimes(\mathbf{q}\cdot\sigma)\big]\Big[\delta\big(\omega - w\mathbf{d}\cdot\mathbf{q} - |\mathbf{q}|\big) - \delta\big(\omega - w\mathbf{d}\cdot\mathbf{q} + |\mathbf{q}|\big)\Big] \tag{2.23}$$

By means of the spectral function, we can rewrite the Green's functions as done in the previous calculation,

$$K^{ij}(i\omega_n,\mathbf{k}) = -\frac{e^2}{\beta}\sum_m\int\frac{d^3q}{(2\pi)^3}\int\frac{d\omega'}{2\pi}\int\frac{d\omega''}{2\pi}\,\mathrm{Tr}\Big[(\tau_z\otimes\sigma^i + wd_i)\frac{A(\omega',\mathbf{k}+\mathbf{q})}{i\omega_n + i\omega_m - \omega'}\times \\ \times(\tau_z\otimes\sigma^j + wd_j)\frac{A(\omega'',\mathbf{q})}{i\omega_m - \omega''}\Big] \tag{2.24}$$

We first sum over Matsubara frequencies, then perform analytic continuation to real frequency and finally integrate out ω''

$$\mathrm{Im}K^{ij}(\omega^+,\mathbf{k}) = -e^2\int\frac{d^3q}{(2\pi)^3}\int\frac{d\omega'}{4\pi}\big[n_F(\omega') - n_F(\omega'-\omega)\big]\times \\ \times\,\mathrm{Tr}\Big[(\tau_z\otimes\sigma^i + wd_i)A(\omega',\mathbf{k}+\mathbf{q})(\tau_z\otimes\sigma^j + wd_j)A(\omega'-\omega,\mathbf{q})\Big] \tag{2.25}$$

We consider the case in which the momentum transfer involved in the process is zero, i.e. $\mathbf{k}=0$. This corresponds to having an external EM field which is approximately constant over the length of our sample. Inserting back the expression for the spectral function we get

$$\mathrm{Im}K^{ij}(\omega^+,\mathbf{0}) = -e^2\int\frac{d^3q}{(2\pi)^3}\int\frac{d\omega'}{4\pi}\pi^2\frac{n_F(\omega') - n_F(\omega'-\omega)}{\mathbf{q}^2}\Big[\delta\big(\omega' - w\mathbf{d}\cdot\mathbf{q} - |\mathbf{q}|\big) - \delta\big(\omega' - w\mathbf{d}\cdot\mathbf{q} + |\mathbf{q}|\big)\Big]\times \tag{2.26}$$
$$\times\Big[\delta\big(\omega' - \omega - w\mathbf{d}\cdot\mathbf{q} - |\mathbf{q}|\big) - \delta\big(\omega' - \omega - w\mathbf{d}\cdot\mathbf{q} + |\mathbf{q}|\big)\Big]\times$$
$$\times\mathrm{Tr}\Big[(\tau_z\otimes\sigma^i + wd_i)((\omega' - w\mathbf{d}\cdot\mathbf{q}) + \tau_z\otimes(\mathbf{q}\cdot\sigma))(\tau_z\otimes\sigma^j + wd_j)((\omega' - \omega - w\mathbf{d}\cdot\mathbf{q}) + \tau_z\otimes(\mathbf{q}\cdot\sigma))\Big]$$

We now perform the sum over ω'

$$\mathrm{Im}K^{ij}(\omega^+,\mathbf{0}) = -e^2\sum_{\alpha=\pm}\int\frac{d^3q}{32\pi^2}\Bigg\{\frac{n_F(w\mathbf{d}\cdot\mathbf{q}+\alpha|\mathbf{q}|) - n_F(w\mathbf{d}\cdot\mathbf{q}+\alpha|\mathbf{q}|-\omega)}{\mathbf{q}^2}\Big[\delta\big(-\omega\big) - \delta\big(2\alpha|\mathbf{q}| - \omega\big)\Big]\times \tag{2.27}$$
$$\times\mathrm{Tr}\Big[(\tau_z\otimes\sigma^i + wd_i)(\alpha|\mathbf{q}| + \tau_z\otimes(\mathbf{q}\cdot\sigma))(\tau_z\otimes\sigma^j + wd_j)(\alpha|\mathbf{q}| - \omega + \tau_z\otimes(\mathbf{q}\cdot\sigma))\Big]\Bigg\}$$

where we introduce $\alpha = \pm 1$ for a more compact notation. We may drop the term $\delta(-\omega)$ since the integrand function is zero for $\omega = 0$. We then compute the trace in the integral,

$$\mathrm{Tr}\Big[(\tau_z\otimes\sigma^i + wd_i)(\alpha|\mathbf{q}| + \tau_z\otimes(\mathbf{q}\cdot\sigma))(\tau_z\otimes\sigma^j + wd_j)(\alpha|\mathbf{q}| - \omega + \tau_z\otimes(\mathbf{q}\cdot\sigma))\Big]$$

Let's introduce

$$A = (\tau_z\otimes\sigma^i + wd_i)(\alpha|\mathbf{q}| + \tau_z\otimes(\mathbf{q}\cdot\sigma)) \\ = \alpha|\mathbf{q}|\tau_z\otimes\sigma^i + \alpha w|\mathbf{q}|d_i + \left(q_i + i\sum_{m,n}\epsilon_{imn}q_m\sigma^n\right) + wd_i\tau_z\otimes(\mathbf{q}\cdot\sigma)$$

and

$$B = (\tau_z\otimes\sigma^j + wd_j)(\alpha|\mathbf{q}| - \omega + \tau_z\otimes(\mathbf{q}\cdot\sigma)) \\ = (\alpha|\mathbf{q}| - \omega)\tau_z\otimes\sigma^j + w(\alpha|\mathbf{q}| - \omega)d_j + \left(q_j + i\sum_{m',n'}\epsilon_{jm'n'}q_{m'}\sigma^{n'}\right) + wd_j\tau_z\otimes(\mathbf{q}\cdot\sigma)$$

We are computing $\mathrm{Tr}[A\cdot B]$, which can seem pretty hard but recall that Pauli matrices are traceless, allowing us to 'discard' all the terms within the trace, that are linear in σ^i (also recall that $\mathrm{Tr}[A\otimes B]=\mathrm{Tr}[A]\mathrm{Tr}[B]$)

$$A\cdot B=\alpha|\mathbf{q}|(\alpha|\mathbf{q}|-\omega)\delta^{ij}+w(2\alpha|\mathbf{q}|-\omega)(\alpha w|\mathbf{q}|d_id_j+d_iq_j+d_jq_i)+ \\ +\left(q_iq_j-\sum_{\substack{m,n\\m',n'}}\epsilon_{imn}\epsilon_{jm'n'}q_mq_{m'}\sigma^n\sigma^{n'}\right)+\mathcal{O}(\sigma^i)$$

where within $\mathcal{O}(\sigma^i)$ are contained all the terms of the product that are linear in the Pauli matrices. Making use of the properties of the Pauli matrices,

$$\begin{aligned}\sum_{\substack{m,n\\m',n'}}\epsilon_{imn}\epsilon_{jm'n'}q_mq_{m'}\sigma^n\sigma^{n'}&=\sum_{\substack{m,n\\m',n'}}\epsilon_{imn}\epsilon_{jm'n'}q_mq_{m'}\delta^{nn'}\\&=\sum_{m,m'}(\delta^{ij}\delta^{mm'}-\delta^{im'}\delta^{jm})q_mq_{m'}\\&=\delta^{ij}q^2-q_iq_j\end{aligned}$$

which brings us to the final result

$$A\cdot B=-\alpha|\mathbf{q}|\omega\delta^{ij}+w(2\alpha|\mathbf{q}|-\omega)(\alpha w|\mathbf{q}|d_id_j+d_iq_j+d_jq_i)+2q_iq_j+\mathcal{O}(\sigma^i)$$

For the sake of simplicity we introduce the tensor

$$T^{ij}=\frac{\mathrm{Tr}[A\cdot B]}{4}=-\alpha|\mathbf{q}|\omega\delta^{ij}+w(2\alpha|\mathbf{q}|-\omega)(\alpha w|\mathbf{q}|d_id_j+d_iq_j+d_jq_i)+2q_iq_j$$

$$\mathrm{Im}K^{ij}(\omega^+,\mathbf{0})=\frac{e^2}{8\pi^2}\sum_{\alpha=\pm}\int d^3q\,T^{ij}\left\{\frac{n_F(w\mathbf{d}\cdot\mathbf{q}+\alpha|\mathbf{q}|)-n_F(w\mathbf{d}\cdot\mathbf{q}+\alpha|\mathbf{q}|-\omega)}{\mathbf{q}^2}\times\right. \\ \left.\times\delta\left(2\alpha|\mathbf{q}|-\omega\right)\right\} \tag{2.28}$$

We set the direction of the tilting to be $\mathbf{d}=(0,0,1)$ and look at the conductivities in the directions parallel and perpendicular to $\mathbf{d}$ to see whether it carries a signature of the tilting term.
In particular we define $\sigma_\parallel=\sigma^{zz}$ and $\sigma_\perp=(\sigma^{xx}+\sigma^{yy})/2$.
Switching to spherical coords, $(q_x,q_y,q_z)\to(q\sin\theta\cos\phi,q\sin\theta\sin\phi,q\cos\theta)$,

$$\frac{T^{xx}+T^{yy}}{2}=-\alpha q\omega+q^2\sin^2\theta$$

$$T^{zz}=-\alpha q\omega+w^2q(2\alpha q-\omega)+2q^2\cos^2\theta+w(2\alpha q-\omega)q\cos\theta$$

For the computation of the above integral one has to consider the different cases, $\omega=\pm|\omega|$.

$$\begin{aligned}\mathrm{Im}\left[\frac{K^{xx}+K^{yy}}{2}\right]&=\frac{e^2}{8\pi^2}\sum_{\alpha=\pm}\int_0^{2\pi}d\phi\int_0^{\pi}d\theta\int_0^{\infty}dq\,q^2\sin\theta\frac{n_F(wq\cos\theta+\alpha q)-n_F(wq\cos\theta+\alpha q-\omega)}{q^2}\times\\&\qquad\times\delta\big(2\alpha q-\omega\big)\left(-\alpha q\omega+q^2\sin^2\theta\right)\\&=\frac{e^2}{4\pi}\sum_{\alpha=\pm}\int_{-1}^{1}dx\int_0^{\infty}dq\left[n_F(wqx+\alpha q)-n_F(wqx+\alpha q-\omega)\right]\times\\&\qquad\times\frac{1}{2}\delta\left(q-\frac{\omega}{2\alpha}\right)\left(-\alpha q\omega+q^2(1-x^2)\right)\\&=-\frac{e^2\omega^2}{32\pi}\int_{-1}^{1}dx\left[n_F\left(\frac{\omega}{2}(wx+1)\right)-n_F\left(\frac{\omega}{2}(wx-1)\right)\right](1+x^2)\end{aligned}$$

Notice that the terms with $\alpha = \pm 1$ correspond to positive and negative frequencies, respectively. Therefore we find the final result for the perpendicular conductivity to be

$$\sigma_\perp(\omega) = \frac{1}{\omega}\mathrm{Im}K_\perp(\omega^+) = -\frac{e^2\omega}{32\pi v_F}\int_{-1}^{1} dx \left[n_F\left(\frac{\omega}{2}(wx+1)\right) - n_F\left(\frac{\omega}{2}(wx-1)\right)\right](1+x^2) \tag{2.29}$$

Where we inserted back the dependence on the Fermi velocity. In analoguous way we compute the parallel conductivity. For ω>0:

$$\begin{aligned}
\mathrm{Im}\left[K^{zz}\right] &= \frac{e^2}{8\pi^2}\sum_{\alpha=\pm}\int_0^{2\pi} d\phi \int_0^{\pi} d\theta \int_0^{\infty} dq\, q^2 \sin\theta \frac{n_F(wq\cos\theta+\alpha q) - n_F(wq\cos\theta+\alpha q-\omega)}{q^2}\times \\
&\qquad \times \delta\big(2q-\omega\big)\left(-\alpha q\omega + w^2 q(2\alpha q-\omega) + 2q^2\cos^2\theta + w(2\alpha q-\omega)q\cos\theta\right) \\
&= \frac{e^2}{4\pi}\sum_{\alpha=\pm}\int_{-1}^{1} dx \int_0^{\infty} dq \left[n_F(wqx+\alpha q) - n_F(wqx+\alpha q-\omega)\right]\times \\
&\qquad \times \frac{1}{2}\delta\left(q-\frac{\omega}{2\alpha}\right)\left(-\alpha q\omega + w^2 q(2\alpha q-\omega) + 2q^2x^2 + w(2\alpha q-\omega)qx\right) \\
&= -\frac{e^2\omega^2}{16\pi}\int_{-1}^{1} dx \left[n_F\left(\frac{\omega}{2}(wx+1)\right) - n_F\left(\frac{\omega}{2}(wx-1)\right)\right](1-x^2)
\end{aligned}$$

From which we get

$$\sigma_\parallel(\omega) = \frac{1}{\omega}\mathrm{Im}K_\parallel(\omega^+) = -\frac{e^2\omega}{16\pi v_F}\int_{-1}^{1} dx \left[n_F\left(\frac{\omega}{2}(wx+1)\right) - n_F\left(\frac{\omega}{2}(wx-1)\right)\right](1-x^2) \tag{2.30}$$

From this calculation we notice that all the crossed terms of the type $d_i q_j$ give no contribution to the conductivity. The effect of the tilting of the Dirac cones is a rather indirect contribution contained in the Fermi-Dirac distribution. A simple check of the result can be made by setting $w = 0$. We compute the longitudinal conductivity:

$$\begin{aligned}
\sigma_L(\omega) &= \sum_i \frac{\sigma^{ii}}{3} = \frac{2\sigma_\perp}{3} + \frac{\sigma_\parallel}{3} \\
&= -\frac{e^2\omega}{24\pi v_F}\int_{-1}^{1} dx \left[n_F\left(\frac{\omega}{2}\right) - n_F\left(-\frac{\omega}{2}\right)\right] = -\frac{e^2\omega}{12\pi v_F}\left[n_F\left(\frac{\omega}{2}\right) - n_F\left(-\frac{\omega}{2}\right)\right]
\end{aligned}$$

which is precisely the result obtained for free massless fermions. It also retains the correct behavior in the zero-temperature limit,

$$\sigma_L(\omega) \overset{T\to 0}{=} \frac{e^2|\omega|}{12\pi v_F} \tag{2.31}$$

in agreement with previous work, [8, 14]. In the general case for which $T \neq 0$ there is no analytical result for eqs. (2.29), (2.30) but the behavior can be studied by solving the equations numerically. We are here interested in how the conductivity changes with the parameter w: in Fig 2.2a is shown the behavior of the conductivity at non-zero temperature. At small values of ω of the external field, the conductivity grows quadratically while it becomes linear in the optical region, that is, for $\omega \gg T$; from the figure is clear that the tilting of the Weyl cone affects mainly this latter region.
We can investigate further the linear region: if we just consider the optical limit, $\omega \gg T$, we can solve analytically eqs. (2.29), (2.30), for in this limit the Fermi-Dirac distribution become simple Heaviside functions and we carry out the angle integration (the limit corresponds to taking the temperature to zero). We suppose $\omega > 0$ and consider $\sigma_\perp$, the term involving the Fermi-Dirac distribution becomes

$$n_F\left(\frac{\omega}{2}(wx+1)\right) - n_F\left(\frac{\omega}{2}(wx-1)\right) \to -\theta(1+wx)\theta(1-wx)$$

which inserted in eq. (2.29) yields

$$\begin{aligned}
\sigma_\perp(\omega) &= -\frac{\omega}{32\pi}\int_{-1}^{1} dx\, \left[-\theta(1+wx)\theta(1-wx)\right](1+x^2) \\
&= \frac{|\omega|e^2}{12\pi v_F} - \theta(w-1)\left(\frac{4}{3} - \frac{3w^2+1}{3w^3}\right)\frac{|\omega|e^2}{16\pi v_F}
\end{aligned}$$

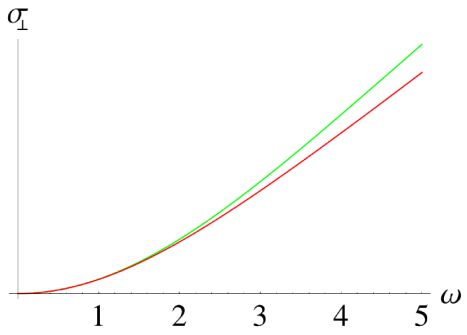

(a) Perpendicular conductivity at $T = 1$ for $w = 0$ (green) and $w = 0.8$ (red).

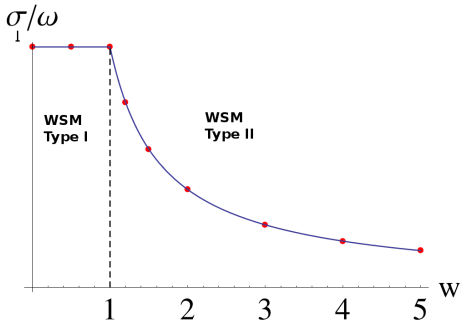

(b) Angular coefficient of the perpendicular conductivity in the optical region as a function of w.

Figure 2.2: *Behavior of the perpendicular conductivity.*

Notice that the absolute value comes from the fact that for $\omega < 0$ the condition expressed via Heaviside function picks up a minus sign. Repeating the same reasoning for the parallel conductivity one obtains

$$\begin{aligned}\sigma_{\parallel}(\omega) &= -\frac{\omega}{16\pi}\int_{-1}^{1} dx\ [-\theta(1+wx)\theta(1-wx)]\,(1-x^2) \\ &= \frac{|\omega|e^2}{12\pi v_F} - \theta(w-1)\left(\frac{2}{3} - \frac{3w^2-1}{3w^3}\right)\frac{|\omega|e^2}{8\pi v_F}\end{aligned}$$

The result is shown in Fig. 2.2b, where the angular coefficient of the perpendicular conductivity in the optical region (thus linear) is plotted. We see that for $|w| < 1$, that is for WSM of type I, the conductivity does not "feel" the tilting of the Weyl cone, hence the conductivity is undistinguishible from that of a normal WSM in the optical region. If the cone is tilted over, though, the conductivity drops to zero as $1/w$. In this sense the conductivity can be employed to classify a WSM in one of the two categories.
We here focus on WSM of type I and try to explain the rather singular behavior of the observable: at first we would have expected the conductivity to show a clear signature of the presence of the tilting term. Although a bit unexpected, a further analysis assures the result makes perfect sense. As we saw earlier, the tilting term enters the expression of the conductivity indirectly, i.e. in the argument of the Fermi-Dirac distribution. Naively, by taking the optical limit (or equivalently the zero-temperature limit) most of the informations stored in the distribution are lost because the only information that matters is the sign of the argument.
If it makes sense on a mathematical basis, the above reasoning is difficult to interpret physically and is worth to bring up a more intuitive argument which is based on a graphical interpretation. We here introduce the concept of **transitions**, a tool that will be used also in the next Chapter, when we will compute the polarization function. A transition is a process in which a particle switches from an initial state $|i\rangle$ to a final state $|f\rangle$, because of an external perturbation or simply a quantum fluctuation. In our case we can interpret the conductivity as given by the transitions of electrons from valence to conduction band caused by the external EM radiation, which exchange with an electron in the valence band an energy ω and a momentum $\mathbf{k} = 0$, as shown in Fig. 2.3, on the left. For untilted cones, the number of states that can undergo such a transitions are those lying on the circular region corresponding to an energy $E = -\omega/2$, which will get excited to the region specular region at energy $E = \omega/2$. Because the process does not involve momentum transfer, then the transition corresponds to a vertical "jump".
If we now consider the additional tilting term, the states that can be excited from valence to conduction band lie on an ellipsoid, tilted itself. Naively we could expect the conductivity to grow since, if the number of states is proportional to the length of the region, there should be more transitions available for the process. However the number of states is given by the line integral over the region of the density of states, and this latter changes along the ellipse. The two effects, length of the region and varying density of states, compensate each other, in such a way that only the **projection** of the shaded areas onto the $\omega = 0$ plane matters.
We thus see that the conductivity does not change as long as the Weyl cone is not tilted over. We now address a problem that the reader might have already recognized in the above reasoning, in particular by just looking at Fig. 2.2. In fact, we showed that the discrepancy between tilted and untilted Weyl cones

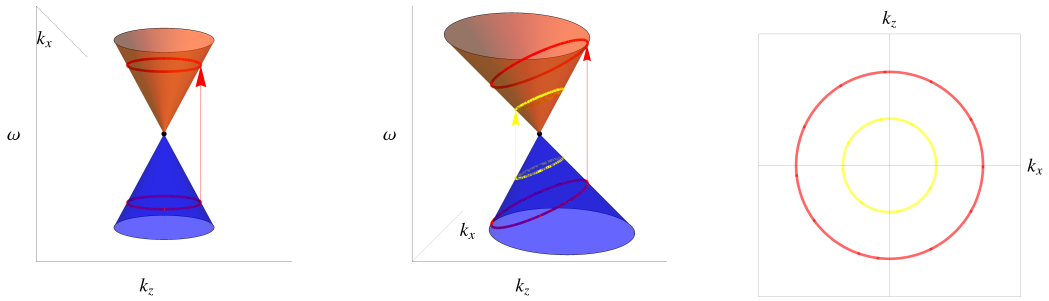

Figure 2.3: *Graphical interpretation of the conductivity. Transitions at $\omega = 2$ (red) and $\omega = 1$ (yellow) and their projection on the $\omega = 0$ plane.*

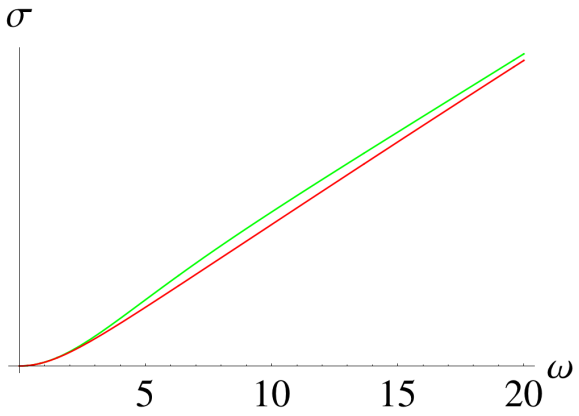

Figure 2.4: *Perpendicular conductivity for $T = 0$ and $w = 0$ (green) and $w = 0.8$ (red).*

can be evinced by looking at the conductivity in the optical limit, for $\omega \gg T$, and soon after that the same quantity does not change when taking the zero-temperature limit. The two seem statements seem to be contradictory, and the two graphics shown in the picture appear to belong to different physical quantities. The loophole lies in the fact that the Fig. 2.2a does not show the proper optical limit, but rather a region in which ω is bigger than the temperature, of at most one order of magnitude. If we were to plot the true optical limit we would see the behavior shown in Fig. 2.4, where it is clear that the difference in the conductivity arises for $T < \omega \sim 1$, while in the optical limit, or equivalently for temperatures nearly zero, the behavior is the one depicted in Fig. 2.2b.

2.5 Conclusions

In the Chapter we computed the optical conductivity for different systems: first massive Dirac electrons and then massless Dirac electrons moving on a tilted cone. The former case served us to get acquainted with different mathematical tools and physical objects, such as the spectral function, that we then used for the case of our interest. We found that for massive Dirac electrons the longitudinal conductivity shows a correction due to the mass at the fourth order in m/ω, thus to all purposes irrelevant in the optical regime, where the scale of the observable is set by the external frequency, ω.
Moving onto the case of our interest, we found that the optical conductivity carries a signature of the tilting of Weyl cones, that shows up at non-zero temperature in the optical regime, that is, where the conductivity grows linearly with ω. For the more we find that the conductivity in the direction parallel to the tilting vector $\sigma_{\parallel}$ is different from that in the plane perpendicular to it, $\sigma_{\perp}$. This can be read as a signature of the additional tilting term in an observable such as the conductivity. We then investigated the zero-temperature limit and found an analytic expression for both perpendicular and parallel conductivity which shows that in this region the conductivity does not care about the tilting of the Dirac cone. Two different explanations have been given, motivating us to believe it is indeed the result we should expect if we are to compute the optical conductivity for an external field constant over our sample, i.e. $\mathbf{k} = 0$.

Chapter 3

The polarization function

3.1 Introduction

In the previous Chapter we introduced the theory of linear response and used it to compute the general expression of the Kubo formula for conductivity in the case of Dirac fields. Here we focus on the computation of an analytic expression for the polarization function, which corresponds to K^{00} in the formalism of Sec. 2.2. It represents the density-density response function of the system, that is, the density fluctuations of the system induced by a density probe.
The polarization function is a very useful tool, both for experimental measurements and for theoretical calculations. Important quantities can be obtained from it, such as the screening length, the plasmons dispersion relation, the particle-hole spectrum and so on.
The fact that plasmons can be manipulated with a very good precision in the experiments, gave rise to a whole new branch of physics, that of plasmonics, which studies how these quasiparticles can be coupled to external sources and what new features can be obtained from it, [12, 21]. In particular polaritons, obtained via coupling plasmons to an electromagnetic field, are now matter of an intense experimental research.
In this Chapter we shall first review the theory of plasmons, then move on considering the 2D case, that of graphene, for which the result for the polarization function is well known, to get acquainted with the calculations.
Finally we will investigate the behaviour of WSM, both at finite electron doping and with the additional tilting term.

3.2 Plasmons in a nutshell

Before diving into the calculation of an analytic expression for the polarization function, we shall first review the theory of plasmons: what they are, how they arise and lastly why they are important to us. In the Drude model, a metal consists of gas of noninteracting electrons that moves around fixed ions. Because of their mobility and of their charge, we expect the electrons to displace when an external field is applied. The electron gas moves as a whole with respect to the ion background, creating an internal electric field that acts as a restoring force on the gas.
The motion of electrons is described by the differential equation

$$\frac{d^2x}{dt^2} = -4\pi n e^2 x$$

which is the EOM of an harmonic oscillator, thus the electrons will move back and forth with respect to the ions core. Here n denotes the electron density.
These collective longitudinal oscillations of the electron gas are called **plasma oscillations**; the picture given above is in fact a bit too naive and a serious calculation has to include the scattering of the electrons from impurities as well as interactions between electrons. This results in an additional term to be added in the above equation which is proportional to the velocity of the electrons, i.e. of the form $\gamma\dot{x}$ and constitues a damping effect.
In general plasma oscillations will make the external perturbation to be disperded in the material, because of the damping effect, however there exist particular frequencies for which the electron motion will not be damped, thus resulting in resonances[1].

[1] We here omit an exhaustive description of the phenomenon, which can be found in any book of solid state physics, for instance [18] or [22]

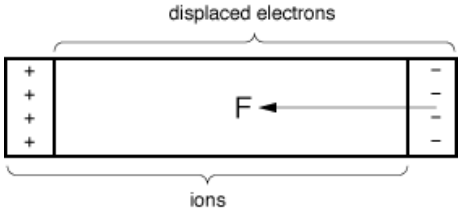

Figure 3.1: *Classical representation of plasma oscillations.*

A **plasmon** is the quasiparticle arising from the quantization of plasma oscillations, its spectrum can be experimentally measured via scattering experiments and important quantities, such as the screening length, can be derived from it. The relation between plasmons and polarization function is provided by another important quantity that emerges in solid state physics, the dielectric function, $\epsilon(\nu, \mathbf{q})$, given by the relation

$$\epsilon(\nu, \mathbf{q}) = 1 - V_0(\mathbf{q})\pi(\nu, \mathbf{q}) \tag{3.1}$$

where $V(\mathbf{q})$ is the Coulomb potential and $\pi(\nu, \mathbf{q})$ is precisely the polarization function. The meaning of the dielectric constant can be understood by considering the static limit, i.e. $\epsilon(\nu = 0, \mathbf{q})$: in this region it represents the ratio between the microscopic potential and the effective one, that is the ratio between the potential a test particle would feel was it in vacuum and the one it feels in the medium, because of interactions.

$$\epsilon(0, \mathbf{q}) = \frac{V_0(\mathbf{q})}{V_{eff}(\mathbf{q})}$$

The dielectric function just introduced is related to plasmons: the dispersion relation of these latter is given precisely by the poles of $1/\epsilon$, thus one way to compute the plasmon spectrum is to begin with the polarization function, compute the dielectric function and find where it has its poles. It should be pointed out that because of the complex structure of the polarization function, eq. (3.1) constitues a set of two equations: one for the real part of the dielectric function and one for the imaginary part.
This means that the dispersion relation of plasmons has, in general, both a real and an imaginary part; the latter corresponds to the quasiparticle to have a finite lifetime. This behavior reproduces the classical pictures of the damping of plasma oscillations by means of the scattering of electrons with impurities or core ions and is physically very important.
Another thing that should be remarked is that eq. (3.1) is exact provided that in the RHS is used the expression for the full polarization, i.e. including interactions and not restricted to first orders in perturbations. We compute here the polarization function for a system without electron-electron interaction, thus in principle it cannot be used to evaluate the plasmon spectrum but nevertheless results very useful for computing correction to, for instance, the self-energy (RPA approximation) and a rough extimation of plasmon spectrum.

3.3 The 2D case: graphene

We begin with the calculation of the polarization function for graphene. As we shall later see, the calculation can be extended without much changes to the three-dimensional case, that is the one we are interested in. We will limit our calculation to spinless graphene, however the result is very general: because the Hamiltonian does not include spin-spin interactions, we can regard the two type of spin as independent particles. The Hamiltonian of the system is given by:

$$\mathcal{H}(\mathbf{k}) = v_F \mathbf{k} \cdot \sigma - \mu \qquad , \qquad \mathbf{k} = (k_x, k_y)$$

which gives the eigenvalyues

$$E_\pm = -\mu \pm v_F |\mathbf{k}|$$

The Green's function of the system is obtained from its inverse,

$$G^{-1}(i\omega_n, \mathbf{k}) = i\omega_n - \mathcal{H}(\mathbf{k}) = (i\omega_n + \mu)\,\mathbb{I}_2 - v_F \mathbf{k} \cdot \sigma$$

$$G(i\omega_n, \mathbf{k}) = \frac{(i\omega_n + \mu)\,\mathbb{I}_2 + v_F \mathbf{k} \cdot \sigma}{(i\omega_n + \mu)^2 - v_F^2 \mathbf{k}^2} \quad .$$

3.3.1 The semimetallic regime: $\mu = 0$

The polarizability is just the density-density correlation function, which can be expressed in terms of Green's function as

$$\pi(i\nu, \mathbf{k}) = -\frac{1}{\beta}\sum_m \int \frac{d^2q}{(2\pi)^2}\mathrm{Tr}\Big[G(i\nu + i\omega_m, \mathbf{k}+\mathbf{q})G(i\omega_m, \mathbf{q})\Big] \tag{3.2}$$
$$= -\frac{1}{\beta}\sum_m \int \frac{d^2q}{(2\pi)^2}\mathrm{Tr}\left[\frac{(i\nu + i\omega_m + v_F(\mathbf{k}+\mathbf{q})\cdot\sigma)(i\omega_m + v_F\mathbf{q}\cdot\sigma)}{\big[(i\nu + i\omega_m)^2 - v_F^2(\mathbf{k}+\mathbf{q})^2\big]\big[(i\omega_m)^2 - v_F^2\mathbf{q}^2\big]}\right]$$

We begin by evaluating the trace:

$$\mathrm{Tr}\big[(i\nu + i\omega_m + v_F(\mathbf{k}+\mathbf{q})\cdot\sigma)(i\omega_m + v_F\mathbf{q}\cdot\sigma)\big] = 2\big[i\omega_m(i\nu + i\omega_m) + v_F^2(\mathbf{k}+\mathbf{q})\cdot\mathbf{q}\big]$$

so that we get

$$\pi(i\nu, \mathbf{k}) = -\frac{2}{\beta}\sum_m \int \frac{d^2q}{(2\pi)^2}\left[\frac{-\omega_m(\nu+\omega_m) + v_F^2(\mathbf{k}+\mathbf{q})\cdot\mathbf{q}}{\big[(\nu+\omega_m)^2 + v_F^2(\mathbf{k}+\mathbf{q})^2\big]\big[\omega_m^2 + v_F^2\mathbf{q}^2\big]}\right]$$

Now recall that Matsubara frequencies have $\Delta\omega = 2\pi/\beta$, thus for small temperatures, $\beta \to \infty$, $\Delta\omega \to 0$. Then at $T = 0$ we can replace the sum with an integral, that is

$$\frac{1}{\beta}\sum_m \quad \to \quad \int_{-\infty}^{\infty}\frac{d\omega}{2\pi}$$

where $\omega = \omega_m$. The previous equation becomes

$$\pi(i\nu, \mathbf{k}) = -2\int_{-\infty}^{\infty}\frac{d\omega}{2\pi}\int \frac{d^2q}{(2\pi)^2}\left[\frac{-\omega(\nu+\omega) + v_F^2(\mathbf{k}+\mathbf{q})\cdot\mathbf{q}}{\big[(\nu+\omega)^2 + v_F^2(\mathbf{k}+\mathbf{q})^2\big]\big[\omega^2 + v_F^2\mathbf{q}^2\big]}\right]$$

At this point we make use of the Feynman trick, that is

$$\frac{1}{AB} = \int_0^1 dx\,\frac{1}{[xA + (1-x)B]^2}$$

We choose

$$A = (\nu+\omega)^2 + v_F^2(\mathbf{k}+\mathbf{q})^2 \qquad , \qquad B = \omega^2 + v_F^2\mathbf{q}^2$$

and rewrite the denominator of the integrand function as follows

$$\frac{1}{AB} = \int_0^1 dx\left(\frac{1}{x\big[(\nu+\omega)^2 + v_F^2(\mathbf{k}+\mathbf{q})^2\big] + (1-x)\big[\omega^2 + v_F^2\mathbf{q}^2\big]}\right)^2$$

Let's look at the denominator:

$$x\big[\nu^2 + \omega^2 + 2\nu\omega + v_F^2\mathbf{k}^2 + v_F^2\mathbf{q}^2 + 2v_F^2\mathbf{k}\cdot\mathbf{q}\big] + (1-x)\big[\omega^2 + v_F^2\mathbf{q}^2\big] \quad .$$

Completing the square we get

$$x^2\nu^2 + 2x\nu\omega + \omega^2 + v_F^2(x^2\mathbf{k}^2 + 2x\mathbf{k}\cdot\mathbf{q} + \mathbf{q}^2) - x^2\nu^2 + x\nu^2 - v_F^2x^2\mathbf{k}^2 + v_F^2x\mathbf{k}^2$$
$$(x\nu + \omega)^2 + v_F^2(x\mathbf{k} + \mathbf{q})^2 + x(x-1)(\nu^2 + v_F^2\mathbf{k}^2) \quad .$$

Finally,

$$\pi(i\nu, \mathbf{k}) = -2\int_{-\infty}^{\infty}\frac{d\omega}{2\pi}\int \frac{d^2q}{(2\pi)^2}\int_0^1 dx\,\frac{-\omega(\nu+\omega) + v_F^2(\mathbf{k}+\mathbf{q})\cdot\mathbf{q}}{[(x\nu+\omega)^2 + v_F^2(x\mathbf{k}+\mathbf{q})^2 + x(x-1)(\nu^2 + v_F^2\mathbf{k}^2)]^2} \quad .$$

The usefulness of the Feynman trick comes in at this point. The denominator of the integrand function has become rotationally invariant for the variables ω and $\mathbf{q}$, thus we can perform a shift over the integration domain, that is $\omega \to \omega - x\nu$, $\mathbf{q} \to \mathbf{q} - x\mathbf{k}$ to get

$$\pi(i\nu, \mathbf{k}) = -2\int_{-\infty}^{\infty}\frac{d\omega}{2\pi}\int \frac{d^2q}{(2\pi)^2}\int_0^1 dx\,\frac{-(\omega - x\nu)(\nu + \omega - x\nu) + v_F^2(\mathbf{k}+\mathbf{q}-x\mathbf{k})\cdot(\mathbf{q}-x\mathbf{k})}{[\omega^2 + v_F^2\mathbf{q}^2 + x(1-x)(\nu^2 + v_F^2\mathbf{k}^2)]}$$

Since the integration domains $d\omega$ and d^2q are even, odd terms in the integral can be dropped and the integral can be solved via contour integration. We make use of the following:

$$\int_{-\infty}^{\infty} dx\ \frac{x^2}{(Ax^2+B)^2} = \frac{\pi}{2}\frac{1}{\sqrt{A^3B}}$$
$$\int_{-\infty}^{\infty} dx\ \frac{1}{(Ax^2+B)^2} = \frac{\pi}{2}\frac{1}{\sqrt{AB^3}}$$

Then performing the integration over ω one gets

$$\begin{aligned}\pi(i\nu,\mathbf{k}) &= -\frac{1}{8\pi^2}\int d^2q\int_0^1 dx\left[\frac{-1}{[v_F^2\mathbf{q}^2 - x(x-1)(\nu^2+v_F^2\mathbf{k}^2)]^{1/2}} + \frac{x\nu(\nu-x\nu)+v_F^2\mathbf{q}^2 - v_F^2x\mathbf{k}\cdot(\mathbf{k}-x\mathbf{k})}{[v_F^2\mathbf{q}^2 + x(1-x)(\nu^2+v_F^2\mathbf{k}^2)]^{3/2}}\right]\\ &= -\frac{1}{8\pi^2}\int d^2q\int_0^1 dx\ \frac{2v_F^2\mathbf{k}^2x(x-1)}{[v_F^2\mathbf{q}^2 + x(1-x)(\nu^2+v_F^2\mathbf{k}^2)]^{3/2}}\\ &= \frac{-1}{4\pi}\int_0^1 dx\int_0^\infty 2q\,dq\ \frac{v_F^2\mathbf{k}^2x(x-1)}{[v_F^2\mathbf{q}^2 + x(1-x)(\nu^2+v_F^2\mathbf{k}^2)]^{3/2}}\end{aligned}$$

The integration over momentum can be done analytically and gives

$$\int_0^\infty 2qdq\ \frac{1}{[Aq^2+B]^{3/2}} = \frac{-2}{A}\frac{1}{[Aq^2+B]^{1/2}}\bigg|_0^\infty = \frac{2}{A\sqrt{B}} \quad . \tag{3.3}$$

Then

$$\begin{aligned}\pi(i\nu,\mathbf{k}) &= \frac{-1}{2\pi}\int_0^1 dx\ \frac{\mathbf{k}^2x(x-1)}{[x(1-x)(\nu^2+v_F^2\mathbf{k}^2)]^{1/2}}\\ &= \frac{-\mathbf{k}^2}{2\pi\sqrt{\nu^2+v_F^2\mathbf{k}^2}}\int_0^1 dx\ \frac{x(x-1)}{\sqrt{x(1-x)}}\\ &= \frac{\mathbf{k^2}}{16\sqrt{\nu^2+v_F^2\mathbf{k}^2}}\end{aligned}$$

where the last integral comes from the properties of the Beta function.
In particular,

$$\int_0^1 dx\sqrt{x}\sqrt{1-x} = \frac{\Gamma(\frac{3}{2})\Gamma(\frac{3}{2})}{\Gamma(3)} = \frac{(\sqrt{\pi}/2)^2}{2} = \frac{\pi}{8} \quad .$$

By analytic continuation we find the polarization function to be

$$\pi(\nu_+,\mathbf{k}) = \frac{\mathbf{k}^2}{16\sqrt{-\nu^2+v_F^2\mathbf{k}^2}} \tag{3.4}$$

It becomes imaginary for $\nu > v_F|\mathbf{k}|$. In this region plasmons have a finite lifetime and the system dissipates the incoming radiation. The explanation is that plasmonic excitations are not exact eigenmodes of the system, thus they are overdamped. The physical origin of this damping term lays in the ability of the system to absorbe incoming energy by generating electron-hole pairs.

3.3.2 Graphene at finite doping

We evaluate the polarizability as done before, we set $v_F = 1$

$$\begin{aligned}\pi(i\nu,\mathbf{k}) &= -\frac{1}{\beta}\sum_m\int\frac{d^2q}{(2\pi)^2}\mathrm{Tr}\Big[G(i\nu+i\omega_m,\mathbf{k}+\mathbf{q})G(i\omega_m,\mathbf{q})\Big] \qquad (3.5)\\ &= -\frac{2}{\beta}\sum_m\int\frac{d^2q}{(2\pi)^2}\frac{(i\nu+i\omega_m+\mu)(i\omega_m+\mu)+(\mathbf{k}+\mathbf{q})\cdot\mathbf{q}}{\big[(i\nu+i\omega_m+\mu)^2-(\mathbf{k}+\mathbf{q})^2\big]\big[(i\omega_m+\mu)^2-\mathbf{q}^2\big]}\end{aligned}$$

Performing Matsubara summation one finds the analogue of the Lindhard function for the case of graphene, see Appendix B:

$$\pi(i\nu,\mathbf{k}) = -\int\frac{d^2q}{(2\pi)^2}\sum_{s,s'=\pm}\frac{n_F(s|\mathbf{q}|)-n_F(s'|\mathbf{k}+\mathbf{q}|)}{i\nu+s|\mathbf{q}|-s'|\mathbf{k}+\mathbf{q}|}\frac{1+ss'\cos\Theta}{2}$$

where Θ is the angle between vector $\mathbf{q}$ and $\mathbf{q}+\mathbf{k}$ and we define the form factor $F^{ss'}(\mathbf{k},\mathbf{q}) = \frac{1+ss'\cos\Theta}{2}$. This term comes from the band-overlap of the electron wave functions and constitues the main difference between graphene and a 2DEG. From now on the calculation follows closely [34]; the idea is to perform immediatly the analytic continuation, which furnishes a way to compute the imaginary part of the polarization function. Once this latter is computed, the real part can be reconstructed by means of the Kramers-Kronig relation. As we will see, the calculation itself is not difficult but has to be done very carefully. We here report the main steps while the details of the full calculation are to be found in Appendix B.

ad First of all we introduce an auxiliary function

$$\chi^{\pm}_{\Lambda}(\nu,\mathbf{q}) = \frac{1}{4\pi^2}\int_{|\mathbf{k}|\leq\Lambda} d^2k \sum_{\alpha=\pm} \frac{\alpha F^{\pm}(\mathbf{k},\mathbf{q})}{\nu+\alpha|\mathbf{k}|\mp\alpha|\mathbf{k}+\mathbf{q}|+i\varepsilon} \tag{3.6}$$

with

$$F^{\pm}(\mathbf{k},\mathbf{q}) = \frac{1}{2}\left(1 \pm \frac{\mathbf{k}\cdot(\mathbf{k}+\mathbf{q})}{|\mathbf{k}||\mathbf{k}+\mathbf{q}|}\right) \quad .$$

The $+(-)$ sign defines the inter(intra)-band transitions and Λ is a momentum cut-off. The function just defined comes in very handy when considering transitions at zero-temperature: in this limit the Fermi-Dirac distribution boils down to a step-function and the polarization function can be computed easily if χ is known. To get some confidence with the new concepts we explore two different cases:

- $\underline{\mu = 0}$: from eq. (B.1) we see that the only transitions allowed are those for which $s = -s'$. We can summarize what happens in a table:

s/s'	1	-1
1	no states	allowed
-1	allowed	Pauli blocking

  In short, at zero doping intraband transitions are prohibited: there are no states in the conduction band, since it is empty, and transitions within the valence band cannot take place because of Pauli blocking. The polarization function reads

$$\pi_0(\nu,\mathbf{q}) = \chi^{-}_{\Lambda}(\nu,\mathbf{q})$$

- $\underline{\mu > 0}$: at finite electron doping the situation changes. Now intraband transitions within the conduction band are allowed. The polarization function has an additional term

$$\pi_\mu(\nu,\mathbf{q}) = \pi_0(\nu,\mathbf{q}) + \Delta\pi(\nu,\mathbf{q}) \tag{3.7}$$

$$\Delta\pi(\nu,\mathbf{q}) = -\chi^{-}_{\mu}(\nu,\mathbf{q}) - \chi^{+}_{\mu}(\nu,\mathbf{q})$$

  Notice that the first part serves to regularize the transitions from valence to conduction band.

Now that we got a bit acquainted with these concepts we can start the actual calculation. Since $\pi(-\nu,\mathbf{q}) = [\pi(\nu,\mathbf{q})]^*$ we take the external frequency to be positive. We will start with the $\mu = 0$ case to check the new method with the result obtained in the previous section and then switch on the chemical potential.
We will consider the real and imaginary part separately

Imaginary part

The imaginary part is obtained by analytic continuation taking the limit for $\varepsilon \to 0$ in eq. (3.6)

$$\begin{aligned}\mathrm{Im}[\chi^{\beta}_{\Lambda}] &= -\frac{1}{4\pi}\int_{|\mathbf{k}|\leq\Lambda} d^2k \sum_{\alpha=\pm}\left(\alpha f^{\beta}(\mathbf{k},\mathbf{q})\,\delta(\nu+\alpha|\mathbf{k}|-\alpha\beta|\mathbf{k}+\mathbf{q}|)\right)\\ &= -\frac{1}{4\pi}\int_0^{\Lambda} dk \sum_{\alpha=\pm} I^{\alpha\beta}(\nu,\mathbf{k},\mathbf{q})\end{aligned}$$

Within $I^{\alpha\beta}$ is encoded the plasmon spectrum for all the possible inter(intra)band transitions with at doping. Observe that while for the imaginary part the introduction of an auxiliary function results very natural,

the same do not apply to the real part.
We switch to polar coordinates and perform the integration:

$$I^{\alpha\beta}(\nu,\mathbf{k},\mathbf{q}) = \frac{\alpha k}{2}\int_0^{2\pi} d\theta \left(1+\beta\frac{k+q\cos\theta}{\sqrt{k^2+q^2+2kq\cos\theta}}\right)\delta\big(\nu+\alpha(k-\beta\sqrt{k^2+q^2+2kq\cos\theta})\big) \quad .$$

The integral is non-zero as long as a solution to the delta function exists and lies within the codomain of the cosine function, $[-1,1]$.

$$\nu+\alpha(k-\beta\sqrt{k^2+q^2+2kq\cos\theta})=0 \qquad \longrightarrow \qquad \sqrt{k^2+q^2+2kq\cos\theta}=\beta(\alpha\nu+k)$$

- if $\beta(\alpha\nu+k)>0$,

$$\cos\theta = \frac{\nu^2+2\alpha\nu k-q^2}{2kq}$$

The solutions to the previous always come in pairs, because of the periodicity of the cosine function: we shall multiply the result by a factor 2. We incorporate the above conditions in the final result by means of Heaviside functions, see Appendix B for details.

$$I^{\alpha\beta}(\nu,\mathbf{k},\mathbf{q}) = \alpha\sqrt{\frac{(2\alpha k+\nu)^2-q^2}{q^2-\nu^2}}\times\left\{\theta(\beta)\theta(q-\nu)\theta\left(k-\frac{q-\alpha\nu}{2}\right)+\right. \tag{3.8}$$
$$\left.+\theta(-\alpha)\theta(-\beta)\theta(\nu-q)\left[\theta\left(\frac{q+\nu}{2}-k\right)-\theta\left(\frac{\nu-q}{2}-k\right)\right]\right\}$$

We are now able to compute the imaginary part of the polarization function. We can check the method by computing the result for the case of undoped graphene, for which we already know the result, eq. (3.4).

$$\begin{aligned}
\mathrm{Im}\left[\pi_0(\nu,\mathbf{q})\right] = \mathrm{Im}\left[\chi^-_\Lambda(\nu,\mathbf{q})\right] &= -\frac{1}{4\pi}\int_0^\Lambda dk\sum_{\alpha=\pm} I^{\alpha-}(\nu,\mathbf{k},\mathbf{q}) \\
&= \frac{1}{4\pi}\frac{\theta(\nu-q)}{\sqrt{q^2-\nu^2}}\int_{\frac{\nu-q}{2}}^{\frac{\nu+q}{2}} dk\,\sqrt{(\nu-2k)^2-q^2} \\
&= -\frac{i}{8\pi}\frac{\theta(\nu-q)}{\sqrt{\nu^2-q^2}}\int_{-q}^{q} dk\,\sqrt{k^2-q^2} \\
&= -\frac{i}{8\pi}\frac{\theta(\nu-q)}{\sqrt{\nu^2-q^2}}\left[-\frac{q^2}{2}\log\frac{q}{-q}\right] = \theta(\nu-q)\frac{q^2}{16\sqrt{\nu^2-q^2}}
\end{aligned}$$

which is precisely the result obtained before via contour integration. We then move to the case of doped graphene, that is, $\mu>0$.
The analysis done previously still holds at finite electron doping and we can compute the imaginary part of $\Delta\pi$ by means of the auxiliary function defined above, eq. (3.6).

$$\begin{aligned}
\mathrm{Im}\left[\Delta\pi(\nu,\mathbf{q})\right] &= -\mathrm{Im}\left[\chi^+_\mu(\nu,\mathbf{q})+\chi^-_\mu(\nu,\mathbf{q})\right] \\
&= \frac{1}{4\pi}\int_0^\mu dk\sum_{\alpha=\pm} I^{\alpha+}(\nu,\mathbf{k},\mathbf{q})+I^{\alpha-}(\nu,\mathbf{k},\mathbf{q})
\end{aligned}$$

Before proceding with the momentum integration it is very convenient to introduce an auxiliary function, $g_2(x)$, defined as

$$g_2(x) = x\sqrt{x^2-1}-\log\left(x+\sqrt{x^2-1}\right) \tag{3.9}$$

The subscript indicates the dimensions of the system we are investigating and its introduction will become clearer later on. We shall briefly investigate the behavior of the function just introduced; recall that

$$\cosh^{-1}(x) = \log(x+\sqrt{x^2-1}) \qquad , \qquad x\in[1,\infty)$$

$$\cos^{-1}(x) = -i\log(x+i\sqrt{1-x^2}) \qquad , \qquad x\in[-1,1]$$

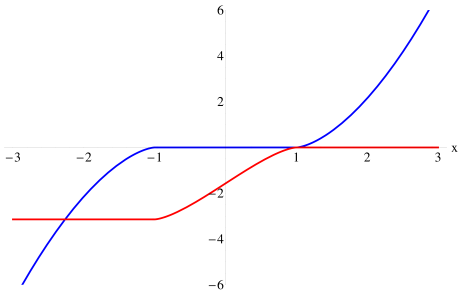

Figure 3.2: *Behavior of the auxiliary function $g_2(x)$, real and imaginary part are represented by blue and red line, respectively.*

then we can rewrite the auxiliary function as

$$g_2(x) = \begin{cases} x\sqrt{x^2-1} - \log\left(x+\sqrt{x^2-1}\right) & x > 1 \\ i\left[x\sqrt{1-x^2} + i\log\left(x+i\sqrt{1-x^2}\right)\right] & |x| < 1 \\ -x\sqrt{x^2-1} - \log\left(-x+\sqrt{x^2-1}\right) - i\pi & x < -1 \end{cases}$$

that can be recast making use of the inverse trigonometric or hyperbolic functions as

$$g_2(x) = \begin{cases} x\sqrt{x^2-1} - \cosh^{-1}(x) & x > 1 \\ i\left[x\sqrt{1-x^2} - \cos^{-1}(x)\right] & |x| < 1 \\ -x\sqrt{x^2-1} - \cosh^{-1}(-x) - i\pi & x < -1 \end{cases} \tag{3.10}$$

For $x > 1$ the function $G(x)$ has only a real part, for $|x| < 1$ it only has an imaginary component, while for $x < 1$ it has both real and imaginary part. The behavior is shown in Fig. 3.2. At this point we are ready to do the momentum integration: we integrate the two terms, $I^{\alpha+}$ and $I^{\alpha-}$, separately,

$$\frac{1}{4\pi}\sum_{\alpha=\pm}\int_0^\mu dk\, I^{\alpha+}(\nu,\mathbf{k},\mathbf{q}) = \frac{\theta(q-\nu)}{16\pi\sqrt{q^2-\nu^2}}q^2\left\{\theta\left(\frac{2\mu+\nu}{q}-1\right)g_2\left(\frac{2\mu+\nu}{q}\right) - \theta\left(\frac{2\mu-\nu}{q}-1\right)g_2\left(\frac{2\mu-\nu}{q}\right)\right\}$$

$$\begin{aligned}\frac{1}{4\pi}\sum_{\alpha=\pm}\int_0^\mu dk\, I^{\alpha-}(\nu,\mathbf{k},\mathbf{q}) = -\frac{\theta(\nu-q)}{16\pi\sqrt{q^2-\nu^2}}q^2\Bigg\{&i\pi\theta\left(\frac{2\mu-\nu}{q}+1\right)+ \\ &+\left[\theta\left(1-\frac{2\mu-\nu}{q}\right)-\theta\left(-1-\frac{2\mu-\nu}{q}\right)\right]g_2\left(\frac{2\mu-\nu}{q}\right)\Bigg\}\end{aligned}$$

Summing up the two results we get the imaginary part of $\Delta\pi$,

$$\begin{aligned}\mathrm{Im}\left[\Delta\pi(\nu,\mathbf{q})\right] = f(\nu,\mathbf{q})\Bigg\{&\theta(q-\nu)\left[\theta\left(\frac{2\mu+\nu}{q}-1\right)g_2\left(\frac{2\mu+\nu}{q}\right) - \theta\left(\frac{2\mu-\nu}{q}-1\right)g_2\left(\frac{2\mu-\nu}{q}\right)\right]+ \\ &+i\theta(\nu-q)\left[i\pi\theta\left(\frac{2\mu-\nu}{q}+1\right)+\left[\theta\left(1-\frac{2\mu-\nu}{q}\right)-\theta\left(-1-\frac{2\mu-\nu}{q}\right)\right]g_2\left(\frac{2\mu-\nu}{q}\right)\right]\Bigg\}\end{aligned} \tag{3.11}$$

where we introduced

$$f(\nu,q) = \frac{1}{16\pi}\frac{q^2}{\sqrt{|\nu^2-q^2|}}$$

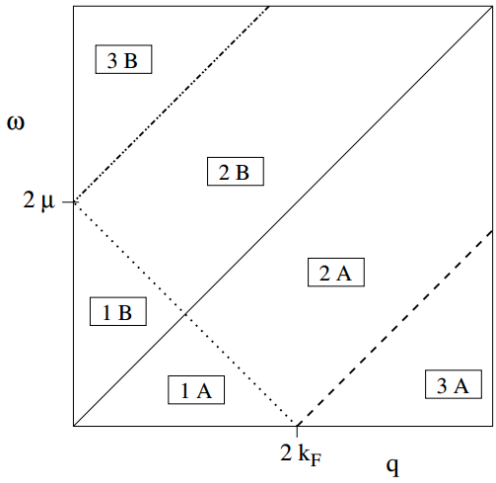

Figure 3.3: *Different regions delimited by the Heaviside functions appearing in the calculation. In our units, $k_f = \mu$, $\omega = \nu$. Taken from [34].*

To better visualize this last result it is convenient to introduce a table showing the different regions delimited by the Heaviside functions, Fig. 3.3. In particular we have that

$$\begin{aligned} 1A + 1B &\rightarrow \theta\left(\frac{2\mu-\nu}{q} - 1\right) \\ 3A &\rightarrow \theta\left(1 - \frac{2\mu+\nu}{q}\right) \\ 3B &\rightarrow \theta\left(-1 - \frac{2\mu-\nu}{q}\right) \end{aligned}$$

This are the Heaviside functions we need to express our result, eq. (3.11), in terms of the regions shown in the Fig. 3.3.

$$\mathrm{Im}\left[\Delta\pi(\nu,\mathbf{q})\right] = f(\nu,\mathbf{q}) \times \begin{cases} g_2\left(\frac{2\mu+\nu}{q}\right) - g_2\left(\frac{2\mu-\nu}{q}\right) & 1A \\ -\pi & 1B \\ g_2\left(\frac{2\mu+\nu}{q}\right) & 2A \\ ig_2\left(\frac{\nu-2\mu}{q}\right) & 2B \\ 0 & 3A \\ 0 & 3B \end{cases}$$

where in the sector $2B$ we used that $i\pi + g_2(x) = -g_2(x)$ for $|x| < 1$.

Real part

In principle one can compute the real part of the polarization function once the imaginary one is known, by means of the Kramers-Kronig relation. However we here follow a slightly different procedure. All we have to compute is $\Delta\pi$: we will make use a result[2] that allows us to compute the real part without making use of the Kramers-Kronig relations (it also allows us to compute the imaginary part, but we the result is the same as the one aready obtained)

$$\lim_{\varepsilon\to 0}\int_0^{2\pi} \frac{d\phi}{a + b\cos\phi \pm i\varepsilon} = \frac{2\pi}{\sqrt{|a^2-b^2|}}\left[\theta(a^2-b^2)\mathrm{sgn}(a) \mp i\theta(b^2-a^2)\right] \tag{3.12}$$

[2] see for instance [26]

We start by rearranging the expression for $\Delta\pi$:

$$\begin{aligned}
\Delta\pi(\nu,\mathbf{q}) &= -\chi_\mu^-(\nu,\mathbf{q}) - \chi_\mu^+(\nu,\mathbf{q}) \\
&= -\frac{1}{4\pi^2}\int_{|\mathbf{k}|<\mu} d^2k \sum_{\alpha,\beta=\pm}\left\{\frac{\alpha f^+(\mathbf{k},\mathbf{q})}{\nu+\alpha|\mathbf{k}|-\alpha|\mathbf{k}+\mathbf{q}|+i\varepsilon} + \frac{\beta f^-(\mathbf{k},\mathbf{q})}{\nu+\beta|\mathbf{k}|+\beta|\mathbf{k}+\mathbf{q}|+i\varepsilon}\right\} \\
&= -\frac{1}{8\pi^2}\int_{|\mathbf{k}|<\mu} d^2k\ (1+\cos\Theta)\left[\frac{1}{\nu+|\mathbf{k}|-|\mathbf{k}+\mathbf{q}|+i\varepsilon} - \frac{1}{\nu-|\mathbf{k}|+|\mathbf{k}+\mathbf{q}|+i\varepsilon}\right] + \\
&\qquad + (1-\cos\Theta)\left[\frac{1}{\nu+|\mathbf{k}|+|\mathbf{k}+\mathbf{q}|+i\varepsilon} - \frac{1}{\nu-|\mathbf{k}|-|\mathbf{k}+\mathbf{q}|+i\varepsilon}\right] \\
&= -\frac{1}{4\pi^2}\int_{|\mathbf{k}|<\mu} d^2k\ \left[\frac{\nu+|\mathbf{k}|+|\mathbf{k}+\mathbf{q}|\cos\Theta}{(\nu+|\mathbf{k}|+i\varepsilon)^2-|\mathbf{k}+\mathbf{q}|^2} - \frac{\nu-|\mathbf{k}|-|\mathbf{k}+\mathbf{q}|\cos\Theta}{(\nu-|\mathbf{k}|+i\varepsilon)^2-|\mathbf{k}+\mathbf{q}|^2}\right] \\
&= -\frac{1}{4\pi^2}\int_{|\mathbf{k}|<\mu} d^2k \sum_{\alpha=\pm}\frac{\alpha\nu+|\mathbf{k}|+|\mathbf{k}+\mathbf{q}|\cos\Theta}{(\nu+\alpha|\mathbf{k}|+i\varepsilon)^2-|\mathbf{k}+\mathbf{q}|^2}
\end{aligned} \tag{3.13}$$

We introduce an auxiliary function J^α in analogy with the previous case

$$\mathrm{Re}\left[\Delta\pi(\nu,\mathbf{q})\right] = -\frac{1}{4\pi^2}\int_0^\mu dk \sum_{\alpha=\pm} J^\alpha(\nu,\mathbf{k},\mathbf{q}) \tag{3.14}$$

As done before, we switch to polar coordinates and perform the integration over the angle variable; we start by working out the RHS of eq. (3.13)

$$\begin{aligned}
\int_0^{2\pi} d\theta\, k\frac{\alpha\nu+2k+q\cos\theta}{(\nu+\alpha k+i\varepsilon)^2-k^2-q^2-2kq\cos\theta} &= \int_0^{2\pi} d\theta\, k\frac{\alpha\nu+2k+q\cos\theta}{(\nu^2+2\alpha\nu k-q^2)+i\varepsilon(\nu+\alpha k)-2kq\cos\theta} \\
&= \int_0^{2\pi} d\theta\, k\frac{q}{-2kq}\frac{\frac{\alpha\nu+2k}{q}+\cos\theta}{\frac{\nu^2+2\alpha\nu k-q^2+i\varepsilon(\nu+\alpha k)}{-2kq}+\cos\theta} \\
&= -\frac{1}{2}\int_0^{2\pi} d\theta\ \frac{\frac{\alpha\nu+2k}{q}+\cos\theta}{z+\cos\theta} \\
&= -\frac{1}{2}\int_0^{2\pi} d\theta\ \left(1+\frac{\frac{\alpha\nu+2k}{q}-z}{z+\cos\theta}\right) \\
&= -\pi - \frac{1}{2}\left(\frac{(2\alpha k+\nu)^2-q^2}{2kq}\right)\int_0^{2\pi} d\theta\ \frac{1}{z+\cos\theta}
\end{aligned}$$

where we introduced $z = \frac{\nu^2+2\alpha\nu k-q^2+i\varepsilon(\nu+\alpha k)}{-2kq}$. We now use the result given in eq. (3.12) to extract the real part

$$\begin{aligned}
J^\alpha(\nu,\mathbf{k},\mathbf{q}) = -\pi + \pi\sqrt{\frac{(2\alpha k+\nu)^2-q^2}{\nu^2-q^2}}\Bigg\{&\theta(q-\nu)\theta\left(\frac{q-\alpha\nu}{2}-k\right) + \\
&+\theta(\nu-q)\left[\theta(\alpha)+\theta(-\alpha)\left(\theta\left(\frac{\nu-q}{2}-k\right)-\theta\left(k-\frac{\nu+q}{2}\right)\right)\right]\Bigg\}
\end{aligned} \tag{3.15}$$

This constitues an operative expression to compute the real part of the polarization function for doped graphene: in fact, the latter is obtained by inserting eq. (3.15) in eq. (3.14). After the momentum integration we find

$$\begin{aligned}
-\frac{1}{4\pi^2}\int_0^\mu dk\ J^+(\nu,\mathbf{k},\mathbf{q}) = \frac{\mu}{4\pi} - \frac{\theta(q-\nu)}{16\pi\sqrt{\nu^2-q^2}}q^2\left\{\theta\left(1-\frac{2\mu+\nu}{q}\right)g_2\left(\frac{2\mu+\nu}{q}\right)-g_2\left(\frac{\nu}{q}\right)\right\} - \\
-\frac{\theta(\nu-q)}{16\pi\sqrt{\nu^2-q^2}}q^2\left\{g_2\left(\frac{2\mu+\nu}{q}\right)-g_2\left(\frac{\nu}{q}\right)\right\}
\end{aligned}$$

$$-\frac{1}{4\pi^2}\int_0^\mu dk\, J^-(\nu,\mathbf{k},\mathbf{q}) = \frac{\mu}{4\pi} - \frac{\theta(q-\nu)}{16\pi\sqrt{\nu^2-q^2}}q^2\left\{\theta\left(1-\frac{2\mu-\nu}{q}\right)g_2\left(\frac{2\mu-\nu}{q}\right) - g_2\left(-\frac{\nu}{q}\right)\right\} -$$
$$- \frac{\theta(\nu-q)}{16\pi\sqrt{\nu^2-q^2}}q^2\left\{\theta\left(-1-\frac{2\mu-\nu}{q}\right)g_2\left(\frac{2\mu-\nu}{q}\right) - i\pi\theta\left(1+\frac{2\mu-\nu}{q}\right) - g_2\left(-\frac{\nu}{q}\right)\right\} +$$
$$+ \frac{\theta(\nu-q)}{16\pi\sqrt{\nu^2-q^2}}q^2\theta\left(\frac{2\mu-\nu}{q}+1\right)g_2\left(\frac{2\mu-\nu}{q}\right)$$

where we made use of the auxiliary function $G(x)$ defined in eq. (3.9). Pulling the two results together and using that $G(x)+G(-x) = -i\pi$, we find for eq. (3.14),

$$\begin{aligned}\mathrm{Re}\left[\Delta\pi(\nu,\mathbf{q})\right] &= -\frac{1}{4\pi^2}\int_0^\mu dk\, \sum_{\alpha=\pm} J^\alpha(\nu,\mathbf{k},\mathbf{q}) \\ &= \frac{\mu}{2\pi} - f(\nu,\mathbf{q})\left\{-i\theta(q-\nu)\left[i\pi + \theta\left(1-\frac{2\mu+\nu}{q}\right)g_2\left(\frac{2\mu+\nu}{q}\right) + \theta\left(1-\frac{2\mu-\nu}{q}\right)g_2\left(\frac{2\mu-\nu}{q}\right)\right] + \right. \\ &\left. +\theta(\nu-q)\left[g_2\left(\frac{2\mu+\nu}{q}\right) + \theta\left(-\frac{2\mu-\nu}{q}-1\right)\left[i\pi + g_2\left(\frac{2\mu-\nu}{q}\right)\right] - \theta\left(\frac{2\mu-\nu}{q}-1\right)g_2\left(\frac{2\mu-\nu}{q}\right)\right]\right\}\end{aligned} \tag{3.16}$$

we can rewrite the result in a more compact form by using the table showed in Fig. 3.3,

$$\mathrm{Re}\left[\Delta\pi(\nu,\mathbf{q})\right] = \frac{\mu}{2\pi} - f(\nu,\mathbf{q}) \times \begin{cases} \pi & 1A \\ g_2\left(\frac{2\mu+\nu}{q}\right) - g_2\left(\frac{2\mu-\nu}{q}\right) & 1B \\ -ig_2\left(\frac{\nu-2\mu}{q}\right) & 2A \\ g_2\left(\frac{2\mu+\nu}{q}\right) & 2B \\ ig_2\left(\frac{2\mu+\nu}{q}\right) - ig_2\left(\frac{\nu-2\mu}{q}\right) & 3A \\ g_2\left(\frac{2\mu+\nu}{q}\right) - g_2\left(\frac{\nu-2\mu}{q}\right) & 3B \end{cases}$$

Summing up real and imaginary parts one find the final result for $\Delta\pi$[3],

$$\begin{aligned}\Delta\pi(\nu,\mathbf{q}) =& \frac{\mu}{2\pi} - f(\nu,\mathbf{q})\left\{g_2\left(\frac{2\mu+\nu}{q}\right) - \theta\left(\frac{2\mu-\nu}{q}-1\right)\left[g_2\left(\frac{2\mu-\nu}{q}\right) - i\pi\right] - \right. \\ &\left. -\theta\left(\frac{\nu-2\mu}{q}+1\right)g_2\left(\frac{\nu-2\mu}{q}\right)\right\}\end{aligned} \tag{3.17}$$

and the full polarization function is obtained by summing up the doped and undoped results, as in eq. (3.7). The result is well established as of now and has been derived by many authors, [3, 4, 15, 34].

3.4 The 3D case: Weyl semimetals

We now move on to the calculation we are interested in, that is the one for WSM of type I. We compute the polarization function in the case of undoped WSM of type I and then we do the calculation for untilted WSM with finite doping. As we shall later see, the calculation for WSM with tilted cone is much more involved than the untilted case: in some special case it is possible to reduce the former to the latter one, but not for finite chemical potential. The most general Hamiltonian describing our system is

$$\mathcal{H}(\mathbf{k},\mathbf{d}) = v_f\left(\mathbf{k}\cdot\sigma + w\mathbf{d}\cdot\mathbf{k}\,\mathbb{I}_2\right) - \mu\,\mathbb{I}_2 \qquad , \qquad \mathbf{k} = (k_x,k_y,k_z) \quad , \quad w<1$$

which gives the eigenvalues

$$E_\pm = v_F\left(w\mathbf{d}\cdot\mathbf{k} \pm |\mathbf{k}|\right) - \mu$$

in the following we shall, as usual, set $v_F = 1$. The Green's function of the system is obtained from its inverse,

$$G^{-1}(i\omega,\mathbf{k},\mathbf{d}) = i\omega\,\mathbb{I}_2 - \mathcal{H}(\mathbf{k},\mathbf{d}) = (i\omega - \mu - w\mathbf{d}\cdot\mathbf{k})\,\mathbb{I}_2 - \sigma\cdot\mathbf{k}$$
$$G(i\omega,\mathbf{k},\mathbf{d}) = \frac{(i\omega-\mu-w\mathbf{d}\cdot\mathbf{k})\,\mathbb{I}_2 + \sigma\cdot\mathbf{k}}{(i\omega-\mu-w\mathbf{d}\cdot\mathbf{k})^2 - \mathbf{k}^2} \quad .$$

It should be clear by now the matrix structure of the Hamiltonian and of the Green's function derived from it, therefore explicit coupling to the identity matrices will be sometimes omitted.

[3] this result, eq. (3.17), was not obtained in the present work, but it was checked numerically that it matches with the results obtained so far.

3.4.1 The semimetallic untilted system: $\mu = 0$, $w = 0$

The calculation of the polarization function follows up closely what seen before in the graphene case. The only difference is that we now work in $d = 3$ dimensions, therefore we might expect the result to be different, for instance how it scales with momentum.

$$\begin{aligned}\pi(i\nu,\mathbf{q}) &= -\frac{1}{\beta}\sum_m \int \frac{d^3k}{(2\pi)^3}\,\mathrm{Tr}\left[G(i\nu+i\omega_m,\mathbf{k}+\mathbf{q})G(i\omega_m,\mathbf{k})\right]\\ &= -\frac{2}{\beta}\sum_m \int \frac{d^3k}{(2\pi)^3}\,\frac{i\omega_m(i\omega_m+i\nu)+\mathbf{k}\cdot(\mathbf{k}+\mathbf{q}))}{\left[(i\omega_m+i\nu)^2-|\mathbf{k}+\mathbf{q}|^2\right]\left[(i\omega_m)^2-|\mathbf{k}|^2\right]}\end{aligned}$$

in the zero-temperature limit we can turn the sum over Matsubara frequencies into an integral, and we also make use of the Feynman trick in order to make the denominator rotational invariant,

$$\frac{1}{\beta}\sum_m \;\to\; \int \frac{d\omega}{2\pi} \quad , \qquad \frac{1}{AB} = \int_0^1 dx\,\frac{1}{[xA+(1-x)B]^2}$$

$$\begin{aligned}\pi(i\nu,\mathbf{q}) &= -\int_{-\infty}^{\infty}\frac{d\omega}{\pi}\int_0^1 dx\int \frac{d^3k}{(2\pi)^3}\,\frac{-\omega(\omega+\nu)+\mathbf{k}\cdot(\mathbf{k}+\mathbf{q}))}{\left[x(\omega+\nu)^2+x|\mathbf{k}+\mathbf{q}|^2+(1-x)(\omega^2+|\mathbf{k}|^2)\right]^2}\\ &= -\int_{-\infty}^{\infty}\frac{d\omega}{\pi}\int_0^1 dx\int \frac{d^3k}{(2\pi)^3}\,\frac{-\omega(\omega+\nu)+\mathbf{k}\cdot(\mathbf{k}+\mathbf{q}))}{\left[(\omega+x\nu)^2+(\mathbf{k}+x\mathbf{q})^2+x(1-x)(\nu^2+\mathbf{q}^2)\right]^2}\end{aligned}$$

in the last step we rearranged the denominator such that it can be simplified via the change of variables $\omega \to \omega + x\nu$ and $\mathbf{k} \to \mathbf{k} + x\mathbf{q}$

$$\begin{aligned}&= -\int_{-\infty}^{\infty}\frac{d\omega}{\pi}\int_0^1 dx\int \frac{d^3k}{(2\pi)^3}\,\frac{-(\omega-x\nu)(\omega+\nu-x\nu)+(\mathbf{k}-x\mathbf{q})\cdot(\mathbf{k}+\mathbf{q}-x\mathbf{q}))}{\left[\omega^2+\mathbf{k}^2+x(1-x)(\nu^2+\mathbf{q}^2)\right]^2}\\ &= -\int_{-\infty}^{\infty}\frac{d\omega}{\pi}\int_0^1 dx\int \frac{d^3k}{(2\pi)^3}\,\frac{-\omega^2+\mathbf{k}^2+x(1-x)(\nu^2-\mathbf{q}^2)}{\left[\omega^2+\mathbf{k}^2+x(1-x)(\nu^2+\mathbf{q}^2)\right]^2}\\ &= -\int_{-\infty}^{\infty}\frac{d\omega}{\pi}\int_0^1 dx\int_0^{\Lambda} \frac{dk}{(2\pi)^3}\,4\pi k^2\,\frac{-\omega^2+k^2+x(1-x)(\nu^2-q^2)}{\left[\omega^2+k^2+x(1-x)(\nu^2+q^2)\right]^2}\\ &= \frac{1}{2\pi^2}\int_0^1 dx\int_0^{\Lambda} dk\,\frac{x(1-x)q^2k^2}{\left[k^2+x(1-x)(\nu^2+q^2)\right]^{3/2}}\\ &= \frac{q^2}{24\pi^2}\left\{\log\left(1+\frac{4\Lambda^2}{Q^2}\right)+\frac{8\Lambda^3}{Q^3}\arctan\left(\frac{Q}{2\Lambda}\right)-\frac{4\Lambda^2}{Q^2}\right\}\end{aligned}$$

where $Q^2 = \nu^2 + q^2$. Notice that because of the divergence of the integral we had to introduce a momentum cut-off Λ. Let's see what is the order of the divergence by looking at how it scales at high momenta, $\Lambda \gg 1$:

$$\begin{aligned}\pi(i\nu,\mathbf{q}) &= \frac{q^2}{24\pi^2}\left\{\log\left(\frac{4\Lambda^2}{Q^2}\right)+\log\left(1+\frac{Q^2}{4\Lambda^2}\right)+\frac{8\Lambda^3}{Q^3}\arctan\left(\frac{Q}{2\Lambda}\right)-\frac{4\Lambda^2}{Q^2}\right\}\\ &\overset{\Lambda\gg 1}{\sim} \frac{q^2}{24\pi^2}\left\{\log\left(\frac{4\Lambda^2}{Q^2}\right)+\left(\frac{Q^2}{4\Lambda^2}\right)+\ldots+\frac{8\Lambda^3}{Q^3}\left(\left(\frac{Q}{2\Lambda}\right)-\frac{1}{3}\left(\frac{Q}{2\Lambda}\right)^3+\frac{1}{5}\left(\frac{Q}{2\Lambda}\right)^5+\ldots\right)-\frac{4\Lambda^2}{Q^2}\right\}\\ &= \frac{q^2}{24\pi^2}\left\{\log\left(\frac{4\Lambda^2}{Q^2}\right)+\frac{1}{3}+\frac{Q^2}{3\Lambda^2}+\mathcal{O}\left(\left(\frac{Q}{\Lambda}\right)^3\right)\right\}\end{aligned}$$

from which we see that the polarization function diverges logarithmically with the cut-off Λ.
As for the 2D case, we are interested in the plasmonic spectrum of our system, that is the region in which the imaginary part of the polarization function is non-zero. In order to investigate the region, we first extend analytically our result into the domain of real frequencies, $i\nu \to \nu + i\delta$:

$$\pi(\nu,\mathbf{q}) = \frac{q^2}{24\pi^2}\left\{\log\left(1+\frac{4\Lambda^2}{q^2-\nu^2}\right)+\frac{8\Lambda^3}{(q^2-\nu^2)^{3/2}}\arctan\left(\frac{\sqrt{q^2-\nu^2}}{2\Lambda}\right)-\frac{4\Lambda^2}{q^2-\nu^2}\right\} \tag{3.18}$$

we introduce two auxiliary functions, $\pi^+(\nu,\mathbf{q})$ and $\pi^-(\nu,\mathbf{q})$ such that

$$\pi(\nu,\mathbf{q}) = \theta(q-\nu)\pi^+(\nu,\mathbf{q}) + \theta(\nu-q)\pi^-(\nu,\mathbf{q}) \quad .$$

It is easy to see that π^+ is always real so that the imaginary component of the polarization function comes from π^-:

$$\pi^-(\nu,\mathbf{q}) = \frac{q^2}{24\pi^2}\left\{\log\left(1-\frac{4\Lambda^2}{\nu^2-q^2}\right) + \frac{8i\Lambda^3}{(\nu^2-q^2)^{3/2}}\arctan\left(\frac{i\sqrt{\nu^2-q^2}}{2\Lambda}\right) + \frac{4\Lambda^2}{\nu^2-q^2}\right\} \quad .$$

If we take $\Lambda \gg \nu, q$ we see that the logarithm always carries an imaginary part, since its argument is negative. A deeper analysis shows that it actually carries all the imaginary part:

$$\pi^-(\nu,\mathbf{q}) = \frac{q^2}{24\pi^2}\left\{\log\left|1-\frac{4\Lambda^2}{\nu^2-q^2}\right| + i\pi - \frac{4\Lambda^3}{(\nu^2-q^2)^{3/2}}\log\left(\frac{2\Lambda+\sqrt{\nu^2-q^2}}{2\Lambda-\sqrt{\nu^2-q^2}}\right) + \frac{4\Lambda^2}{\nu^2-q^2}\right\}$$

where we used the logarithm representation of the inverse tangent. We thus see that plasmonic excitations are overdamped in the region for which $\nu > q$ and, in particular,

$$\mathrm{Im}\left[\pi(\nu,\mathbf{q})\right] = \theta(\nu-q)\frac{q^2}{24\pi} \quad . \tag{3.19}$$

3.4.2 Weyl semimetals at finite doping

We here analyse the expression for the polarization function when our system presents an electron doping, $\mu > 0$: we will see that the result is a generalization to 3D of the calculation for graphene. We start from eq. (3.30), where we set $v_F = 1$ and $w = 0$:

$$\pi(i\nu,\mathbf{q}) = -\frac{1}{8\pi^3}\int d^3k \sum_{s,s'=\pm}\frac{n_F(s|\mathbf{k}|) - n_F(s'|\mathbf{k}+\mathbf{q}|)}{i\nu + s|\mathbf{k}| - s'|\mathbf{k}+\mathbf{q}|}\,\frac{1+ss'\cos\Theta}{2} \quad .$$

The exactly same analysis in terms of inter(intra)band transitions that was made earlier for the graphene case applies here, therefore we shall jump directly to the calculation skipping some details. We introduce the auxiliary function

$$\chi^{\pm}_{\Lambda}(\nu,\mathbf{q}) = \frac{1}{8\pi^3}\int_{|\mathbf{k}|\le\Lambda} d^3k \sum_{\alpha=\pm}\frac{\alpha f^{\pm}(\mathbf{k},\mathbf{q})}{\nu + \alpha|\mathbf{k}| \mp \alpha|\mathbf{k}+\mathbf{q}| + i\varepsilon} \tag{3.20}$$

with

$$f^{\pm}(\mathbf{k},\mathbf{q}) = \frac{1}{2}\left(1 \pm \frac{\mathbf{k}\cdot(\mathbf{k}+\mathbf{q})}{|\mathbf{k}||\mathbf{k}+\mathbf{q}|}\right)$$

As before, we can express the full polarization function by means of the auxiliary function χ just introduced:

- $\underline{\mu = 0}$:
$$\pi_0(\nu,\mathbf{q}) = \chi^-_{\Lambda}(\nu,\mathbf{q})$$
- $\underline{\mu > 0}$:
$$\pi_\mu(\nu,\mathbf{q}) = \pi_0(\nu,\mathbf{q}) + \Delta\pi(\nu,\mathbf{q})$$
$$\Delta\pi(\nu,\mathbf{q}) = -\chi^-_{\mu}(\nu,\mathbf{q}) - \chi^+_{\mu}(\nu,\mathbf{q})$$

In the same way we carried on the calculations for graphene case, we split between real and imaginary part of the polarization function. As seen before there are very different ways to compute the two of them. We shall employ the same used earlier, which turn out to be the most convenient.

Imaginary part:

The imaginary part is obtained by analytic continuation taking the limit $\varepsilon \to 0$ in eq. (3.20):

$$\begin{aligned}\mathrm{Im}[\chi^{\beta}_{\Lambda}] &= -\frac{1}{8\pi^2}\int_{|\mathbf{k}|\le\Lambda} d^3k \sum_{\alpha=\pm}\left(\alpha f^{\beta}(\mathbf{k},\mathbf{q})\,\delta(\nu+\alpha|\mathbf{k}| - \alpha\beta|\mathbf{k}+\mathbf{q}|)\right) \\ &= -\frac{1}{8\pi^2}\int_0^{\Lambda} dk \sum_{\alpha=\pm}\alpha I^{\alpha\beta}(\nu,\mathbf{k},\mathbf{q})\end{aligned} \tag{3.21}$$

Where we introduce $I^{\alpha\beta}$ which encodes the plasmon spectrum for all the possible inter(intra)band transitions at varying doping.
We switch to spherical coordinates and perform the integration:

$$I^{\alpha\beta}(\mathbf{k},\mathbf{q}) = \int_0^{2\pi} d\phi \int_0^{\pi} d\theta \, \frac{k^2 \sin\theta}{2} \left(1 + \beta \frac{k + q\cos\theta}{\sqrt{k^2+q^2+2kq\cos\theta}}\right) \delta\big(\nu + \alpha(k - \beta\sqrt{k^2+q^2+2kq\cos\theta})\big)$$

The integral is non-zero as long as a solution to the Dirac delta exists and lies within the codomain of the cosine function, $[-1,1]$. The difference with the previous, 2D case is that the solution, if exists, is unique (while in the 2D case one picks up a factor 2 from the integration). We here summarize the result that was found earlier,

$$\nu + \alpha(k - \beta\sqrt{k^2+q^2+2kq\cos\theta}) = 0 \qquad \rightarrow \qquad \sqrt{k^2+q^2+2kq\cos\theta} = \beta(\alpha\nu + k)$$

- if $\beta(\alpha\nu + k) > 0$,

$$\cos\theta = \frac{\nu^2 + 2\alpha\nu k - q^2}{2kq}$$

$$\begin{aligned}
I^{\alpha\beta}(\mathbf{k},\mathbf{q}) &= 2\pi k^2 \int_{-1}^{1} d(\cos\theta) \, \frac{1}{2}\left(1 + \beta\frac{k+q\cos\theta}{\sqrt{k^2+q^2+2kq\cos\theta}}\right) \frac{-(\alpha\nu+k)}{\alpha kq} \, \delta\left(\cos\theta - \frac{\nu^2+2\alpha\nu k - q^2}{2kq}\right) \\
&= -\pi k^2 \left(1 + \frac{2k^2+\nu^2+2\alpha\nu k - q^2}{2k(\alpha\nu+k)}\right) \left|\frac{\alpha\nu+k}{-\alpha kq}\right| \\
&= -\pi k^2 \frac{(2\alpha k+\nu)^2 - q^2}{2k(\alpha\nu+k)} \, \frac{\alpha\nu+k}{\alpha kq} \\
&= -\frac{\pi}{2} \frac{(2\alpha k+\nu)^2 - q^2}{\alpha q}
\end{aligned}$$

the full result after the angle integration reads

$$\begin{aligned}
I^{\alpha\beta}(\mathbf{k},\mathbf{q}) &= -\frac{\pi}{2} \frac{(2\alpha k+\nu)^2 - q^2}{\alpha q} \times \theta(\beta(\alpha\nu+k))\theta\left(1 - \left(\frac{\nu^2+2\alpha\nu k - q^2}{2kq}\right)^2\right) \qquad (3.22) \\
&= -\frac{\pi}{2} \frac{(2\alpha k+\nu)^2 - q^2}{\alpha q} \times \Big\{\theta(\beta)\theta(q-\nu)\theta\left(k - \frac{q-\alpha\nu}{2}\right) + \\
&\qquad + \theta(-\alpha)\theta(-\beta)\theta(\nu-q)\left[\theta\left(\frac{q+\nu}{2} - k\right) - \theta\left(\frac{\nu-q}{2} - k\right)\right]\Big\}
\end{aligned}$$

where we made use of a result already obtained for the case of graphene. In order to check our derivation, we compute the plasmon spectrum for the case of zero chemical potential and compare it with the result obtained in the previous section.

$$\begin{aligned}
\mathrm{Im}[\pi_0(\nu,\mathbf{q})] &= -\frac{1}{8\pi^2} \int_0^{\Lambda} dk \sum_{\alpha=\pm} \alpha I^{\alpha-}(\nu,\mathbf{k},\mathbf{q}) \\
&= \frac{1}{16\pi} \int_0^{\Lambda} dk \sum_{\alpha=\pm} \frac{(2\alpha k+\nu)^2 - q^2}{q} \theta(-\alpha)\theta(\nu-q)\left[\theta\left(\frac{q+\nu}{2} - k\right) - \theta\left(\frac{\nu-q}{2} - k\right)\right] \\
&= \frac{\theta(\nu-q)}{16\pi} \int_{\frac{\nu-q}{2}}^{\frac{\nu+q}{2}} dk \, \frac{(\nu-2k)^2 - q^2}{q} \\
&= -\theta(\nu-q) \, \frac{q^2}{24\pi}
\end{aligned}$$

which is consistend with eq. (3.19).
We are not going to compute the real part of the polarization function since it was already computed

previously and the imaginary parts coincides. The real part can ten be obtained through the Kramers-Kronig relations and has to give the same result.
We turn to the case of WSM at finite electron doping; the calculation follows up closely the one for the 2D case and we here summarize the main steps, without going into detailed calculations. As we shall see in a short while, evaluating the polarization function for Dirac materials at finite doping turns out to be simpler in 3D than in 2D, the reason lying in the Jacobian of the coordinate transformation. As one can already notice, eq. (3.22) is a polynomial in the variable k we are going to integrate.

$$\begin{aligned}\mathrm{Im}[\Delta\pi(\nu,\mathbf{q})] &= -\mathrm{Im}[\chi_\mu^+(\nu,\mathbf{q})+\chi_\mu^-(\nu,\mathbf{q})]\\ &= \frac{1}{8\pi^2}\int_0^\mu dk\,\sum_{\alpha=\pm}\alpha[I^{\alpha+}(\nu,\mathbf{q})+I^{\alpha-}(\nu,\mathbf{q})]\end{aligned}$$

Before writing down the full result we introduce an auxiliary function as we saw for the case of graphene. We will call the function $g_3(x)$, defined as

$$g_3(x) = x\left(\frac{x^2}{3}-1\right)+\frac{2}{3} \tag{3.23}$$

Notice that the auxiliary function is much simpler in the 3D case, it is always real and does not have annoying features as for instance branch cuts in the complex plane, contrary to the analogous 2D case. We evaluate the contribution of the two terms, I^{α^+} and I^{α^-}:

$$\frac{1}{8\pi^2}\int_0^\mu dk\, I^{\alpha+}(\nu,\mathbf{q}) = -\sum_{\alpha=\pm}\frac{q^2}{32\pi}\theta(q-\nu)\theta\left(\frac{2\mu+\alpha\nu}{q}-1\right)g_3\left(\frac{2\mu+\alpha\nu}{q}\right)$$

$$\begin{aligned}\frac{1}{8\pi^2}\int_0^\mu dk\,\sum_{\alpha=\pm} I^{\alpha-}(\nu,\mathbf{k},\mathbf{q}) = -\frac{q^2}{32\pi}\theta(\nu-q)\Bigg\{&\theta\left(1-\frac{2\mu-\nu}{q}\right)g_3\left(\frac{2\mu-\nu}{q}\right)\\ &-\theta\left(-1-\frac{2\mu-\nu}{q}\right)g_3\left(\frac{2\mu-\nu}{q}\right)-\frac{4}{3}\theta\left(\frac{2\mu-\nu}{q}+1\right)\Bigg\}\end{aligned}$$

$$\begin{aligned}\mathrm{Im}[\Delta\pi(\nu,\mathbf{q})] = -\frac{q^2}{32\pi}\Bigg\{&\theta(q-\nu)\left[\theta\left(\frac{2\mu+\nu}{q}-1\right)g_3\left(\frac{2\mu+\nu}{q}\right)+\theta\left(\frac{2\mu-\nu}{q}-1\right)g_3\left(\frac{2\mu-\nu}{q}\right)\right]+\\ &\theta(\nu-q)\left[\theta\left(1-\frac{2\mu-\nu}{q}\right)g_3\left(\frac{2\mu-\nu}{q}\right)-\theta\left(-1-\frac{2\mu-\nu}{q}\right)g_3\left(\frac{2\mu-\nu}{q}\right)\right]-\\ &-\frac{4}{3}\theta\left(\frac{2\mu-\nu}{q}+1\right)\Bigg\}\end{aligned} \tag{3.24}$$

We can visualize better the result recalling Fig. 3.3 and rewrite the result in terms of the regions shown,

$$\mathrm{Im}[\Delta\pi(\nu,\mathbf{q})] = -\frac{q^2}{32\pi}\times\begin{cases} g_3\left(\frac{2\mu+\nu}{q}\right)+g_3\left(\frac{2\mu-\nu}{q}\right) & 1A\\ -\frac{4}{3} & 1B\\ g_3\left(\frac{2\mu+\nu}{q}\right) & 2A\\ g_3\left(\frac{2\mu-\nu}{q}\right)-\frac{4}{3} & 2B\\ 0 & 3A\\ 0 & 3B\end{cases}$$

Real part:

The real part can be obtained from the imaginary part by making use of the Kramers-Kronig relations, however there are several other methods that may result more straightforward. We saw that for the 2D case it results much more convenient to rearrange the expression for $\Delta\pi$ such that the the integration can be easily done; we here follow the same procedure. Generalizing eq. (3.13) to the 3D case,

$$\Delta\pi(\nu,\mathbf{q}) = -\frac{1}{8\pi^3}\int_{|\mathbf{k}|<\mu} d^3k\,\sum_{\alpha=\pm}\frac{\alpha\nu+|\mathbf{k}|+|\mathbf{k}+\mathbf{q}|\cos\Theta}{(\nu+\alpha|\mathbf{k}|+i\varepsilon)^2-|\mathbf{k}+\mathbf{q}|^2} \tag{3.25}$$

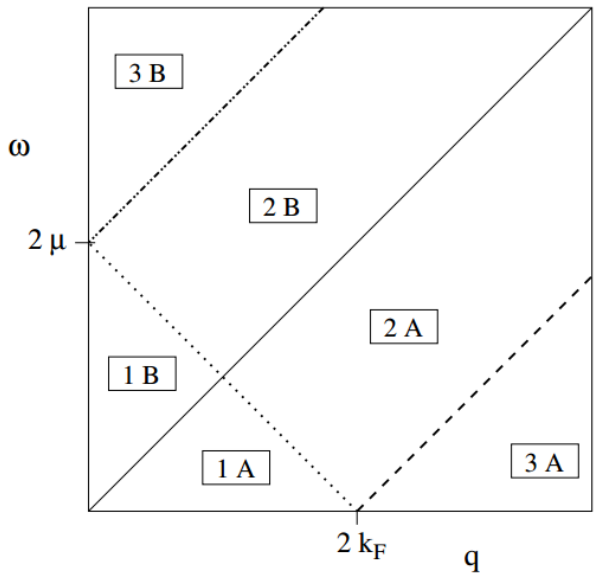

Different regions delimited by the Heaviside functions appearing in the calculation. In our units, $k_f = \mu$, $\omega = \nu$. Taken from [34].

A detailed procedure of how the calculations are carried on was already explained for the graphene case, therefore we shall skip some technical steps. We go to spherical coordinates,

$$\begin{aligned}\Delta\pi(\nu,\mathbf{q}) &= -\frac{1}{8\pi^3}\int_0^\mu dk\int_0^\pi d\theta\sum_{\alpha=\pm}2\pi k^2\sin\theta\frac{\alpha\nu+k+k+q\cos\theta}{(\nu+\alpha k+i\varepsilon)^2-k^2-q^2-2kq\cos\theta}\\ &= -\frac{1}{8\pi^3}\int_0^\mu dk\int_0^\pi d\theta\sum_{\alpha=\pm}2\pi k^2\sin\theta\frac{q}{-2kq}\frac{\frac{\alpha\nu+2k}{q}+\cos\theta}{\frac{\nu^2+2\alpha\nu k-q^2+i\varepsilon(\nu+\alpha k)}{-2kq}+\cos\theta}\\ &= -\frac{1}{8\pi^3}\int_0^\mu dk\int_0^\pi d\theta\sum_{\alpha=\pm}-\pi k\sin\theta\left(1+\frac{\frac{\alpha\nu+2k}{q}-z}{z+\cos\theta}\right)\end{aligned}$$

with $z=\frac{\nu^2+2\alpha\nu k-q^2+i\varepsilon(\nu+\alpha k)}{-2kq}$. The integral is easier than in the 2D case, because of the different Jacobian. We integrate out the angle variable to get

$$\Delta\pi(\nu,\mathbf{q}) = -\frac{1}{8\pi^3}\int_0^\mu dk\sum_{\alpha=\pm}(-\pi k)\int_0^\pi d\theta\left[\sin\theta+\left(\frac{\alpha\nu+2k}{q}-z\right)\frac{\sin\theta}{z+\cos\theta}\right]$$

It is clear that the only term that requires extra care is the second one. We shall analyse it separately,

$$\int_0^\pi d\theta\frac{\sin\theta}{z+\cos\theta}=\int_{-1}^1 dx\frac{1}{z+x}=\int_{-1}^1 dx\frac{1}{a+x\pm i\varepsilon}=\log\left|\frac{a+1}{a-1}\right|+\theta(1-a^2)(\mp i\pi\varepsilon)$$

Notice that the imaginary component guarantees the convergence of the integral. Then

$$\Delta\pi(\nu,\mathbf{q}) = -\frac{1}{8\pi^3}\int_0^\mu dk\sum_{\alpha=\pm}\left\{-2\pi k-\pi k\left(\frac{\alpha\nu+2k}{q}-z\right)\left[\log\left|\frac{\mathrm{Re}z+1}{\mathrm{Re}z-1}\right|+\theta(1-(\mathrm{Re}z)^2)(\mp i\pi\,\mathrm{sgn}(\mathrm{Im}z))\right]\right\}$$

It is easy to verify that the imaginary part is consistent with what seen above and coincides with what is obtained by substituing eq. (3.22) in eq. (3.21). In analogy with what done for the imaginary part, we introduce an auxiliary function J^α which contains all the information regarding the real part of the polarization function,

$$\mathrm{Re}\left[\Delta\pi(\nu,\mathbf{q})\right] = -\frac{1}{8\pi^3}\int_0^\mu dk\sum_{\alpha=\pm}J^\alpha(\nu,\mathbf{k},\mathbf{q}) \tag{3.26}$$

With the above definition we find

$$J^{\alpha}(\nu,\mathbf{k},\mathbf{q}) = -2\pi k - \pi\frac{(2\alpha k+\nu)^2-q^2}{2q}\log\left|\frac{(\alpha\nu-q)(2k+\alpha\nu+q)}{(\alpha\nu+q)(2k+\alpha\nu-q)}\right| \tag{3.27}$$

We split the momentum integration into the two different cases, $\alpha = \pm 1$.

$$\begin{aligned}\int_0^{\mu} dk\, J^{+}(\nu,\mathbf{k},\mathbf{q}) &= -\pi\mu^2 - \pi\int_0^{\mu} dk\,\frac{(2k+\nu)^2-q^2}{2q}\log\left|\frac{(\nu-q)(2k+\nu+q)}{(\nu+q)(2k+\nu-q)}\right| \\ &= -\pi\mu^2 - \frac{\pi}{12q}\Big\{4q\mu(\mu+\nu) + (2q+2\mu+\nu)(2\mu+\nu-q)^2\log\left|\frac{q-\nu}{2\mu+\nu-q}\right| + \\ &\qquad (2q-2\mu-\nu)(2\mu+\nu+q)^2\log\left|\frac{\nu+q}{2\mu+\nu+q}\right|\Big\} \\ &= -\pi\mu^2 - \frac{\pi}{12}\Big\{4\mu(\mu+\nu) + q^2\left(g_3\left(\frac{2\mu+\nu}{q}\right)\right)\log\left|\frac{q-\nu}{2\mu+\nu-q}\right| + \\ &\qquad +q^2\left(-g_3\left(\frac{2\mu+\nu}{q}\right)+\frac{4}{3}\right)\log\left|\frac{\nu+q}{2\mu+\nu+q}\right|\Big\}\end{aligned}$$

$$\int_0^{\mu} dk\, J^{-}(\nu,\mathbf{k},\mathbf{q}) = -\pi\mu^2 - \pi\int_0^{\mu} dk\,\frac{(\nu-2k)^2-q^2}{2q}\log\left|\frac{(-\nu-q)(2k-\nu+q)}{(q-\nu)(2k-\nu-q)}\right|$$

This second result comes for free if we observe that the parameter α is always associated to the external frequency ν, therefore changing sign to the former is equivalent to doing the operation on the latter, i.e. we can substitue $\nu \to -\nu$ in the final result for J^{+}:

$$\begin{aligned}\int_0^{\mu} dk\, J^{-}(\nu,\mathbf{k},\mathbf{q}) = -\pi\mu^2 - \frac{\pi}{12}\Big\{&4\mu(\mu-\nu) + q^2\left(g_3\left(\frac{2\mu-\nu}{q}\right)\right)\log\left|\frac{q+\nu}{2\mu+\nu-q}\right| + \\ &+q^2\left(-g_3\left(\frac{2\mu-\nu}{q}\right)+\frac{4}{3}\right)\log\left|\frac{q-\nu}{2\mu-\nu+q}\right|\Big\}\end{aligned}$$

where G was defined in eq. (3.23). Before summarizing the results for the real part of the polarization function, it seems convenient to introduce another auxiliary function,

$$H(\nu,q) = \log\left|\frac{2\mu+\nu-q}{q-\nu}\right| \tag{3.28}$$

$$\begin{aligned}\mathrm{Re}\left[\Delta\pi(\nu,\mathbf{q})\right] = \frac{\mu^2}{3\pi^2} + \frac{q^2}{96\pi^2}\Big\{&g_3\left(\frac{2\mu+\nu}{q}\right)H(\nu,q) + \left(-g_3\left(\frac{2\mu+\nu}{q}\right)+\frac{4}{3}\right)H(\nu,-q) \\ &g_3\left(\frac{2\mu-\nu}{q}\right)H(-\nu,q) + \left(-g_3\left(\frac{2\mu-\nu}{q}\right)+\frac{4}{3}\right)H(-\nu,-q)\Big\}\end{aligned} \tag{3.29}$$

We find the result to be in agreement with [36]. We end the section by showing two plots, one for undoped WSM and the other one for the doped case, Fig. 3.4 and Fig. 3.5. By comparison of the two plots we can relate different transitions to different areas of the plot: interband transitions, that are the only one allowed in the case of undoped WSM, characterize the region for which $\nu > q$, while intraband transitions the region in which $\nu + 2\mu > q > \nu$.

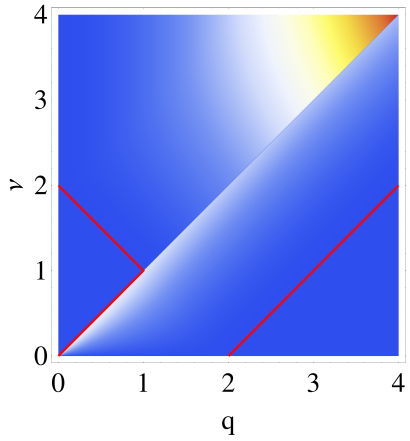

Figure 3.4: -Imπ_μ *with* $\mu = 1$. *Red lines enclose regions for which* Im$\pi_\mu = 0$.

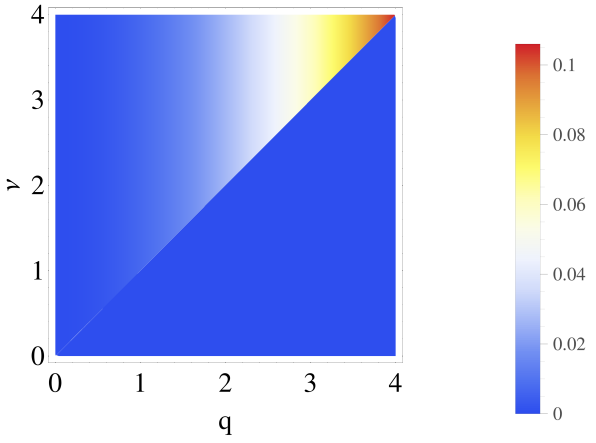

Figure 3.5: -Imπ_μ *with* $\mu = 0$.

3.4.3 Weyl semimetals with tilting term

We now consider turn to the case of a spinless WSM with tilted Dirac cones: the polarization function has become familiar by now,

$$\begin{aligned}\pi(i\nu,\mathbf{q},\mathbf{d}) &= -\frac{1}{\beta}\sum_m \int \frac{d^3k}{(2\pi)^3}\mathrm{Tr}\Big[G(i\omega_m + i\nu, \mathbf{k}+\mathbf{q},\mathbf{d})G(i\omega_m,\mathbf{q},\mathbf{d})\Big] \\ &= -\frac{2}{\beta}\sum_m \int \frac{d^3k}{(2\pi)^3}\frac{(i\omega_m - w\mathbf{d}\cdot\mathbf{k})(i\nu + i\omega_m - w\mathbf{d}\cdot(\mathbf{k}+\mathbf{q})) + \mathbf{k}\cdot(\mathbf{k}+\mathbf{q})}{\big[(i\omega_m - w\mathbf{d}\cdot\mathbf{k})^2 - \mathbf{k}^2\big]\big[(i\omega_m + i\nu - w\mathbf{d}\cdot(\mathbf{k}+\mathbf{q}))^2 - |\mathbf{k}+\mathbf{q}|^2\big]}\end{aligned}$$

As already seen in the doped graphene case, turning the Matsubara summation into an integral and making use of the Feynman trick is a very hard path, for one will have to do contour integration with double poles: here for the more the poles depend on the internal momentum so that this way is not feasible. A different approach would be the one used in the previous section: getting rid of the Matsubara frequency as soon as possible by performing analytic continuation and then carry out the integration by taking good care of all the different conditions by means of Heaviside functions.
We will follow this latter approach: performing Matsubara summation, see Appendix sec?, yields

$$\pi(i\nu,\mathbf{q},\mathbf{d}) = -\int \frac{d^3k}{(2\pi)^3}\sum_{s,s'=\pm1}\frac{n_F(s|\mathbf{k}| + w\mathbf{d}\cdot\mathbf{k}) - n_F(s'|\mathbf{k}+\mathbf{q}| + w\mathbf{d}\cdot(\mathbf{k}+\mathbf{q}))}{i\nu - w\mathbf{d}\cdot\mathbf{q} + s|\mathbf{k}| - s'|\mathbf{k}+\mathbf{q}|}\times\frac{1+ss'\cos\Theta}{2} \tag{3.30}$$

It is not a coincidence that the expression for the polarization function looks like the one for graphene but is due to the structure of the Hamiltonian, in particular to the presence of Dirac points. It constitues the generalized version of the Lindhard function for Dirac materials.
We want to recover an analytical expression for the polarization function for the system and in order to do this it results better to focus on eq. (3.30). There are a couple of important observations here: the first regards the Fermi-Dirac distributions:

$$n_F(s|\mathbf{k}| + w\mathbf{d}\cdot\mathbf{k}) = n_F(s|\mathbf{k}|(1+w\cos\varphi)) \quad , \qquad \cos\varphi = \frac{\mathbf{d}\cdot\mathbf{k}}{|\mathbf{k}|}$$

in particular

$$1 + w\cos\varphi > 0 \quad \forall\varphi \in [0,2\pi] \qquad \text{since} \qquad w < 1$$

when taking the zero temperature limit, then, the above Fermi-Dirac distribution becomes

$$n_F(s|\mathbf{k}|(1+w\cos\varphi)) \quad \overset{T\to0}{\longrightarrow} \quad \theta(-s|\mathbf{k}|(1+w\cos\varphi)) = \theta(-s)$$

The take-home message here is that the presence of the tilting term within the Fermi-Dirac distribution **does not influence at all** their behaviour: indeed we may just drop them from eq. (3.30). The second

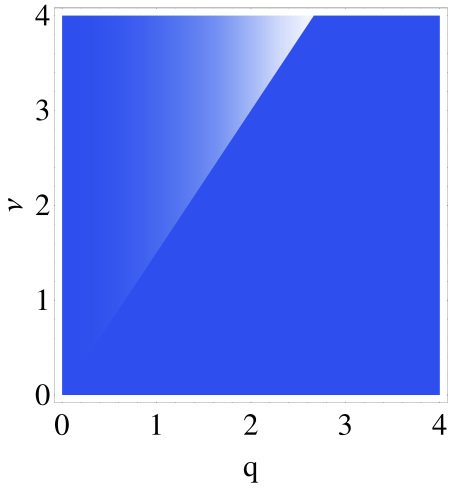

Figure 3.6: *$\mathrm{Im}\pi(\nu, \mathbf{q}, \mathbf{d})$ for tilted WSM. The legend is the same as in the previous two figures.*

observation is that the angle Θ does not depend on the tilting of the Dirac cones and we can absorb the term $w\mathbf{d}\cdot\mathbf{q}$ at the denominator in the frequency ν, by redefining it. After analytic continuation we obtain

$$\pi(\nu + w\mathbf{d}\cdot\mathbf{q}, \mathbf{q}, \mathbf{d}) = -\int \frac{d^3k}{(2\pi)^3} \sum_{s,s'=\pm 1} \frac{n_F(s|\mathbf{k}|) - n_F(s'|\mathbf{k}+\mathbf{q}|)}{\nu + s|\mathbf{k}| - s'|\mathbf{k}+\mathbf{q}| + i\varepsilon} \times \frac{1 + ss'\cos\Theta}{2} \tag{3.31}$$

At this point is clear that we can identify the right-hand-side with the polarization function for untilted WSM, which was calculated just above, eq. (3.18):

$$\begin{aligned}\pi(\nu, \mathbf{q}) = \frac{q^2}{24\pi^2}\Bigg\{&\log\left(1 + \frac{4\Lambda^2}{q^2 - (\nu - w\mathbf{d}\cdot\mathbf{q})^2}\right) + \\ &+ \frac{8\Lambda^3}{(q^2 - (\nu - w\mathbf{d}\cdot\mathbf{q})^2)^{3/2}} \arctan\left(\frac{\sqrt{q^2 - (\nu - w\mathbf{d}\cdot\mathbf{q})^2}}{2\Lambda}\right) - -\frac{4\Lambda^2}{q^2 - (\nu - w\mathbf{d}\cdot\mathbf{q})^2}\Bigg\}\end{aligned} \tag{3.32}$$

We can compute the plasmons spectrum by looking at the imaginary part of the polarization function, as done before. The very same analysis brings to the result

$$\mathrm{Im}\left[\pi(\nu, \mathbf{q})\right] = \theta(\nu - w\mathbf{d}\cdot\mathbf{q} - q)\,\frac{q^2}{24\pi} \tag{3.33}$$

The result is interesting: it seems that the presence of the tilting velocity only reflects in a shift in the frequencies. However it is not totally unexpected. We already saw how this term tilts the Dirac cones, that is, the dispersion relation of the system. For zero chemical potential, there are only excitations from valence to conduction band, be the cones tilted or not: the only difference in the excitations is found in the energy, which is, indeed, characterized by $w\mathbf{d}\cdot\mathbf{q}$.
A plot of the imaginary part of the polarization function is shown in Fig. 3.6. We see that the effect of tilting simply increases the steepness of the line that separates regions in which the polarization function is zero from the others.

3.5 Conclusions

In the Chapter we investigated the behavior of the polarization function for a very wide variety of Dirac systems. We found a generalized formula for the Lindhard function that seems to preserve the same form for any Dirac materials,

$$\pi(i\nu, \mathbf{q}) = -\int \frac{d^Dk}{(2\pi)^D} \sum_{s,s'=\pm 1} \frac{n_F(E_s(\mathbf{k})) - n_F(E_{s'}(\mathbf{k}+\mathbf{q}))}{i\nu + E_s(\mathbf{k}) - E_{s'}(\mathbf{k}+\mathbf{q})} \times \frac{1 + ss'\cos\Theta}{2}$$

where $E_s(\mathbf{k})$ denotes the energy of an electron in the band indicated by s, e.g. valence or conduction band, and D sets the dimensionality. It is to be remarked the emergence in the equation of the form factor

$F^{ss'} = (1 + ss' \cos\Theta)/2$, being Θ the angle between vector $\mathbf{k}$ and $\mathbf{k} + \mathbf{q}$. This additional term is a feature of Dirac materials and keeps track of the overlapping of the electronic wavefunctions.
We computed analytic expressions for the polarization function in the case of doped graphene, doped WSM and finally undoped tilted WSM of type I: from these it is possible to extract the regions in which plasmons are more likely to arise, i.e those for which $\mathrm{Im}\pi = 0$, and also their dispersion relation can be obtained, according to eq. (3.1). It shall be noted that this latter constitues an exact relation provided that the full polarization function is used; in our case we computed the polarization function in the case there are no interactions within the system. A possible further work would be to compute the correction, at least to first order, to the polarization function, due to the electron-electron interactions.
By comparison of the result for the polarization function in the doped and undoped cases it is possible to relate regions in the $(\mathbf{q}, \nu)$ diagram with the corresponding inter-or-intra band transitions. As one could expect from the fact that the generalized Lindhard function has the same form for any Dirac material, the polarization function is very similar between graphene and WSM: we found an analytic expression for both cases and by comparison is clear that the only change is in the auxiliary function, namely g_2 and g_3.
Finally the polarization function for the case of undoped tilted WSM was computed, where we made use of a very useful trick that applies for WSM of type I when considering the zero-temperature limit. The response function can be related to the one of the untilted WSM which results much easier to compute analytically.

Chapter 4

A renormalization group approach

4.1 Introduction

So far we have investigated different properties of our system by looking at the response functions. In this Chapter we propose to study what happens once we include in the theory the interaction between electrons. In particular we are interested in studying whether the system becomes more stable because of the interactions or, on the contrary, more unstable. The theoretical framework we will work in is that of renormalization group (RG): we start the chapter by outlining the renormalization technique we will employ, then we compute the relevant Feynman diagrams and from these the RG equations are derived. In the last part we solve the equations numerically and analyze the plots that come out of them, hence draw some conclusions.

4.2 The energy shell renormalization scheme

When it comes to use the renormalization technique, a big variety of procedures can be equally employed. The scheme we will use for our purpose can be addressed as an "energy shell" renormalization scheme. We proceed as follows: first we introduce the Coulomb potential in our Hamiltonian. This latter is given by

$$H = \int d^3r\ \bar{\psi}(\mathbf{r})(-i\hbar v_F \nabla\cdot\sigma - i\hbar\tilde{w}\mathbf{d}\cdot\nabla)\psi(\mathbf{r}) + \frac{e^2}{8\pi\epsilon}\int d^3r \int d^3r'\ \bar{\psi}(\mathbf{r})\psi(\mathbf{r})\frac{1}{|\mathbf{r}-\mathbf{r}'|}\bar{\psi}(\mathbf{r}')\psi(\mathbf{r}') \qquad (4.1)$$

Notice the presence of the parameter $\tilde{w}$ which now has the dimension of a velocity and is to be distinguished from the parameter w, adimensional, which was used in the previous Chapters. The reason for this redefinition will become clear later, here we just state that since we are interested in seeing how the different parameters of the Hamiltonian change, we want them to be independent of each other.
In the equation, $\epsilon = \epsilon_0\epsilon_r$ is the product of the vacuum dielectric constant and the medium one, respectively. The interaction term introduced in the Hamiltonian describes an istantaneous interaction between the electric charges, thus we are here neglecting any retardation effect that could come from the propagation of the photon field (which is also not included in the Hamiltonian). The approximation is justified if we assume that the ratio between the velocity at which electrons and photons propagate is small, so that we can regard to all purposes the photon propagation as instantaneous (in graphene, for instance, $v_F/c \sim 1/300$). This is equivalent to what is obtained by starting with the usual QED Lagrangian, where the fermionic field is coupled to a photon field, and performing a Hubbard-Stratanovich transformation to integrate out the bosonic field, [14]. It shall be remarked that there is a subtle but important difference between the two approaches: while the Lagrangian formulation of QED depends explicitly on the velocity of light c, in our theory there is no trace of it[1]. The reason lies in the assumption of instantaneous interaction between electrons and we shall bear it in mind.
The idea behind RG theory is that, although the system has a natural ultraviolet cut-off, which is set by the lattice spacing, we are interested in the low-energy physics, processes that take place in a narrow energy strip around the Fermi surface. To this aim we integrate out all the momenta above a certain energy cut-off and find an effective, low-energy description for our system. The price to pay is the introduction of an artificial cut-off in our system, on which the Hamiltonian's parameters will now depend. With the tool of RG theory we can understand this dependence and study how the parameters flow with the cut-off.
To be concrete, imagine to do the following operation: we slowly move the energy cut-off Λ to a value

[1] A discussion for the 2D case can be found in [11]

$\Lambda' = \Lambda - \delta\Lambda$. The operation will involve only those terms that depends on the cut-off, precisely the one obtained from the Feynman diagrams.

$$H(\Lambda) \quad \rightarrow \quad \tilde{H}(\Lambda') = H(\Lambda) + \delta H$$

With this operation the bare parameters are promoted to cut-off dependent parameters and they are then said to flow.

We can study how interactions affects the system by doing perturbation theory: this corresponds to computing the Feynman diagrams that contribute to the renormalization of our parameters. We here restrict ourselves to the first order expansion, that is 1-loop diagrams. The Hamiltonian's parameters are the Fermi velocity, v_F, the tilting velocity, $\tilde{w}$ and the coupling constant e^2/ϵ.

We start by recasting the Coulomb potential in momentum space:

$$\begin{aligned}
\mathcal{H}_c &= \frac{e^2}{8\pi\epsilon} \int d^3r \int d^3r' \, \frac{\rho(\mathbf{r})\rho(\mathbf{r}')}{|\mathbf{r}-\mathbf{r}'|} \\
&= \frac{e^2}{8\pi\epsilon} \int \frac{d^3q}{(2\pi)^3} \int \frac{d^3q'}{(2\pi)^3} \int d^3r \int d^3r' \, \frac{\rho(\mathbf{q})e^{-i\mathbf{q}\mathbf{r}}\rho(\mathbf{q}')e^{-i\mathbf{q}'\mathbf{r}'}}{|\mathbf{r}-\mathbf{r}'|} \\
&= \frac{e^2}{8\pi\epsilon} \int d^3q \int d^3R \, \rho(\mathbf{q})\rho(-\mathbf{q}) \frac{1}{|\mathbf{R}|} \frac{e^{-i\mathbf{q}\mathbf{R}}}{(2\pi)^3} \\
&= \frac{e^2}{8\pi\epsilon} \int \frac{d^3q}{(2\pi)^3} \, \rho(\mathbf{q})\rho(-\mathbf{q}) \int d^3R \, \frac{1}{|\mathbf{R}|} e^{-i\mathbf{q}\mathbf{R}}
\end{aligned}$$

We make use of the result

$$\int d^3R \, \frac{1}{|\mathbf{R}|} e^{-i\mathbf{q}\mathbf{R}} = \frac{4\pi}{\mathbf{q}^2}$$

to obtain the expression for the Coulomb potential in momentum space, $V = V(\nu, \mathbf{q})$,

$$V(\nu, \mathbf{q}) = \frac{e^2}{2\epsilon} \frac{1}{\mathbf{q}^2}$$

The Feynman diagram associated to the Coulomb interaction is shown in Fig. 4.2, diagrams shown in Fig. 4.3 correspond to its 1-loop order corrections. These will be computed in the next section.

We conclude with an important remark: absorbing the interaction effects in a redefinition of the system's parameter corresponds to the requirement that the microscopic description must retain the same structure, i.e. the form of the Hamiltonian should not change. This latter requirement is in fact far from being verified in most cases and is connected to the concept of renormalizability of a theory; we avoid here a deep discussion on the topic and assume our theory in indeed renormalizable.
The last part of the chapter will be devoted to the study of the RG flow equations and we will investigate, at least numerically, the solutions. This will allow us to draw some conclusions about the effect of the interactions within our system.

4.3 Feynman diagrams

Self energy

The full propagator can be expressed in terms of a free part and a correction coming from the interacting part, the self-energy $\Sigma(\omega, \mathbf{q})$:

$$G(\omega, \mathbf{q})^{-1} = G_0(\omega, \mathbf{q})^{-1} - \Sigma(\omega, \mathbf{q}) \tag{4.2}$$

The self-energy term has an expansion in terms of one-particle-irreducible (1PI) diagrams; in our calculation we will restrict to the first-order terms, that is the one-loop 1PI. To this order in perturbation theory, there is only one diagram contributing to the self-energy, shown in Fig. 4.1, and sometimes referred to as "sunrise".

$$\Sigma(i\omega, \mathbf{q}) = \frac{1}{\beta} \sum_{\nu} \int \frac{d^3k}{(2\pi)^3} \, G_0(i\omega_n + i\nu, \mathbf{k}+\mathbf{q}) V_c(-\nu, -\mathbf{k}) \tag{4.3}$$

Figure 4.1: *Self-energy diagram*

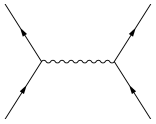

Figure 4.2: *Coulomb interaction diagram*

V_c being the Coulomb interaction, $V_c(-\nu,-\mathbf{k}) = e^2/16\pi^2\epsilon\mathbf{k}^2$ (independent of the internal frequency) and the Green's function is obtained as usual from the Bloch Hamiltonian,

$$G_0(i\omega_n,\mathbf{k},\mathbf{d})^{-1} = i\omega_n - \mathcal{H}(\mathbf{k},\mathbf{d}) \qquad , \qquad \mathcal{H}(\mathbf{k},\mathbf{d}) = v_F\,\mathbf{k}\cdot\sigma + w\,\mathbf{d}\cdot\mathbf{k}$$

$$G_0(i\omega_n,\mathbf{k},\mathbf{d}) = \frac{i\omega_n - w\mathbf{d}\cdot\mathbf{k} + v_F\mathbf{k}\cdot\sigma}{(i\omega_n - w\mathbf{d}\cdot\mathbf{k})^2 - v_F^2\mathbf{k}^2}$$

where we set $v_F = 1$. We now turn to the computation of eq. (4.3): taking the zero temperature limit the sum over Matsubara frequencies becomes an integral and it reads

$$\begin{aligned}\Sigma(i\omega,\mathbf{q}) &= \frac{e^2}{2\epsilon}\int\frac{d\nu}{2\pi}\int\frac{d^3k}{(2\pi)^3}\,\frac{i\omega_n + i\nu - w\mathbf{d}\cdot(\mathbf{k}+\mathbf{q}) + v_F(\mathbf{k}+\mathbf{q})\cdot\sigma}{(i\omega_n + i\nu - w\mathbf{d}\cdot(\mathbf{k}+\mathbf{q}))^2 - v_F^2|\mathbf{k}+\mathbf{q}|^2}\,\frac{1}{\mathbf{k}^2}\\ &= \frac{e^2}{2\epsilon}\int\frac{d\nu}{2\pi}\int\frac{d^3k}{(2\pi)^3}\,\frac{i\nu - w\mathbf{d}\cdot\mathbf{k} + v_F\mathbf{k}\cdot\sigma}{(i\nu - w\mathbf{d}\cdot\mathbf{k})^2 - v_F^2|\mathbf{k}|^2}\,\frac{1}{|\mathbf{k}-\mathbf{q}|^2}\\ &= \frac{e^2}{2\epsilon}\int\frac{d^3k}{(2\pi)^3}\,\frac{1}{|\mathbf{k}-\mathbf{q}|^2}\int\frac{d\nu}{2\pi}\,\frac{i\nu - w\mathbf{d}\cdot\mathbf{k} + v_F\mathbf{k}\cdot\sigma}{(i\nu - w\mathbf{d}\cdot\mathbf{k})^2 - v_F^2|\mathbf{k}|^2}\end{aligned}$$

Performing the frequency integration, see Appendix C, one find the expression for the self-energy,

$$\Sigma(\omega,\mathbf{q}) = -\frac{e^2}{4\epsilon v_F}\int\frac{d^3k}{(2\pi)^3}\,\frac{\mathbf{k}\cdot\sigma}{|\mathbf{k}||\mathbf{k}-\mathbf{q}|^2} \tag{4.4}$$

it results much more convenient, for later calculations, to work out a bit the expression in order to get a cleaner result. We can generalize the Feynman trick to get

$$\frac{1}{A^2B} = \frac{1}{2}\int_0^1 dx\,\frac{1}{\sqrt{1-x}}\,\frac{1}{[xA^2 + (1-x)B^2]^{3/2}}$$

which inserted in the above gives,

$$\begin{aligned}\Sigma(\omega,\mathbf{q}) &= -\frac{e^2}{4\epsilon v_F}\int\frac{d^3k}{(2\pi)^3}\,\frac{(\mathbf{k}+\mathbf{q})\cdot\sigma}{|\mathbf{k}+\mathbf{q}||\mathbf{k}|^2}\\ &= -\frac{e^2}{8\epsilon v_F}\int_0^1 dx\,\frac{1}{\sqrt{1-x}}\int\frac{d^3k}{(2\pi)^3}\,\frac{(\mathbf{k}+(1-x)\mathbf{q})\cdot\sigma}{[\mathbf{k}^2 + x(1-x)\mathbf{q}^2]^{3/2}}\end{aligned}$$

we conclude by stating that the term linear in $\mathbf{k}$ gives zero contribution, an assumption that will be later justified.

Coulomb interaction

We investigate the effect of the Coulomb interaction by looking if, and how, the interaction itself gets renormalized. The Feynman graphs that contribute at one loop to the renormalization are shown in Fig. 4.3.

Here and in the remainder we choose ω and $\mathbf{p}$ to be the *internal* frequency and momentum, respectively. As for the external momentum and frequency, the total momentum involved in the process is $\mathbf{k}+\mathbf{q}+\mathbf{k}'$, being $\mathbf{k}+\mathbf{q}$ the bottom-left incoming momentum and $\mathbf{k}'$ the bottom-right incoming momentum. The external frequencies are η, η'. Time flows bottom to top.
We start by computing the contribution of Fig. 4.3a.

$$I_a(i\nu,\mathbf{q}) = -\int_{-\infty}^{\infty}\frac{d\omega}{2\pi}\int\frac{d^3p}{(2\pi)^3}V^2(\nu,\mathbf{q})\mathrm{Tr}\left[G(i\omega+i\nu,\mathbf{p}+\mathbf{q})G(i\omega,\mathbf{p})\right]$$

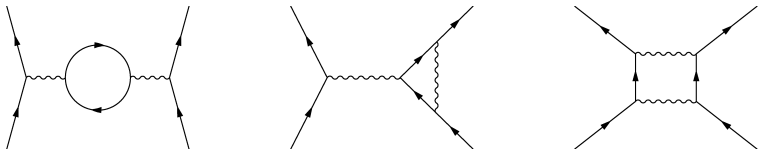

Figure 4.3: *Feynman graphs contributing to the charge renormalization up to one-loop corrections.*

where the minus sign comes from the closed fermion loop. The contibution results easy to compute since both the interactions don't depend on internal variables and we can factorize them outside the integral. Then we are left with an expression already familiar for us, it's simply the polarization bubble that was computed earlier. As we shall later see, there are some differences between this contribution and the polarization function we saw, therefore we don't carry out the full calculation. We omit the description of the single steps as it is precisely the same seen for the polarization function.

$$\begin{aligned} I_a(i\nu,\mathbf{q}) &= -\left(\frac{e^2}{2\epsilon|\mathbf{q}|^2}\right)^2 \int_{-\infty}^{\infty}\frac{d\omega}{\pi}\int\frac{d^3p}{(2\pi)^3}\frac{-\omega(\omega+\nu)+v_F^2\mathbf{p}\cdot(\mathbf{p}+\mathbf{q})}{[(\omega+\nu)^2+v_F^2|\mathbf{p}+\mathbf{q}|^2]\,[\omega^2+v_F^2|\mathbf{p}|^2]} \\ &= -\left(\frac{e^2}{2\epsilon|\mathbf{q}|^2}\right)^2 \int_{-\infty}^{\infty}\frac{d\omega}{\pi}\int_0^1 dx\int\frac{d^3p}{(2\pi)^3}\frac{-\omega^2+v_F^2\mathbf{p}^2+x(1-x)(\nu^2-v_F^2\mathbf{q}^2)}{[\omega^2+v_F^2\mathbf{p}^2+x(1-x)(\nu^2+v_F^2\mathbf{q}^2)]^2} \\ &= \left(\frac{e^2}{2\epsilon|\mathbf{q}|^2}\right)^2 \int_0^1 dx\int\frac{d^3p}{(2\pi)^3}\frac{x(1-x)v_F^2\mathbf{q}^2}{[v_F^2\mathbf{p}^2+x(1-x)(\nu^2+v_F^2\mathbf{q}^2)]^{3/2}} \end{aligned}$$

we postpone the evaluation of this last integral and analyse the contribution of the next Feynman diagram.

Contribution of Fig. 4.3b

$$\begin{aligned} I_b(\nu,\mathbf{q}) &= \int_{-\infty}^{\infty}\frac{d\omega}{2\pi}\int\frac{d^3p}{(2\pi)^3}V(i\nu,\mathbf{q})G(i\omega,\mathbf{p})V(i\omega-i\eta',\mathbf{p}-\mathbf{k}')G(i\omega+i\nu,\mathbf{p}+\mathbf{q}) \\ &= \left(\frac{e^2}{2\epsilon|\mathbf{q}|}\right)^2 \int\frac{d\omega}{2\pi}\int\frac{d^3p}{(2\pi)^3}\frac{1}{|\mathbf{p}-\mathbf{k}'|^2}G(i\omega+i\nu,\mathbf{p}+\mathbf{q})G(i\omega,\mathbf{p}) \end{aligned}$$

We see that in this case we cannot take out of the integral both Coulomb potentials, since one of them depends upon the internal momentum. The presence of the potential within the integral has the effect of lowering the overall divergence of the Feynman graph: it is not possible, however, to discard such a graph. A naive power counting argument would give the following: the denominator goes as p^2 and the denominator as p^6, since we are in dimension $d=4$ the contribution will be **at most** logarithmic.
We see that it is a priori not possible to discard the graph, but we have to keep it into account for the charge renormalization. A naive rule can be extracted from the above reasoning, though: when looking at the graphs that may contribute to the renormalization of a certain physical parameter, we can discard those terms that by power counting goes to zero faster than a logarithm (that is, power of the form $p^{-\alpha}$ with $\alpha > 1$).

Let's start by computing the matrix product between the two Green's functions,

$$G(i\omega+i\nu,\mathbf{p}+\mathbf{q})G(i\omega,\mathbf{p}) = \frac{\left[-\omega(\omega+\nu)+v_F^2\mathbf{p}\cdot(\mathbf{p}+\mathbf{q})\right]}{[(\omega+\nu)^2+v_F^2|\mathbf{p}+\mathbf{q}|^2][\omega^2+v_F^2|\mathbf{p}|^2]}\mathbb{I}_2+\frac{i\omega v_F(\mathbf{p}+\mathbf{q})+(i\omega+i\nu)v_F\mathbf{p}}{[(\omega+\nu)^2+v_F^2|\mathbf{p}+\mathbf{q}|^2][\omega^2+v_F^2|\mathbf{p}|^2]}\cdot\sigma$$

The contribution of the Feynman integral is thus rewritten as

$$I_b(\nu,\mathbf{q}) = \left(\frac{e^2}{2\epsilon|\mathbf{q}|}\right)^2 \int_{\infty}^{\infty}\frac{d\omega}{2\pi}\int\frac{d^3p}{(2\pi)^3}\frac{v_F^2}{v_F^2|\mathbf{p}-\mathbf{k}'|^2}\left\{\frac{\left[-\omega(\omega+\nu)+v_F^2\mathbf{p}\cdot(\mathbf{p}+\mathbf{q})\right]\mathbb{I}_2+[i\omega v_F(\mathbf{p}+\mathbf{q})+(i\omega+i\nu)v_F\mathbf{p}]\cdot\sigma}{[(\omega+\nu)^2+v_F^2|\mathbf{p}+\mathbf{q}|^2][\omega^2+v_F^2|\mathbf{p}|^2]}\right\}$$

We make use of the generalized Feynman trick,

$$\frac{1}{ABC} = 2\int_0^1 dx\int_0^{1-x} dy\,\frac{1}{[A+x(B-A)+y(C-A)]^3}$$

to rewrite I_b as

$$I_b(\nu,\mathbf{q},\mathbf{k}') = 2v_F^2\left(\frac{e^2}{2\epsilon|\mathbf{q}|}\right)^2 \int_{-\infty}^{\infty}\frac{d\omega}{2\pi}\int\frac{d^3p}{(2\pi)^3}\int_0^1 dx\int_0^{1-x}dy$$
$$\left\{\frac{\left[-\omega(\omega+\nu)+v_F^2\mathbf{p}\cdot(\mathbf{p}+\mathbf{q})\right]\mathbb{I}_2+\left[i\omega v_F(\mathbf{p}+\mathbf{q})+(i\omega+i\nu)v_F\mathbf{p}\right]\cdot\sigma}{[\omega^2+v_F^2|\mathbf{p}|^2+x(\nu^2+2\omega\nu+v_F^2\mathbf{q}^2+2v_F^2\mathbf{p}\cdot\mathbf{q})+y(v_F^2\mathbf{k}'^2-2v_F^2\mathbf{p}\cdot\mathbf{k}'-\omega^2)]^3}\right\}$$

It is convenient to introduce two terms, Γ^0 and Γ^1 defined as follows,

$$I_b(\nu,\mathbf{q},\mathbf{k}') = 2v_F^2\left(\frac{e^2}{2\epsilon|\mathbf{q}|}\right)^2\left(\mathbb{I}_2\,\Gamma^0(\nu,\mathbf{q},\mathbf{k}')+\sigma\cdot\mathbf{\Gamma}(\nu,\mathbf{q},\mathbf{k}')\right)$$

such that

$$\Gamma^0(\nu,\mathbf{k}',\mathbf{q}) = \int_{-\infty}^{\infty}\frac{d\omega}{2\pi}\int\frac{d^3p}{(2\pi)^3}\int_0^1 dx\int_0^{1-x}dy\,\frac{-\omega(\omega+\nu)+v_F^2\mathbf{p}\cdot(\mathbf{p}+\mathbf{q})}{[(1-y)\omega^2+v_F^2|\mathbf{p}|^2+x(\nu^2+2\omega\nu+v_F^2\mathbf{q}^2+2v_F^2\mathbf{p}\cdot\mathbf{q})+y(v_F^2\mathbf{k}'^2-2v_F^2\mathbf{p}\cdot\mathbf{k}')]^3}$$

$$\mathbf{\Gamma}(\nu,\mathbf{k}',\mathbf{q}) = \int_{-\infty}^{\infty}\frac{d\omega}{2\pi}\int\frac{d^3p}{(2\pi)^3}\int_0^1 dx\int_0^{1-x}dy\,\frac{i\omega v_F(\mathbf{p}+\mathbf{q})+(i\omega+i\nu)v_F\mathbf{p}}{[(1-y)\omega^2+v_F^2|\mathbf{p}|^2+x(\nu^2+2\omega\nu+v_F^2\mathbf{q}^2+2v_F^2\mathbf{p}\cdot\mathbf{q})+y(v_F^2\mathbf{k}'^2-2v_F^2\mathbf{p}\cdot\mathbf{k}')]^3}$$

Now substituing $\omega\to\omega-x\nu$ and $\mathbf{p}\to\mathbf{p}-x\mathbf{q}+y\mathbf{k}'$ in both expressions and integrating out ω via contour integration,

$$\int_{-\infty}^{\infty}d\omega\,\frac{A+B\omega+C\omega^2}{(D\omega^2+E)} = \frac{\pi}{8}\frac{3AD+CE}{D^{3/2}E^{5/2}}$$

we get

$$\Gamma^0(\nu,\mathbf{k}',\mathbf{q}) = \frac{1}{8}\int\frac{d^3p}{(2\pi)^3}\int_0^1 dx\int_0^{1-x}dy\,\frac{1}{(1-y)^{3/2}}$$
$$\frac{(2-3y)v_F^2\mathbf{p}^2+x(1-x)(2-3y)\nu^2+(3y-4)v_F^2\mathbf{q}^2+(4y^2-3y^3-y)v_F^2\mathbf{k}'^2+3(1-y)v_F^2\mathbf{p}\cdot(\mathbf{q}-2x\mathbf{q}+2y\mathbf{k}')+3y(1-y)v_F^2\mathbf{q}\cdot\mathbf{k}'}{[v_F^2\mathbf{p}^2+x(1-x)v_F^2\mathbf{q}^2+y(1-y)v_F^2\mathbf{k}'^2+x(1-x)\nu^2-2xyv_F^2\mathbf{q}\cdot\mathbf{k}']^{5/2}} \tag{4.5}$$

$$\mathbf{\Gamma}(\nu,\mathbf{k}',\mathbf{q}) = \frac{1}{8}\int\frac{d^3p}{(2\pi)^3}\int_0^1 dx\int_0^{1-x}dy\,\frac{3i\nu}{\sqrt{1-y}}\frac{v_F\mathbf{p}(1-2x)+v_F\mathbf{q}(2x^2-2x)+v_F\mathbf{k}'(y-2xy)}{[v_F^2\mathbf{p}^2+x(1-x)v_F^2\mathbf{q}^2+y(1-y)v_F^2\mathbf{k}'^2+x(1-x)\nu^2-2xyv_F^2\mathbf{q}\cdot\mathbf{k}']^{5/2}} \tag{4.6}$$

An analytic result for the two expression is in principle feasible but the calculation is very lengthy and out of the present purpose. In fact, we want to investigate the behaviour of the integral for large values of $\mathbf{p}$, for later we are going to do shell integration.
To this end, we can do the further approximations: the term that couples to Pauli matrices, $\mathbf{\Gamma}$, will give just a finite contribution, as the integrand goes at most like $\int dpp^{-2}$, therefore we shall drop it. This is consistent with the fact that our interaction vertex couples to the identity matrix and not to the Pauli one; in order to absorbe the divergent terms in a redefinition of our coupling parameter, then, these have to be of the same matrix form.
We focus on the computation of Γ^0 and keep only the leading term in $\mathbf{p}$ at the numerator,

$$\Gamma^0(\nu,\mathbf{k}',\mathbf{q}) = \frac{1}{8}\int\frac{d^3p}{(2\pi)^3}\int_0^1 dx\int_0^{1-x}dy\,\frac{2-3y}{(1-y)^{3/2}}\,\frac{v_F^2\mathbf{p}^2}{[v_F^2\mathbf{p}^2+D^2]^{5/2}}$$

$$D^2 = x(1-x)v_F^2\mathbf{q}^2+y(1-y)v_F^2\mathbf{k}'^2+x(1-x)\nu^2-2xyv_F^2\mathbf{q}\cdot\mathbf{k}'$$

In the variable D is stored all the information concerning the external momentum and energy. The integral still looks hard to perform if one wants an analytic result, however we are interested only in the on-shell

behavior, that is for $\mathbf{p} \sim \Lambda$, where Λ is our energy cut-off, chosen such that $\Lambda \gg \nu, |\mathbf{k}'|, |\mathbf{q}|$. We can then regard D as a constant and perform the integrations over the Feynman parameters, x and y. Because of symmetry,

$$\int_0^1 dx \int_0^{1-x} dy \, \frac{2-3y}{(1-y)^{3/2}} = 0$$

thus also the contribution of Γ^0 is just zero. We find that the Feynman diagram given in Fig. 4.3b does not give contribution in the RG sense.

Contribution of Fig. 4.3c

$$I_c(\nu, \mathbf{q}) = \int_{-\infty}^{\infty} \frac{d\omega}{2\pi} \int \frac{d^3p}{(2\pi)^3} V(i\omega, \mathbf{p}) G(i\eta + i\nu - i\omega, \mathbf{k} + \mathbf{q} - \mathbf{p}) V(i\nu - i\omega, \mathbf{q} - \mathbf{p}) G(i\omega + i\eta', \mathbf{p} + \mathbf{k}')$$

The integral does not need to be computed, is is finite and thus give no contribution in the RG scheme. This can be seen thanks to an observation made above: integrals that give finite contribution can be found by using the rule of power counting. In the present case, fermion propagators goes like $1/p$, and interaction potential as $1/p^2$. Because both Coulomb potential depends on the integration variable, $\mathbf{p}$, the integral goes like $\int dp p^{-2}$ and the contribution is finite.

4.4 The flow equations

We have all the elements needed to compute the contribution of the Feynman diagram that plays a role in the RG scheme. We start with the half-oyster diagram, i.e. the one representing the self-energy, that renormalizes the Fermi velocity. Using it as an example to show the general procedure, the calculations for the remaining two diagrams are trivial and the flow equations are derived.

Self-energy:

In order to study the scaling behaviour of our theory, we imagine to move the energy cut-off Λ to a value $\Lambda' = \Lambda - \delta\Lambda$ and look how the parameters of our system are modified by the operation, how they "scale".

$$H(\Lambda) \quad \rightarrow \quad \tilde{H}(\Lambda') = H(\Lambda) + \delta H$$

where δH contains the quantities that changes in the operation. As we saw above, if one considers the correction to the parameter of the Hamiltonian to, let's say, first order, i.e. to the first loop correction to Feynman diagram, the outcomes are corrections depending on the energy cut-off Λ. This are indeed the quantities that show up in δH when the cut-off is moved, the contribution being

$$\delta H_{SE} = -\frac{\pi e^2}{8\epsilon} \int_0^1 dx \, \frac{1}{\sqrt{1-x}} \int_{\delta E} \frac{d^3k}{(2\pi)^3} \, \frac{(1-x)\mathbf{q}\cdot\sigma}{[\mathbf{k}^2 + x(1-x)\mathbf{q}^2]^{3/2}}$$

Under the assumption that $\Lambda >> |\mathbf{q}|$, ν we can apply what seen for the ellipsoidal integral, to find

$$\begin{aligned} \delta H_{SE} &= -\frac{e^2}{8\epsilon} \int_0^1 dx \, \frac{1}{\sqrt{1-x}} \frac{(1-x)\mathbf{q}\cdot\sigma}{\pi^2} \frac{1}{1-\frac{w^2}{v_F^2}} \log\left(\frac{\Lambda}{\Lambda'}\right) \\ &= -\frac{e^2}{12\pi^2\epsilon} \frac{\mathbf{q}\cdot\sigma}{1-\frac{w^2}{v_F^2}} \log\left(\frac{\Lambda}{\Lambda'}\right) \end{aligned}$$

We introduce

$$\alpha = \frac{e^2}{\epsilon v_F}$$

which is usually referred to as the *effective fine structure constant* and describes the strength of Coulomb interaction in the system, in analoguous way to the fine structure constant in QED. In particular, α is the ratio between the potential energy due to electron-electron interaction and the kinetic energy, represented

by v_F. The bigger its value, the more important the interactions and viceversa.
By shifting the momentum cut-off the Hamiltonian transforms as

$$\begin{aligned} H(\Lambda') &= H(\Lambda) + \delta H_{SE} \\ &= v_F \mathbf{k}\cdot\sigma + w\mathbf{d}\cdot\mathbf{k} - \frac{\alpha}{12\pi^2}\frac{v_F}{1-\frac{w^2}{v_F^2}}\mathbf{k}\cdot\sigma\log\frac{\Lambda}{\Lambda'} \\ &= v_F\mathbf{k}\cdot\sigma\left(1-\frac{\alpha}{12\pi^2}\frac{1}{1-\frac{w^2}{v_F^2}}\log\frac{\Lambda}{\Lambda'}\right) + w\mathbf{d}\cdot\mathbf{k} \end{aligned}$$

we thus find that

$$v_F(\Lambda) = v_F\left(1-\frac{\alpha}{12\pi^2}\frac{1}{1-\frac{w^2}{v_F^2}}\log\Lambda\right) \tag{4.7}$$

The effect of the self-energy is to renormalize the Fermi velocity; this is to be expected since we know from QED that the diagram renormalizes the fermionic field and in the condensed-matter corresponding picture the only parameter of the field is the velocity of the electron. On the other hand, the tilting velocity doesn't get renormalized at all, which at a first glance may come as a surprise.
My guess is that this latter enters the Hamiltonian as a time-component term, which is even more evident by taking a look at the calculation done above. However since we assumed the potential to be instantaneous, it does not carry any time component and the tilting term does not show up in any self-energy diagram. It seems that we have to include a retardation effect in the potential in order for the term to be renormalized. This is in agreement with some recent works on graphene with tilted cones, [16].
The flow of the Fermi velocity is given by

$$\begin{aligned} \frac{d\,v_F}{d\Lambda} &= \lim_{\delta\Lambda\to 0}\frac{v_F(\Lambda)-v_F(\Lambda')}{\delta\Lambda} \\ &= \frac{\alpha v_F}{12\pi^2}\frac{1}{1-\frac{w^2}{v_F^2}}\lim_{\delta\Lambda\to 0}\frac{1}{\delta\Lambda}\log\left(\frac{\Lambda-\delta\Lambda}{\Lambda}\right) = -\frac{\alpha v_F}{12\pi^2}\frac{1}{1-\frac{w^2}{v_F^2}}\frac{1}{\Lambda} \end{aligned}$$

from which we get the RG equation,

$$\frac{d\,v_F}{d\log\Lambda} = -\frac{\alpha v_F}{12\pi^2}\frac{1}{1-\frac{w^2}{v_F^2}} \tag{4.8}$$

We can already see what the effect of the tilting is: although $\tilde{w}$ does not get renormalized itself, it contributes to the renormalization of the Hamiltonian's parameters. If we set $\tilde{w}$ to zero in eq. (4.8) we would recover the usual flow for the Fermi velocity in Weyl semimetals, [14, 30]; for non-zero values of $\tilde{w}$, instead, the flow of the parameter gets modified.

Coulomb interaction:

We saw that the only diagram that contributes is the bubble one, corresponding to the polarization function.

$$\begin{aligned} I_a(i\nu,\mathbf{q}) &= \left(\frac{e^2}{2\epsilon|\mathbf{q}|^2}\right)^2\int_0^1 dx\int_{\delta E}\frac{d^3p}{(2\pi)^3}\,\frac{x(1-x)v_F^2\mathbf{q}^2}{[v_F^2\mathbf{p}^2+x(1-x)(\nu^2+v_F^2\mathbf{q}^2)]^{3/2}} \\ &= \left(\frac{e^2}{2\epsilon|\mathbf{q}|}\right)^2\frac{1}{v_F}\int_0^1 dx\frac{x(1-x)}{\pi^2}\frac{1}{1-\frac{w^2}{v_F^2}}\log\left(\frac{\Lambda}{\Lambda'}\right) \\ &= \left(\frac{e^2}{2\epsilon|\mathbf{q}|}\right)^2\frac{1}{v_F}\frac{1}{6\pi^2}\frac{1}{1-\frac{w^2}{v_F^2}}\log\left(\frac{\Lambda}{\Lambda'}\right) \end{aligned}$$

We then find

$$\frac{e^2}{\epsilon}(\Lambda) = \frac{e^2}{2\epsilon}\left(1+\frac{\alpha}{12\pi^2}\frac{1}{1-\frac{w^2}{v_F^2}}\log\Lambda\right) \tag{4.9}$$

$$\frac{d}{d\log\Lambda}\frac{e^2}{\epsilon} = \frac{\alpha e^2}{24\pi^2\epsilon}\frac{1}{1-\frac{w^2}{v_F^2}} \tag{4.10}$$

We know that e has to be constant, because of gauge invariance; we can then recast the previous equation in terms of the dielectric constant, ϵ, which is indeed the quantity that gets renormalized,

$$\frac{d}{d\log\Lambda}\left(\frac{1}{\epsilon}\right) = -\frac{1}{\epsilon^2}\frac{d\epsilon}{d\log\Lambda}$$

$$\frac{d\epsilon}{d\log\Lambda} = -\frac{\alpha\epsilon}{24\pi^2}\frac{1}{1-\frac{w^2}{v_F^2}} \tag{4.11}$$

At last, we can study how the parameter α, which describes the interaction of the system, gets renormalized,

$$\begin{aligned}\frac{d\alpha}{d\log\Lambda} &= \frac{d}{d\log\Lambda}\left(\frac{e^2}{\epsilon v_F}\right)\\ &= -\frac{e^2}{\epsilon v_F^2}\frac{dv_F}{d\log\Lambda} - \frac{e^2}{\epsilon^2 v_F}\frac{d\epsilon}{d\log\Lambda}\\ &= \frac{\alpha^2}{12\pi^2}\frac{1}{1-\frac{w^2}{v_F^2}} + \frac{\alpha^2}{24\pi^2}\frac{1}{1-\frac{w^2}{v_F^2}}\\ &= \frac{\alpha^2}{8\pi^2}\frac{1}{1-\frac{w^2}{v_F^2}}\end{aligned} \tag{4.12}$$

We study the behavior of the Fermi velocity v_F and the coupling parameter α by solving the flow equations,

$$\begin{cases}\frac{d\,v_F}{d\log\Lambda} &= -\frac{\alpha v_F}{12\pi^2}\frac{1}{1-\frac{w^2}{v_F^2}}\\ \frac{d\alpha}{d\log\Lambda} &= \frac{\alpha^2}{8\pi^2}\frac{1}{1-\frac{w^2}{v_F^2}}\end{cases} \tag{4.13}$$

The two equations are coupled, that is, they depend on each other; thus we need an expression that relates the two of them, such that we can employ it to decouple the above system. The expression is obtained by dividing the two equations by each other,

$$\begin{aligned}\frac{d\alpha}{dv_F} &= \frac{d\alpha}{d\log\Lambda}\frac{d\log\Lambda}{dv_F}\\ &= -\frac{3\alpha}{2v_F}\end{aligned}$$

that can be recasted in the more convenient form

$$\frac{d\alpha}{\alpha} = -\frac{3}{2}\frac{dv_F}{v_F} \quad .$$

We integrate the differential equation from a larger value of the energy cut-off, Λ_0, to a smaller one, Λ. We define $v_0 = v_F(\Lambda_0)$, $\alpha_0 = \alpha(\Lambda_0)$. The value of the initial parameters can be measured experimentally: once the energy is known, Λ_0, measurements will fix the v_0 and α_0. The powerfullness of the renormalization technique lies in the fact that these parameters can be chosen at any energy of choice; once they are known, the flow equations will predict their values at any other energy scale.
Integration on both sides yields

$$\alpha(\Lambda) = \alpha_0\left(\frac{v_F(\Lambda)}{v_0}\right)^{-\frac{3}{2}} \tag{4.14}$$

This latter provides precisely the relation we were looking for and we can insert it in the previous set of equation, eqs. (4.13), to get

$$\begin{cases}\frac{d\,v_F}{d\log\Lambda} &= -\frac{\alpha v_F}{12\pi^2}\frac{1}{1-\frac{w^2}{v_F^2}}\\ \alpha(\Lambda) &= \alpha_0\left(\frac{v_F(\Lambda)}{v_0}\right)^{-\frac{3}{2}}\end{cases}$$

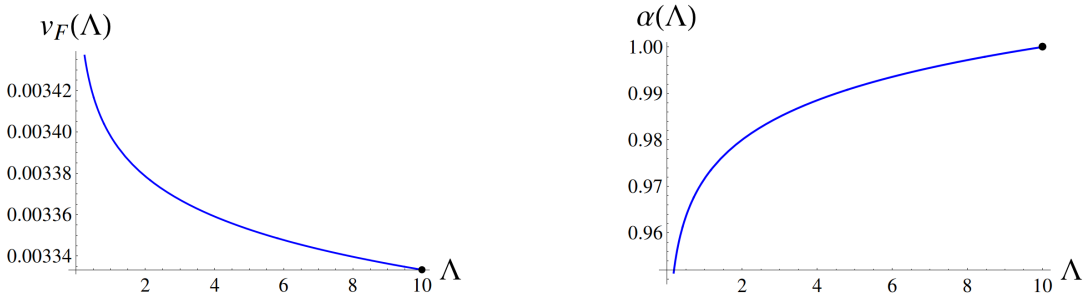

Figure 4.4: *Flow of the Fermi velocity (left) and of the coupling constant (right) for untilted WSM. The initial parameter are taken to be $\Lambda_0 = 10$, $v_0 = 1/300$, $\alpha_0 = 1$. The black dot indicates the point at which the flow starts.*

At this point we can solve for v_F, since the first equation in the system has become an ordinary differential equation,

$$\frac{d\, v_F(\Lambda)}{d \log \Lambda} = -\alpha_0 \left(\frac{v_F(\Lambda)}{v_0} \right)^{-\frac{3}{2}} \frac{v_F(\Lambda)}{12\pi^2} \frac{1}{1 - \frac{w^2}{v_F^2(\Lambda)}}$$

rearranging one finds

$$\left(\frac{v_F^2(\Lambda) - w^2}{v_F^{3/2}(\Lambda)} \right) dv_F = -\frac{\alpha_0 v_0^{3/2}}{12\pi^2} d \log \Lambda$$

then integrating both sides yields

$$\left(\frac{2}{3} v_F^{3/2} + \frac{2w^2}{v_F^{1/2}} \right) \Bigg|_{v_0}^{v_F(\Lambda)} = -\frac{\alpha_0 v_0^{3/2}}{12\pi^2} \log \frac{\Lambda}{\Lambda_0}$$

which gives

$$\frac{v_F^2(\Lambda) + 3w^2}{v_F^{1/2}(\Lambda)} = \frac{v_0^2 + 3w^2}{v_0^{1/2}} - \frac{\alpha_0 v_0^{3/2}}{8\pi^2} \log \frac{\Lambda}{\Lambda_0} \quad .$$

At this point one solves for v_F: this can be done by substitution, for instance introducing $y = v_F^{1/2}$, and results in a quartic equation, which will give four solutions. Of the four of them only one is correct and this is usually seen on the basis of physical interpretation: we know that for $w = 0$, lowering the cut-off Λ makes the Fermi velocity to grow. The solution then has to reproduce this behavior when taking the limit for $w \to 0$.
We can check the correctness of our result, so far, by setting $w = 0$; we recover the usual equation for untilted WSM,

$$v_F(\Lambda) = v_0 \left(1 - \frac{\alpha_0}{8\pi^2} \log \frac{\Lambda}{\Lambda_0} \right)^{\frac{2}{3}} \tag{4.15}$$

which diverges as Λ approaches zero. The analytic solution to the flow equations can in principle be obtained, for instance by using the method sketched earlier. However since we are interested in the modifications to the flow that the tilting term brings, we can solve the equations numerically and analyse the plots that come out of them. A set of equations like in (4.13) is easy for Mathematica; before starting we make use of eq. (4.15) to compute $\alpha(\Lambda)$ for untilted WSM and present the result in Fig. 4.4.

$$\alpha(\Lambda) = \alpha_0 \left(1 - \frac{\alpha_0}{8\pi^2} \log \frac{\Lambda}{\Lambda_0} \right)^{-1} \tag{4.16}$$

By numerically solving eqs. (4.13) we can study the flow of the parameters v_F and α when the additional tilting term is present, i.e. $\tilde{w} \neq 0$. The numerical results are reported in Fig. 4.5. As was expected, the presence of the tilting term has the effect og incresing the "velocity" at which the parameters get renormalized. It makes sense to study also how the $\tilde{w}$-dependent factor, that is introduced by the additional term in the Hamiltonian, flows. In fact this factor is the main difference between our case and the standard RG flow for a WSM. We define

$$f(\tilde{w}, \Lambda) = \frac{v_F^2(\Lambda)}{v_F^2(\Lambda) - \tilde{w}^2}$$

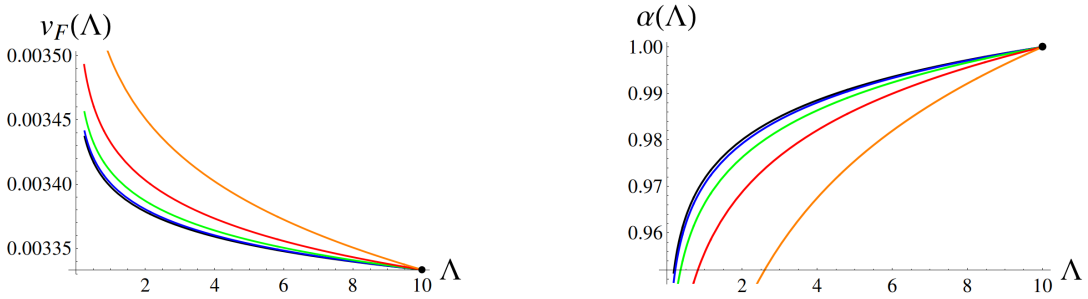

Figure 4.5: *Flow of the Fermi velocity (left) and of the coupling constant (right) for tilted WSM. The initial parameter are taken to be $\Lambda_0 = 10$, $v_0 = 1/300$, $\alpha_0 = 1$. Different colors correspond to different values of the tilting parameter, $\tilde{w} = (0 - 0.8)\, v_0$ (black to orange). The black dot indicates the point at which the flow starts.*

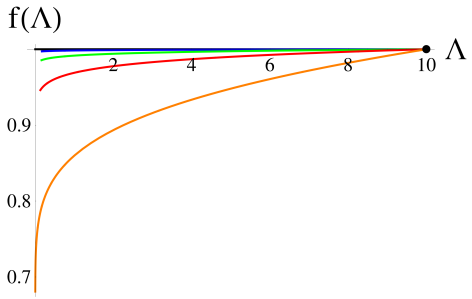

Figure 4.6: *Flow of the $f(\tilde{w}, \Lambda)/f(\tilde{w}, \Lambda_0)$. The initial parameter are taken to be $\Lambda_0 = 10$, $v_0 = 1/300$, $\alpha_0 = 1$. Different colors correspond to different values of the tilting parameter, $\tilde{w} = (0 - 0.8)\, v_0$ (black to orange). The black dot indicates the point at which the flow starts.*

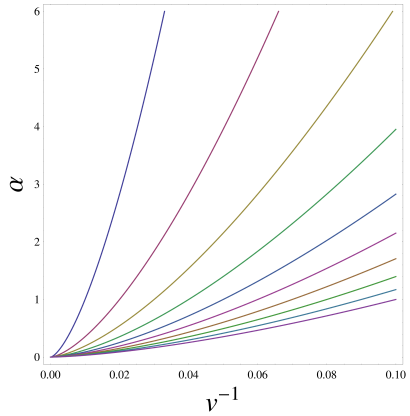

Figure 4.7: *Flow of the system's parameter α and v_F for different initial values.*

It is clear that $f(0, \Lambda) = 1$, for which one recovers the usual behavior; its flow is reported in Fig. 4.6. In order to compare the flow for different values of the tilting velocity $\tilde{w}$ we normalize $f(\tilde{w}, \Lambda)$ to its value at the point where the flow starts, i.e. $f(\tilde{w}, \Lambda_0)$.

An important information that the renormalization group analysis provides is the presence of fixed points. These latter are points to or from which the system's parameter flow and are essential in the study, for instance, of phase transitions. They constitue stable point for the theory and the flow around them determines the kind of stability: for instance if the flow is going towards a stable point, perturbations of the system around this latter will cause the system to go back to their initial state, thus the system is stable against perturbations. On the contrary, if the flow is outgoing from a fixed point, even a small perturbation will cause it to run into instabilities. The flow of the Hamiltonian's parameter in shown in Fig. 4.7, where on the horizontal axis is plotted the inverse of the Fermi velocity. As we can see the system flows towards a fixed point for which $\alpha = 0$ and $v_F \to \infty$.

4.5 Conclusions

In the Chapter we investigated the effect of the electron-electron interaction in our system by means of an energy shell renormalization scheme. We started computing the relevant, i.e. diverging, Feynman diagrams and saw that both the Fermi velocity and the coupling constant get renormalized.
In particular, there are only two relevant diagrams, both diverging logarithmically with the energy cut-off Λ: the half-oyster in Fig. 4.1 and the polarization bubble in Fig. 4.3a, corresponding to Fermi velocity and coupling constant renormalization, respectively. A very important role in our system is played by anisotropy: the introduction of an energy cut-off imposes asymmetric boundaries on the momentum region that has to be integrated, in the on-shell picture. The region becomes an ellipsoid instead of the usual spherical shell and the contribution of the diagrams depends on the shape of the deformed shell. In particular we saw that

it results in an extra factor $f(\tilde{w}) = (1 - \tilde{w}^2/v_F^2)^{-1}$ that therefore characterizes the RG equations.
The effect of this extra factor has been widely investigated, we conclude that the main change, when the additional "tilting" term is added to the Hamiltonian, is that the velocity at which both the Fermi velocity v_F and the coupling constant α gets normalized grows.
Studying the flow of the two parameters we found that the Fermi velocity grows when the cut-off is reduced, as was expected from the experience of, for instance, graphene, where the same behavior is observed. The coupling constant tends to zero when the at low energy scale, meaning our theory is, in this region, free: the electrons moves at high velocity and do not feel each other.

Chapter 5

Conclusions

In the present work we investigated several properties of systems described by eq. 1.2. In Chapter 2, after reproducing the well-established result for 3D Dirac cones, eq. (2.31), we extended it to the case of tilted Dirac cones. Our results are summarized in eqs. (2.30) and (2.29): we find that the conductivity carries a clear signature of the tilting of Dirac cones. This can be seen both in the fact that $\sigma_{\parallel} \neq \sigma_{\perp}$ and by numerical comparison with the conductivity of untilted Dirac cones, Fig. 2.2a.
In Chapter 3 we derived an analytic expression for the polarization function in the case of untilted DSM, both for the undoped and the doped cases. Although the result is not new, [36], it was derived independently by extending the result of [34] to the 3D case. In the Chapter we also investigated the behavior of the polarization function when an additional, tilting term is added to the Hamiltonian. In the case of WSM of type I we find that is possible, for $T = 0$, to relate the polarization function to the one of untilted WSM. This is also justified by reasoning in terms of the possible transitions that can take place. The latter is, as far as I am aware, a novel result.
In Chapter 4 we investigated the effect of the interactions in the system, by studying how the system's parameters renormalize. After we set up an energy-shell renormalization scheme that takes care of the anisotropy of our Hamiltonian, we studied the RG equations of our parameters. In the untilted case, $\tilde{w} = 0$, we recover the correct behavior where both the Fermi velocity v_F and the dielectric constant ϵ renormalize, eqs. (4.8) and (4.11), [14,30]. When lowering the energy cut-off the Fermi velocity grows while the coupling constant goes to zero, indicating the system becomes, at low energy, free: electrons move at high velocity and do not feel each other. Once the anysotropy is introduced in the system, it characterizes the flow equations: they now depend on the tilting "velocity", $\tilde{w}$, via a factor $f(\tilde{w}) = (1 - \tilde{w}^2/v_F^2)^{-1}$. This has the effect of increasing the velocity at which the system's parameters get renormalized, as shown in Fig. 4.5. The tilting velocity $\tilde{w}$ does not get renormalized and the system retains the same low-energy features mentioned earlier for the untilted DSM.

Appendix A

Dirac Lagrangian and Green's function

We use the Dirac Lagrangian

$$\mathcal{L} = \bar{\psi}(i\partial\!\!\!/ - m)\psi \tag{A.1}$$

where the usual Dirac notation, $\partial\!\!\!/ = \gamma^\mu \partial_\mu$ is employed and the gamma matrices are chosen as follows:

$$\{\gamma^\mu, \gamma^\nu\} = -2\eta^{\mu\nu} \ , \qquad \gamma^\mu = \begin{pmatrix} 0 & \sigma^\mu \\ \bar{\sigma}^\mu & 0 \end{pmatrix} \ , \qquad \sigma^\mu = (\mathbb{I}, \vec{\sigma}) \ , \qquad \bar{\sigma}^\mu = (\mathbb{I}, -\vec{\sigma})$$

the metric being $\eta^{\mu\nu} = \eta_{\mu\nu} = \text{diag}\{-,+,+,+\}$. The Green's function is then obtained as the two-point correlation function,

$$G(x,y) = -i\langle \mathcal{T}\,[\psi(x)\bar{\psi}(y)]\rangle = -\frac{i}{\mathcal{Z}} \int \mathcal{D}\bar{\psi}\mathcal{D}\psi \ \psi(x)\bar{\psi}(y) \ e^{\frac{i}{\hbar} S[\bar{\psi},\psi]} \tag{A.2}$$

where S represents the action,

$$S[\bar{\psi},\psi] = \int dt \mathcal{L}(t)$$

We introduce as usual auxiliary currents that couple to the fermionic fields in the Lagrangian, which now reads

$$\mathcal{L} = \bar{\psi}(i\partial\!\!\!/ - m)\psi + \bar{\psi}J + \bar{J}\psi$$

so that we can rewrite the Green's function as

$$\begin{aligned} G(x,y) &= -\frac{i}{\mathcal{Z}} \int \mathcal{D}\bar{\psi}\mathcal{D}\psi \ \ - i^2 \frac{\delta}{\delta J(y)} \frac{\delta}{\delta \bar{J}(x)} \ e^{\frac{i}{\hbar} S[\bar{\psi},\psi,\bar{J},J]} \Big|_{\bar{J}=J=0} \\ &= -\frac{i}{\mathcal{Z}} \frac{\delta}{\delta J(y)} \frac{\delta}{\delta \bar{J}(x)} \int \mathcal{D}\bar{\psi}\mathcal{D}\psi \ e^{\frac{i}{\hbar} S[\bar{\psi},\psi,\bar{J},J]} \Big|_{\bar{J}=J=0} \\ &= -\frac{\delta}{\delta J(y)} \frac{\delta}{\delta \bar{J}(x)} \log \mathcal{Z}[\bar{J},J] \Big|_{\bar{J}=J=0} \end{aligned}$$

[Note the minus that comes from the anti-commutation of the functional derivatives!]
We now focus on the action:

$$\begin{aligned} S[\bar{\psi},\psi,\bar{J},J] &= \int d^4x \ [\bar{\psi}(x)(i\partial\!\!\!/ - m)\psi(x) + \bar{\psi}(x)J(x) + \bar{J}(x)\psi(x)] \\ &= \int\int d^4x d^4y \ [\bar{\psi}(x)(i\partial\!\!\!/ - m)\delta(x-y)\psi(y) + \bar{\psi}(x)\delta(x-y)J(y) + \bar{J}(x)\delta(x-y)\psi(y)] \end{aligned}$$

Now defining the kernel $K(x,y) = (i\partial\!\!\!/ - m)\delta(x-y)$ we rewrite the action

$$S[\bar{\psi},\psi,\bar{J},J] = \int\int d^4x d^4y \left[\left(\bar{\psi}(x) + \int d^4z \bar{J}(z) K^{-1}(z,x)\right) K(x,y) \left(\psi(y) + \int d^4z' K^{-1}(y,z')J(z')\right) - \bar{J}(x)K^{-1}(x,y)J(y) \right]$$

We notice that with the above definition the action has now a term "quadratic" in the Dirac fields and an extra term quadratic in the currents. At this point we can perform the integration over the fields $\bar{\psi}$ and ψ to get the partition function:

$$\mathcal{Z}[\bar{J},J]=\int\mathcal{D}\bar{\psi}\mathcal{D}\psi\; e^{\frac{i}{\hbar}S[\bar{\psi},\psi,\bar{J},J]}=Ce^{\frac{-i}{\hbar}\int\int d^4xd^4y\;\bar{J}(x)K^{-1}(x,y)J(y)}$$

where C is a constant that we can discard since does not depend on the auxiliary currents and therefore will give no contribution.

$$G(x,y)=-K^{-1}(x,y)$$

which can be reformulated as a condition on the Green's function:

$$\int d^4z\;(i\partial\!\!\!/-m)\delta(x-z)G(z,y)=-\delta(x-y) \tag{A.3}$$

The equation is much easier in Fourier space, where $G(x,y)$ can be written

$$G(x,y)=\int\frac{d^4k}{(2\pi)^4}\;G(k)\,e^{ik\cdot(x-y)}$$

because of translational invariance. The equation boils down to

$$\begin{gathered}(k\!\!\!/+m)G(k)=-1\\ \downarrow\\ G(k)=\frac{k\!\!\!/-m}{k^2+m^2}\end{gathered} \tag{A.4}$$

Euclidean space-time

We start by observing that taking a Wick rotation, $\tau=it$, we get

$$\gamma^\mu\partial_\mu=-\gamma^0\partial_t+\vec{\gamma}\cdot\vec{\nabla}\qquad\xrightarrow{\tau=it}\qquad-i\gamma^0\partial_\tau+\vec{\gamma}\cdot\vec{\nabla}=-\gamma^0_\tau\partial_\tau+\vec{\gamma}\cdot\vec{\nabla}=(\gamma^\mu\partial_\mu)_E$$

where for convenience we introduced $\gamma^0_\tau=i\gamma^0$, to preserve the form of the scalar product. Note that with this definition we have $\{\gamma^\mu_E,\gamma^\nu_E\}=\delta^\mu\nu$, being $\delta^{\mu\nu}=\delta_{\mu\nu}=\text{diag}\{+,+,+,+\}$. The Green's function in Euclidean space-time is obtained in the path-integral formalism as

$$G_E(x,y)=-\langle\mathcal{T}_\tau\;[\psi(x)\bar{\psi}(y)]\rangle=-\frac{1}{\mathcal{Z}}\int\mathcal{D}\bar{\psi}\mathcal{D}\psi\;\psi(x)\bar{\psi}(y)\;e^{-\frac{1}{\hbar}\int d\tau\mathcal{L}(\tau)}$$

The procedure is exactly the same done before, the only difference being some "i" coefficients. In the end one finds that the Euclidean Green's function has to satisfy the equation

$$\int d^4z\;(i\partial\!\!\!/_E-m)\delta(x-z)G_E(z,y)=-\delta(x-y) \tag{A.5}$$

As done before, we can rewrite the Green's function in Fourier space, with the prescription that the imaginary part has to be expanded in Fourier series since it has periodic boundary conditions: this expansion is in fact a Matsubara expansion with fermionic frequencies

$$G_E(\tau,\vec{x};\tau',\vec{y})=\frac{1}{\beta}\sum_m\int\frac{d^3k}{(2\pi)^3}\;G(i\omega_m,\vec{k})\,e^{-i\omega_m(\tau-\tau')}\,e^{i\vec{k}\cdot(\vec{x}-\vec{y})} \tag{A.6}$$

Matsubara frequencies are defined as

$$\omega_m=\begin{cases}(2n)\pi/\beta & \text{for bosonic fields}\\ (2n+1)\pi/\beta & \text{for fermionic fields}\end{cases}$$

with $\beta^{-1}=k_BT$ and n an integer. The Green's function becomes

$$\begin{gathered}(\gamma^0_\tau\omega_m-\vec{\gamma}\cdot\vec{k}-m)\,G_E(i\omega_m,\vec{k})=-1\\ \downarrow\\ G_E(i\omega_m,\vec{k})=\frac{k\!\!\!/_E-m}{-(i\omega_m)^2+\vec{k}^2+m^2}\end{gathered} \tag{A.7}$$

The spectral function and

The spectral function reads

$$A(\omega,\mathbf{k}) = -2\mathrm{Im}C^{+}(\omega,\mathbf{k}) \tag{A.8}$$

where C^+ is the retarded correlation function. This is obtained via analytic continuation from the imaginary-time correlation function,

$$C^{\tau}(\tau,\tau') = -\Big\langle T_\tau\, \psi(\tau)\bar{\psi}(\tau')\Big\rangle = G_E(\tau,\tau')$$

In the case of free massive Dirac fields, performing analytic continuation, $i\omega_n \to \omega + i\delta$, yields

$$C^{+}(\omega,\mathbf{k}) = \frac{i\gamma^0_\tau(\omega+i\delta)+\gamma\cdot\mathbf{q}-m}{-(\omega+i\delta)^2+\mathbf{q}^2+m^2} = \frac{-\gamma^0(\omega+i\delta)+\gamma\cdot\mathbf{q}-m}{(\sqrt{\mathbf{k}^2+m^2}+\omega+i\delta)(\sqrt{\mathbf{k}^2+m^2}-\omega-i\delta)}$$

where we used that $\gamma^0_\tau = i\gamma^0$. Now using the identity $\frac{1}{AB} = \frac{1}{A+B}\left(\frac{1}{A}+\frac{1}{B}\right)$ we rewrite the denominator

$$\frac{1}{(\sqrt{\mathbf{k}^2+m^2}+\omega+i\delta)(\sqrt{\mathbf{k}^2+m^2}-\omega-i\delta)} = \frac{1}{2\sqrt{\mathbf{k}^2+m^2}}\left(\frac{1}{\sqrt{\mathbf{k}^2+m^2}+\omega+i\delta}+\right.$$
$$\left.+\frac{1}{\sqrt{\mathbf{k}^2+m^2}-\omega-i\delta}\right)$$

and we get

$$C^{+}(\omega,\mathbf{k}) = \frac{-\gamma^0(\omega+i\delta)+\gamma\cdot\mathbf{q}-m}{2\sqrt{\mathbf{k}^2+m^2}}\left(\frac{1}{\sqrt{\mathbf{k}^2+m^2}+\omega+i\delta}+\frac{1}{\sqrt{\mathbf{k}^2+m^2}-\omega-i\delta}\right)$$

Taking the limit $\delta \to 0$,

$$C^{+}(\omega,\mathbf{k}) = \frac{-\gamma^0\omega+\gamma\cdot\mathbf{q}-m}{2\sqrt{\mathbf{k}^2+m^2}}\left[P\left(\frac{1}{\sqrt{\mathbf{k}^2+m^2}+\omega}\right) - i\pi\delta(\sqrt{\mathbf{k}^2+m^2}+\omega)+\right.$$
$$\left.+P\left(\frac{1}{\sqrt{\mathbf{k}^2+m^2}-\omega}\right)+i\pi\delta(\sqrt{\mathbf{k}^2+m^2}-\omega)\right]$$

From this expression we can easily read off the spectral function, which is defined as

$$A(\omega,\mathbf{k}) = \pi\frac{\not{k}-m}{\sqrt{\mathbf{k}^2+m^2}}\left[\delta(\sqrt{\mathbf{k}^2+m^2}+\omega)-\delta(\sqrt{\mathbf{k}^2+m^2}-\omega)\right] \tag{A.9}$$

The EM kernel

Inserting eq. (A.9) in eq. (2.12),

$$K^{\mu\nu}(i\omega_n,\mathbf{k}) = -e^2\int\frac{d^3q}{(2\pi)^3}\int\frac{d\omega'}{2\pi}\int\frac{d\omega''}{2\pi}\,\mathrm{Tr}\frac{n_F(\omega'')-n_F(\omega')}{i\omega_n-\omega'+\omega''}\gamma^\mu\pi\frac{\not{k}+\not{q}-m}{\sqrt{(\mathbf{k}+\mathbf{q})^2+m^2}}\gamma^\nu\pi\frac{\not{q}-m}{\sqrt{\mathbf{q}^2+m^2}}\times$$
$$\times\left[\delta(\sqrt{(\mathbf{k}+\mathbf{q})^2+m^2}+\omega')-\delta(\sqrt{(\mathbf{k}+\mathbf{q})^2+m^2}-\omega')\right]\left[\delta(\sqrt{\mathbf{q}^2+m^2}+\omega'')-\delta(\sqrt{\mathbf{q}^2+m^2}-\omega'')\right]$$

where[1]

$$\not{k}+\not{q} = -\gamma^0\omega'+\gamma\cdot(\mathbf{k}+\mathbf{q})\,,\qquad \not{q} = -\gamma^0\omega''+\gamma\cdot\mathbf{q}$$

We trace out the gamma matrices:

$$\begin{aligned}\mathrm{Tr}\left[\gamma^\mu(\not{k}+\not{q}-m)\gamma^\nu(\not{q}-m)\right] &= \mathrm{Tr}\left[\gamma^\mu(\gamma^\sigma k_\sigma+\gamma^\sigma q_\sigma-m)\gamma^\nu(\gamma^\rho q_\rho-m)\right]\\ &= \mathrm{Tr}\left[\gamma^\mu\gamma^\sigma\gamma^\nu\gamma^\rho\right](k_\sigma+q_\sigma)q_\rho - \mathrm{Tr}\left[\gamma^\mu\gamma^\sigma\gamma^\nu\right]m(k_\sigma+2q_\sigma)+\mathrm{Tr}\left[\gamma^\mu\gamma^\nu\right]m^2\end{aligned}$$

Let's work out the trace of the above gamma matrices:

[1] Note the slight asymmetry that this definition implies!

- $\mathrm{Tr}[\gamma^\mu\gamma^\nu]$:

$$\begin{aligned}\mathrm{Tr}\left[\gamma^\mu\gamma^\nu\right] =&\mathrm{Tr}\left[-\gamma^\nu\gamma^\mu - 2\eta^{\mu\nu}\right]\\ =&-\mathrm{Tr}\left[\gamma^\nu\gamma^\mu\right] - 2\eta^{\mu\nu}\mathrm{Tr}[\mathcal{I}]\\ =&-\mathrm{Tr}\left[\gamma^\mu\gamma^\nu\right] - 8\eta^{\mu\nu}\\ &\downarrow\\ \mathrm{Tr}[\gamma^\mu\gamma^\nu] =&-4\eta^{\mu\nu}\end{aligned}$$

where we made use of the anti-commutation relation for gamma matrices, $\{\gamma^\mu,\gamma^\mu\} = -2\eta^{\mu\nu}$ and of the fact that the trace operator is invariant under cyclic permutations.

- $\mathrm{Tr}\left[\gamma^\mu\gamma^\nu\gamma^\sigma\right]$:

$$\begin{aligned}\mathrm{Tr}\left[\gamma^\mu\gamma^\nu\gamma^\sigma\right] =&\mathrm{Tr}\left[\gamma^\mu(-2\eta^{\nu\sigma} - \gamma^\sigma\gamma^\nu)\right]\\ =&-2\eta^{\nu\sigma}\mathrm{Tr}[\gamma^\mu] - \mathrm{Tr}\left[\gamma^\mu\gamma^\sigma\gamma^\nu\right]\\ =&-2\eta^{\nu\sigma}\mathrm{Tr}[\gamma^\mu] - \mathrm{Tr}\left[(-2\eta^\mu\sigma - \gamma^\sigma\gamma^\mu)\gamma^\nu\right]\\ =&-2\eta^{\nu\sigma}\mathrm{Tr}[\gamma^\mu] + 2\eta^{\mu\sigma}\mathrm{Tr}[\gamma^\nu] + \mathrm{Tr}[\gamma^\sigma\gamma^\mu\gamma^\nu]\\ &\downarrow\\ \mathrm{Tr}\left[\gamma^\mu\gamma^\nu\gamma^\sigma\right] =&0\end{aligned}$$

- $\mathrm{Tr}\left[\gamma^\mu\gamma^\sigma\gamma^\nu\gamma^\rho\right]$:

$$\begin{aligned}\mathrm{Tr}\left[\gamma^\mu\gamma^\sigma\gamma^\nu\gamma^\rho\right] =&-2\eta^{\nu\rho}\mathrm{Tr}[\gamma^\mu\gamma^\sigma] - \mathrm{Tr}[\gamma^\mu\gamma^\sigma\gamma^\rho\gamma^\nu]\\ =&-2\eta^{\nu\rho}\mathrm{Tr}[\gamma^\mu\gamma^\sigma] + 2\eta^{\sigma\rho}\mathrm{Tr}[\gamma^\mu\gamma^\nu] + \mathrm{Tr}[\gamma^\mu\gamma^\rho\gamma^\sigma\gamma^\nu]\\ =&-2\eta^{\nu\rho}\mathrm{Tr}[\gamma^\mu\gamma^\sigma] + 2\eta^{\sigma\rho}\mathrm{Tr}[\gamma^\mu\gamma^\nu] - 2\eta^{\mu\rho}\mathrm{Tr}[\gamma^\sigma\gamma^\nu] + \mathrm{Tr}[\gamma^\rho\gamma^\mu\gamma^\sigma\gamma^\nu]\\ &\downarrow\\ \mathrm{Tr}\left[\gamma^\mu\gamma^\sigma\gamma^\nu\gamma^\rho\right] =&4\eta^{\mu\sigma}\eta^{\nu\rho} - 4\eta^{\mu\nu}\eta^{\sigma\rho} + 4\eta^{\mu\rho}\eta^{\sigma\nu}\end{aligned}$$

So that we finally get

$$\begin{aligned}\mathrm{Tr}\left[\gamma^\mu(\not{k}+\not{q}-m)\gamma^\nu(\not{q}-m)\right] =&4[\eta^{\mu\sigma}\eta^{\nu\rho} - \eta^{\mu\nu}\eta^{\sigma\rho} + \eta^{\mu\rho}\eta^{\sigma\nu}](k_\sigma+q_\sigma)q_\rho - 4\eta^{\mu\nu}m^2\\ =&-4\eta^{\mu\nu}((k^\rho+q^\rho)q_\rho + m^2) + 4(k^\mu+q^\mu)q^\nu + 4(k^\nu+q^\nu)q^\mu\\ =&T^{\mu\nu}\end{aligned}$$

we will call this generic tensor $T^{\mu\nu}$ for a shorter notation.
We can thus rewrite $K^{\mu\nu}$ as

$$K^{\mu\nu}(i\omega_n,\mathbf{k}) = -e^2\int\frac{d^3q}{(2\pi)^3}\int\frac{d\omega'}{2\pi}\int\frac{d\omega''}{2\pi}\,\pi^2\frac{n_F(\omega'')-n_F(\omega')}{i\omega_n-\omega'+\omega''}\frac{T^{\mu\nu}}{\sqrt{(\mathbf{k}+\mathbf{q})^2+m^2}\sqrt{\mathbf{q}^2+m^2}}\times$$
$$\times\left[\delta(\sqrt{(\mathbf{k}+\mathbf{q})^2+m^2}+\omega') - \delta(\sqrt{(\mathbf{k}+\mathbf{q})^2+m^2}-\omega')\right]\left[\delta(\sqrt{\mathbf{q}^2+m^2}+\omega'') - \delta(\sqrt{\mathbf{q}^2+m^2}-\omega'')\right]$$

Spectral function for massless Dirac fermions with tilting term

We start from the Euclidean Green's function and perform the analytic continuation to real frequencies

$$
\begin{aligned}
G(i\omega_n,\mathbf{q},\mathbf{d}) &= \frac{1}{(i\omega_n - w\mathbf{d}\cdot\mathbf{q})^2 - v_F\mathbf{q}^2}\big[(i\omega_n - w\mathbf{d}\cdot\mathbf{q}) + v_F\tau_z\otimes(\mathbf{q}\cdot\sigma)\big] \\
&= \big[(i\omega_n - w\mathbf{d}\cdot\mathbf{q}) + v_F\tau_z\otimes(\mathbf{q}\cdot\sigma)\big]\frac{1}{2v_F|\mathbf{q}|}\left(\frac{1}{i\omega_n - w\mathbf{d}\cdot\mathbf{q} - v_F|\mathbf{q}|} - \frac{1}{i\omega_n - w\mathbf{d}\cdot\mathbf{q} + v_F|\mathbf{q}|}\right) \\
&\downarrow_{i\omega_n=\omega+i\delta} \\
G(\omega^+,\mathbf{q},\mathbf{d}) &= \lim_{\delta\to 0}\big[(\omega + i\delta - w\mathbf{d}\cdot\mathbf{q}) + v_F\tau_z\otimes(\mathbf{q}\cdot\sigma)\big]\frac{1}{2v_F|\mathbf{q}|}\left(\frac{1}{\omega + i\delta - w\mathbf{d}\cdot\mathbf{q} - v_F|\mathbf{q}|} - \right. \\
&\qquad\qquad \left. - \frac{1}{\omega + i\delta - w\mathbf{d}\cdot\mathbf{q} + v_F|\mathbf{q}|}\right) \\
&= \big[(\omega - w\mathbf{d}\cdot\mathbf{q}) + v_F\tau_z\otimes(\mathbf{q}\cdot\sigma)\big]\frac{1}{2v_F|\mathbf{q}|}\left[P\Big(\frac{1}{\omega - w\mathbf{d}\cdot\mathbf{q} - v_F|\mathbf{q}|}\Big) - P\Big(\frac{1}{\omega - w\mathbf{d}\cdot\mathbf{q} + v_F|\mathbf{q}|}\Big) - \right. \\
&\qquad \left. - i\pi\delta(\omega - w\mathbf{d}\cdot\mathbf{q} - v_F|\mathbf{q}|) + i\pi\delta(\omega - w\mathbf{d}\cdot\mathbf{q} + v_F|\mathbf{q}|)\right]
\end{aligned}
$$

From which one gets

$$
A(\omega^+,\mathbf{q},\mathbf{d}) = \frac{\pi}{v_F|\mathbf{q}|}\big[(\omega - w\mathbf{d}\cdot\mathbf{q}) + v_F\tau_z\otimes(\mathbf{q}\cdot\sigma)\big]\Big[\delta\big(\omega - w\mathbf{d}\cdot\mathbf{q} - v_F|\mathbf{q}|\big) - \delta\big(\omega - w\mathbf{d}\cdot\mathbf{q} + v_F|\mathbf{q}|\big)\Big] \quad \text{(A.10)}
$$

Appendix B

Generalized Lindhard function for graphene

We start with the expression for the polarization function,

$$\pi(i\nu,\mathbf{k}) = -\frac{2}{\beta}\sum_m \int \frac{d^2q}{(2\pi)^2}\frac{(i\nu+i\omega_m+\mu)(i\omega_m+\mu)+v_F^2(\mathbf{k}+\mathbf{q})\cdot\mathbf{q}}{\left[(i\nu+i\omega_m+\mu)^2-v_F^2(\mathbf{k}+\mathbf{q})^2\right]\left[(i\omega_m+\mu)^2-v_F^2\mathbf{q}^2\right]}$$

In order to perform the Matsubara summation, it results convenient to rewrite the integrand function and introduce a more convenient notation: we set $v_F=1$ and define $\varepsilon_q=|\mathbf{q}|$ and $\varepsilon_{q'}=|\mathbf{k}+\mathbf{q}|$

$$\frac{(i\nu+i\omega_m+\mu-\varepsilon_{q'})(i\omega_m+\mu-\varepsilon_q)+\varepsilon_{q'}(i\omega_m+\mu-\varepsilon_q)+\varepsilon_q(i\nu+i\omega_m+\mu-\varepsilon_{q'})+\varepsilon_q\varepsilon_{q'}+\mathbf{q}\cdot(\mathbf{q}+\mathbf{k})}{\left[(i\nu+i\omega_m+\mu-\varepsilon_{q'})(i\nu+i\omega_m+\mu+\varepsilon_{q'})\right]\left[(i\omega_m+\mu-\varepsilon_q)(i\omega_m+\mu+\varepsilon_q)\right]}$$

and consider each term separately:

$$\begin{aligned}
[1] &= \frac{1}{\beta}\sum_m \frac{(i\nu+i\omega_m+\mu-\varepsilon_{q'})(i\omega_m+\mu-\varepsilon_q)}{\left[(i\nu+i\omega_m+\mu-\varepsilon_{q'})(i\nu+i\omega_m+\mu+\varepsilon_{q'})\right]\left[(i\omega_m+\mu-\varepsilon_q)(i\omega_m+\mu+\varepsilon_q)\right]} \\
&= \frac{1}{\beta}\sum_m \frac{1}{(i\nu+i\omega_m+\mu+\varepsilon_{q'})(i\omega_m+\mu+\varepsilon_q)} \\
&= \frac{1}{i\nu+\varepsilon_{q'}-\varepsilon_q}\frac{1}{\beta}\sum_m\left(\frac{1}{i\omega_m+\mu+\varepsilon_q}-\frac{1}{i\omega_m+i\nu+\mu+\varepsilon_{q'}}\right) = \frac{n_F(-\varepsilon_q)-n_F(-\varepsilon_{q'})}{i\nu+\varepsilon_{q'}-\varepsilon_q}
\end{aligned}$$

$$\begin{aligned}
[2] &= \frac{1}{\beta}\sum_m \frac{\varepsilon_{q'}(i\omega_m+\mu-\varepsilon_q)}{\left[(i\nu+i\omega_m+\mu-\varepsilon_{q'})(i\nu+i\omega_m+\mu+\varepsilon_{q'})\right]\left[(i\omega_m+\mu-\varepsilon_q)(i\omega_m+\mu+\varepsilon_q)\right]} \\
&= \frac{1}{\beta}\sum_m \frac{\varepsilon_{q'}}{(i\nu+i\omega_m+\mu-\varepsilon_{q'})(i\nu+i\omega_m+\mu+\varepsilon_{q'})(i\omega_m+\mu+\varepsilon_q)} \\
&= \frac{1}{\beta}\sum_m \frac{1}{2}\frac{1}{i\omega_m+\mu+\varepsilon_q}\left(\frac{1}{i\omega_m+i\nu+\mu-\varepsilon_{q'}}-\frac{1}{i\omega_m+i\nu+\mu+\varepsilon_{q'}}\right) \\
&= \frac{1}{\beta}\sum_m \frac{1}{2}\left[\frac{1}{i\nu-\varepsilon_{q'}-\varepsilon_q}\left(\frac{1}{i\omega_m+\mu+\varepsilon_q}-\frac{1}{i\omega_m+i\nu-\mu+\varepsilon_{q'}}\right)-\right. \\
&\qquad\qquad \left.-\frac{1}{i\nu+\varepsilon_{q'}-\varepsilon_q}\left(\frac{1}{i\omega_m+\mu+\varepsilon_q}-\frac{1}{i\omega_m+i\nu+\mu+\varepsilon_{q'}}\right)\right] \\
&= \frac{1}{2}\left[\frac{n_F(-\varepsilon_q)-n_F(\varepsilon_{q'})}{i\nu-\varepsilon_{q'}-\varepsilon_q}-\frac{n_F(-\varepsilon_q)-n_F(-\varepsilon_{q'})}{i\nu+\varepsilon_{q'}-\varepsilon_q}\right]
\end{aligned}$$

$$
\begin{aligned}
[3] &= \frac{1}{\beta}\sum_m \frac{\varepsilon_q(i\nu + i\omega_m + \mu - \varepsilon_{q'})}{\left[(i\nu + i\omega_m + \mu - \varepsilon_{q'})(i\nu + i\omega_m + \mu + \varepsilon_{q'})\right]\left[(i\omega_m + \mu - \varepsilon_q)(i\omega_m + \mu + \varepsilon_q)\right]} \\
&= \frac{1}{\beta}\sum_m \frac{1}{2}\frac{1}{i\omega_m + i\nu + \mu + \varepsilon_{q'}}\left(\frac{1}{i\omega_m + \mu - \varepsilon_q} - \frac{1}{i\omega_m + \mu + \varepsilon_q}\right) \\
&= \frac{1}{\beta}\sum_m \frac{1}{2}\left[\frac{1}{i\nu + \varepsilon_{q'} + \varepsilon_q}\left(\frac{1}{i\omega_m + \mu - \varepsilon_q} - \frac{1}{i\omega_m + i\nu + \mu + \varepsilon_{q'}}\right)\right. \\
&\qquad\qquad \left. - \frac{1}{i\nu + \varepsilon_{q'} - \varepsilon_q}\left(\frac{1}{i\omega_m + \mu + \varepsilon_q} - \frac{1}{i\omega_m + i\nu + \mu + \varepsilon_{q'}}\right)\right] \\
&= \frac{1}{2}\left[\frac{n_F(\varepsilon_q) - n_F(-\varepsilon_{q'})}{i\nu + \varepsilon_{q'} + \varepsilon_q} - \frac{n_F(-\varepsilon_q) - n_F(-\varepsilon_{q'})}{i\nu + \varepsilon_{q'} - \varepsilon_q}\right]
\end{aligned}
$$

$$
\begin{aligned}
[4] &= \frac{1}{\beta}\sum_m \frac{\mathbf{q}\cdot(\mathbf{k}+\mathbf{q}) + \varepsilon_{q'}\varepsilon_q}{\left[(i\nu + i\omega_m + \mu - \varepsilon_{q'})(i\nu + i\omega_m + \mu + \varepsilon_{q'})\right]\left[(i\omega_m + \mu - \varepsilon_q)(i\omega_m + \mu + \varepsilon_q)\right]} \\
&= \frac{1}{\beta}\sum_m \frac{\mathbf{q}\cdot(\mathbf{k}+\mathbf{q}) + \varepsilon_{q'}\varepsilon_q}{4\varepsilon_q\varepsilon_{q'}}\left(\frac{1}{i\omega_m + i\nu + \mu - \varepsilon_{q'}} - \frac{1}{i\omega_m + i\nu + \mu + \varepsilon_{q'}}\right)\times \\
&\qquad\qquad \times\left(\frac{1}{i\omega_m + i\nu + \mu - \varepsilon_q} - \frac{1}{i\omega_m + i\nu + \mu + \varepsilon_q}\right) \\
&= \frac{1}{\beta}\sum_m \frac{1}{4}\left(1 + \frac{\mathbf{q}\cdot(\mathbf{k}+\mathbf{q})}{\varepsilon_q\varepsilon_{q'}}\right)\left[\frac{1}{i\nu + \varepsilon_q - \varepsilon_{q'}}\left(\frac{1}{i\omega_m + \mu - \varepsilon_q} - \frac{1}{i\omega_m + i\nu + \mu - \varepsilon_{q'}}\right) - \right. \\
&\qquad\qquad - \frac{1}{i\nu - \varepsilon_q - \varepsilon_{q'}}\left(\frac{1}{i\omega_m + \mu + \varepsilon_q} - \frac{1}{i\omega_m + i\nu + \mu - \varepsilon_{q'}}\right) - \\
&\qquad\qquad - \frac{1}{i\nu + \varepsilon_q + \varepsilon_{q'}}\left(\frac{1}{i\omega_m + \mu - \varepsilon_q} - \frac{1}{i\omega_m + i\nu + \mu + \varepsilon_{q'}}\right) + \\
&\qquad\qquad \left. + \frac{1}{i\nu - \varepsilon_q + \varepsilon_{q'}}\left(\frac{1}{i\omega_m + \mu + \varepsilon_q} - \frac{1}{i\omega_m + i\nu + \mu + \varepsilon_{q'}}\right)\right] \\
&= \frac{1 + \cos\Theta}{4}\left[\frac{n_F(\varepsilon_q) - n_F(\varepsilon_{q'})}{i\nu + \varepsilon_q - \varepsilon_{q'}} - \frac{n_F(-\varepsilon_q) - n_F(\varepsilon_{q'})}{i\nu - \varepsilon_q - \varepsilon_{q'}} - \frac{n_F(\varepsilon_q) - n_F(-\varepsilon_{q'})}{i\nu + \varepsilon_q + \varepsilon_{q'}} + \frac{n_F(-\varepsilon_q) - n_F(-\varepsilon_{q'})}{i\nu - \varepsilon_q + \varepsilon_{q'}}\right]
\end{aligned}
$$

in the latter was defined Θ to be the angle comprised between $\mathbf{q}$ and $\mathbf{k}+\mathbf{q}$. Summing up the four terms,

$$
\begin{aligned}
[1] + [2] + [3] + [4] &= \frac{1}{4}\left[\frac{n_F(\varepsilon_q) - n_F(\varepsilon_{q'})}{i\nu + \varepsilon_q - \varepsilon_{q'}} + \frac{n_F(\varepsilon_q) - n_F(-\varepsilon_{q'})}{i\nu + \varepsilon_q + \varepsilon_{q'}} + \right. \\
&\qquad \left. + \frac{n_F(-\varepsilon_q) - n_F(+\varepsilon_{q'} - \mu)}{i\nu - \varepsilon_q - \varepsilon_{q'}} + \frac{n_F(-\varepsilon_q) - n_F(-\varepsilon_{q'})}{i\nu - \varepsilon_q + \varepsilon_{q'}}\right] + \\
&\quad + \frac{\cos\Theta}{4}\left[\frac{n_F(\varepsilon_q) - n_F(\varepsilon_{q'})}{i\nu + \varepsilon_q - \varepsilon_{q'}} - \frac{n_F(\varepsilon_q) - n_F(-\varepsilon_{q'})}{i\nu + \varepsilon_q + \varepsilon_{q'}} - \right. \\
&\qquad \left. - \frac{n_F(-\varepsilon_q) - n_F(+\varepsilon_{q'} - \mu)}{i\nu - \varepsilon_q - \varepsilon_{q'}} + \frac{n_F(-\varepsilon_q) - n_F(-\varepsilon_{q'})}{i\nu - \varepsilon_q + \varepsilon_{q'}}\right]
\end{aligned}
$$

The result can be rewritten in a more compact notation,

$$
[1] + [2] + [3] + [4] = \frac{1}{4}\sum_{s,s'=\pm} \frac{n_F(s\varepsilon_q) - n_F(s'\varepsilon_{q'})}{i\nu + s\varepsilon_q - s'\varepsilon_{q'}} \times (1 + ss'\cos\Theta)
$$

We finally find the expression for the polarization function after one performs the Matsubara summation,

$$
\pi(i\nu, \mathbf{k}) = -\int \frac{d^2q}{(2\pi)^2}\sum_{s,s'=\pm} \frac{n_F(s|\mathbf{q}|) - n_F(s'|\mathbf{k}+\mathbf{q}|)}{i\nu + s|\mathbf{q}| - s'|\mathbf{k}+\mathbf{q}|}\frac{1 + ss'\cos\Theta}{2} \tag{B.1}
$$

This latter result constitues the **generalized Lindhard function** for graphene.

Generalized Lindhard function for WSM with tilted cones

We evaluate the polarizability as done before,

$$\pi(i\nu,\mathbf{q},\mathbf{d}) = -\frac{2}{\beta}\sum_m \int \frac{d^3k}{(2\pi)^3}\frac{(i\omega_m - c\mathbf{d}\cdot\mathbf{k})(i\nu + i\omega_m - c\mathbf{d}\cdot(\mathbf{k}+\mathbf{q})) + \mathbf{k}\cdot(\mathbf{k}+\mathbf{q})}{\left[(i\omega_m - c\mathbf{d}\cdot\mathbf{k})^2 - \mathbf{k}^2\right]\left[(i\omega_m + i\nu - c\mathbf{d}\cdot(\mathbf{k}+\mathbf{q}))^2 - |\mathbf{k}+\mathbf{q}|^2\right]}$$

We start rewriting the integrand function and introducing new variables $\mathbf{k}' = \mathbf{k}+\mathbf{q}$ and $\varepsilon_k = |\mathbf{k}|$

$$\frac{(i\omega_m - c\mathbf{d}\cdot\mathbf{k} - \varepsilon_k)(i\nu + i\omega_m - c\mathbf{d}\cdot\mathbf{k}' - \varepsilon_{k'}) + \varepsilon_k(i\nu + i\omega_m - c\mathbf{d}\cdot\mathbf{k}' - \varepsilon_{k'}) + \varepsilon_{k'}(i\omega_m - c\mathbf{d}\cdot\mathbf{k} - \varepsilon_k) + \mathbf{k}\cdot\mathbf{k}' - \varepsilon_k\varepsilon_{k'}}{(i\omega_n - c\mathbf{d}\cdot\mathbf{k} - \varepsilon_k)(i\omega_n - c\mathbf{d}\cdot\mathbf{k} + \varepsilon_k)(i\omega_m + i\nu - c\mathbf{d}\cdot\mathbf{k}' - \varepsilon_{k'})(i\omega_m + i\nu - c\mathbf{d}\cdot\mathbf{k}' + \varepsilon_{k'})}$$

and consider each term separately:

$$\begin{aligned}
[1] &= \sum_m \frac{(i\omega_m - c\mathbf{d}\cdot\mathbf{k} - \varepsilon_k)(i\nu + i\omega_m - c\mathbf{d}\cdot\mathbf{k}')}{(i\omega_n - c\mathbf{d}\cdot\mathbf{k} - \varepsilon_k)(i\omega_n - c\mathbf{d}\cdot\mathbf{k} + \varepsilon_k)(i\omega_m + i\nu - c\mathbf{d}\cdot\mathbf{k}' - \varepsilon_{k'})(i\omega_m + i\nu - c\mathbf{d}\cdot\mathbf{k}' + \varepsilon_{k'})} \\
&= \sum_m \frac{1}{(i\omega_n - c\mathbf{d}\cdot\mathbf{k} + \varepsilon_k)(i\omega_m + i\nu - c\mathbf{d}\cdot\mathbf{k}' + \varepsilon_{k'})} \\
&= \sum_m \frac{1}{i\nu - c\mathbf{d}\cdot\mathbf{q} - \varepsilon_k + \varepsilon_{k'}}\left(\frac{1}{i\omega_m - c\mathbf{d}\cdot\mathbf{k} + \varepsilon_k} - \frac{1}{i\omega_m + i\nu - c\mathbf{d}\cdot\mathbf{k}' + \varepsilon_{k'}}\right) \\
&= \frac{n_F(-\varepsilon_k + c\mathbf{d}\cdot\mathbf{k}) - n_F(-\varepsilon_{k'} + c\mathbf{d}\cdot\mathbf{k}')}{i\nu - c\mathbf{d}\cdot\mathbf{q} - \varepsilon_k + \varepsilon_{k'}}
\end{aligned}$$

$$\begin{aligned}
[2] &= \sum_m \frac{\varepsilon_k}{(i\omega_n - c\mathbf{d}\cdot\mathbf{k} - \varepsilon_k)(i\omega_n - c\mathbf{d}\cdot\mathbf{k} + \varepsilon_k)(i\omega_m + i\nu - c\mathbf{d}\cdot\mathbf{k}' + \varepsilon_{k'})} \\
&= \sum_m \frac{1}{2}\frac{1}{i\omega_m + i\nu - c\mathbf{d}\cdot\mathbf{k}' + \varepsilon_{k'}}\left(\frac{1}{i\omega_m - c\mathbf{d}\cdot\mathbf{k} - \varepsilon_k} - \frac{1}{i\omega_m - c\mathbf{d}\cdot\mathbf{k} + \varepsilon_k}\right) \\
&= \sum_m \frac{1}{2}\Bigg\{\frac{1}{i\nu - c\mathbf{d}\cdot\mathbf{q} + \varepsilon_k + \varepsilon_{k'}}\left(\frac{1}{i\omega_m - c\mathbf{d}\cdot\mathbf{k} - \varepsilon_k} - \frac{1}{i\nu + i\omega_m - c\mathbf{d}\cdot\mathbf{k}' + \varepsilon_{k'}}\right) - \\
&\qquad - \frac{1}{i\nu - c\mathbf{d}\cdot\mathbf{q} - \varepsilon_k + \varepsilon_{k'}}\left(\frac{1}{i\omega_m - c\mathbf{d}\cdot\mathbf{k} + \varepsilon_k} - \frac{1}{i\nu + i\omega_m - c\mathbf{d}\cdot\mathbf{k}' + \varepsilon_{k'}}\right)\Bigg\} \\
&= \frac{1}{2}\left[\frac{n_F(\varepsilon_k + c\mathbf{d}\cdot\mathbf{k}) - n_F(-\varepsilon_{k'} + c\mathbf{d}\cdot\mathbf{k}')}{i\nu - c\mathbf{d}\cdot\mathbf{q} + \varepsilon_k + \varepsilon_{k'}} - \frac{n_F(-\varepsilon_k + c\mathbf{d}\cdot\mathbf{k}) - n_F(-\varepsilon_{k'} + c\mathbf{d}\cdot\mathbf{k}')}{i\nu - c\mathbf{d}\cdot\mathbf{q} - \varepsilon_k + \varepsilon_{k'}}\right]
\end{aligned}$$

$$\begin{aligned}
[3] &= \sum_m \frac{\varepsilon_{k'}}{(i\omega_n - c\mathbf{d}\cdot\mathbf{k} + \varepsilon_k)(i\omega_m + i\nu - c\mathbf{d}\cdot\mathbf{k}' + \varepsilon_{k'})(i\omega_m + i\nu - c\mathbf{d}\cdot\mathbf{k}' - \varepsilon_{k'})} \\
&= \sum_m \frac{1}{2}\Bigg\{\frac{1}{i\nu - c\mathbf{d}\cdot\mathbf{q} - \varepsilon_k - \varepsilon_{k'}}\left(\frac{1}{i\omega_m - c\mathbf{d}\cdot\mathbf{k} + \varepsilon_k} - \frac{1}{i\nu + i\omega_m - c\mathbf{d}\cdot\mathbf{k}' - \varepsilon_{k'}}\right) - \\
&\qquad - \frac{1}{i\nu - c\mathbf{d}\cdot\mathbf{q} - \varepsilon_k + \varepsilon_{k'}}\left(\frac{1}{i\omega_m - c\mathbf{d}\cdot\mathbf{k} + \varepsilon_k} - \frac{1}{i\nu + i\omega_m - c\mathbf{d}\cdot\mathbf{k}' + \varepsilon_{k'}}\right)\Bigg\} \\
&= \frac{1}{2}\left[\frac{n_F(-\varepsilon_k + c\mathbf{d}\cdot\mathbf{k}) - n_F(\varepsilon_{k'} + c\mathbf{d}\cdot\mathbf{k}')}{i\nu - c\mathbf{d}\cdot\mathbf{q} - \varepsilon_k - \varepsilon_{k'}} - \frac{n_F(-\varepsilon_k + c\mathbf{d}\cdot\mathbf{k}) - n_F(-\varepsilon_{k'} + c\mathbf{d}\cdot\mathbf{k}')}{i\nu - c\mathbf{d}\cdot\mathbf{q} - \varepsilon_k + \varepsilon_{k'}}\right]
\end{aligned}$$

$$
\begin{aligned}
[4] &= \sum_m \frac{\mathbf{k}\cdot\mathbf{k}' - \varepsilon_k\varepsilon_{k'}}{\varepsilon_k\varepsilon_{k'}} \left(\frac{1}{i\nu + i\omega_m - c\mathbf{d}\cdot\mathbf{k}' - \varepsilon_{k'}} - \frac{1}{i\nu + i\omega_m - c\mathbf{d}\cdot\mathbf{k}' + \varepsilon_{k'}}\right)\left(\frac{1}{i\omega_m - c\mathbf{d}\cdot\mathbf{k} - \varepsilon_k} - \frac{1}{i\omega_m - c\mathbf{d}\cdot\mathbf{k} + \varepsilon_k}\right) \\
&= \sum_m \frac{\cos\Theta - 1}{4}\Bigg\{ \frac{1}{i\nu - c\mathbf{d}\cdot\mathbf{q} + \varepsilon_k - \varepsilon_{k'}}\left(\frac{1}{i\omega_m - c\mathbf{d}\cdot\mathbf{k} - \varepsilon_k} - \frac{1}{i\nu + i\omega_m - c\mathbf{d}\cdot\mathbf{k}' - \varepsilon_{k'}}\right) - \\
&\qquad - \frac{1}{i\nu - c\mathbf{d}\cdot\mathbf{q} - \varepsilon_k - \varepsilon_{k'}}\left(\frac{1}{i\omega_m - c\mathbf{d}\cdot\mathbf{k} + \varepsilon_k} - \frac{1}{i\nu + i\omega_m - c\mathbf{d}\cdot\mathbf{k}' - \varepsilon_{k'}}\right) - \\
&\qquad - \frac{1}{i\nu - c\mathbf{d}\cdot\mathbf{q} + \varepsilon_k + \varepsilon_{k'}}\left(\frac{1}{i\omega_m - c\mathbf{d}\cdot\mathbf{k} - \varepsilon_k} - \frac{1}{i\nu + i\omega_m - c\mathbf{d}\cdot\mathbf{k}' + \varepsilon_{k'}}\right) + \\
&\qquad + \frac{1}{i\nu - c\mathbf{d}\cdot\mathbf{q} - \varepsilon_k + \varepsilon_{k'}}\left(\frac{1}{i\omega_m - c\mathbf{d}\cdot\mathbf{k} + \varepsilon_k} - \frac{1}{i\nu + i\omega_m - c\mathbf{d}\cdot\mathbf{k}' + \varepsilon_{k'}}\right)\Bigg\}
\end{aligned}
$$

where Θ is the angle between $\mathbf{k}$ and $\mathbf{k}'$. Summing all the terms up, we get

$$
[1] + [2] + [3] + [4] = \frac{1}{4}\sum_{s,s'=\pm1} \frac{n_F(s\varepsilon_k + c\mathbf{d}\cdot\mathbf{k}) - n_F(s'\varepsilon_{k'} + c\mathbf{d}\cdot\mathbf{k}')}{i\nu - c\mathbf{d}\cdot\mathbf{q} + s\varepsilon_k - s'\varepsilon_{k'}} \times (1 + ss'\cos\Theta)
$$

Finally, we can rewrite the polarization function as

$$
\pi(i\nu, \mathbf{q}, \mathbf{d}) = -\int \frac{d^3k}{(2\pi)^3} \sum_{s,s'=\pm1} \frac{n_F(s|\mathbf{k}| + c\mathbf{d}\cdot\mathbf{k}) - n_F(s'|\mathbf{k}+\mathbf{q}| + c\mathbf{d}\cdot(\mathbf{k}+\mathbf{q}))}{i\nu - c\mathbf{d}\cdot\mathbf{q} + s|\mathbf{k}| - s'|\mathbf{k}+\mathbf{q}|} \times \frac{1 + ss'\cos\Theta}{2} \tag{B.2}
$$

Calculation polarization function graphene

Imaginary part

$$
I^{\alpha\beta}(\mathbf{k}, \mathbf{q}) = \frac{\alpha k}{2}\int_0^{2\pi} d\theta \left(1 + \beta\frac{k + q\cos\theta}{\sqrt{k^2 + q^2 + 2kq\cos\theta}}\right)\delta\big(\nu + \alpha(k - \beta\sqrt{k^2 + q^2 + 2kq\cos\theta})\big)
$$

The integral is non-zero as long as a solution to the delta function exists and lies within the codomain of the cosine function, $[-1, 1]$.

$$
\nu + \alpha(k - \beta\sqrt{k^2 + q^2 + 2kq\cos\theta}) = 0 \qquad \longrightarrow \qquad \sqrt{k^2 + q^2 + 2kq\cos\theta} = \beta(\alpha\nu + k)
$$

- if $\beta(\alpha\nu + k) > 0$,

$$
\cos\theta = \frac{\nu^2 + 2\alpha\nu k - q^2}{2kq}
$$

Note that the solutions to the previous always come in pairs, because of the periodicity of the cosine function: we shall multiply the result by a factor 2. We incorporate the above conditions in the final result by means of Heaviside functions; for now we will assume that a solution exists and we carry out the integration.

$$
\begin{aligned}
I^{\alpha\beta}(\mathbf{k}, \mathbf{q}) &= \alpha k \int \frac{-d\cos\theta}{\sqrt{1 - \cos^2\theta}}\left(1 + \beta\frac{k + q\cos\theta}{\sqrt{k^2 + q^2 + 2kq\cos\theta}}\right)\left|\frac{\beta(\alpha\nu + k)}{-\alpha\beta kq}\right|\delta\left(\cos\theta - \frac{\nu^2 + 2\alpha\nu k - q^2}{2kq}\right) \\
&= \alpha k \frac{2kq}{\sqrt{4k^2q^2 - (\nu^2 + 2\alpha\nu k - q^2)^2}}\left(1 + \frac{2k^2 + \nu^2 + 2\alpha\nu k - q^2}{2k(\alpha\nu + k)}\right)\frac{\alpha\nu + k}{kq} \\
&= \alpha k \frac{2kq}{\sqrt{q^2 - \nu^2}\sqrt{(2\alpha k + \nu)^2 - q^2}}\,\frac{(2\alpha k + \nu)^2 - q^2}{2k(\alpha\nu + k)}\,\frac{\alpha\nu + k}{kq} \\
&= \alpha\sqrt{\frac{(2\alpha k + \nu)^2 - q^2}{q^2 - \nu^2}}
\end{aligned}
$$

then the full result after the angle integration reads

$$I^{\alpha\beta}(\mathbf{k},\mathbf{q}) = \alpha\sqrt{\frac{(2\alpha k+\nu)^2-q^2}{q^2-\nu^2}} \times \theta(\beta(\alpha\nu+k))\theta\left(1-\left(\frac{\nu^2+2\alpha\nu k-q^2}{2kq}\right)^2\right) \tag{B.3}$$

Before the momentum integration we rewrite the Heaviside functions in a more convenient form; first of all we note that

$$\begin{aligned}\theta\left(1-\left(\frac{\nu^2+2\alpha\nu k-q^2}{2kq}\right)^2\right) &= \theta\left(1-\frac{\nu^2+2\alpha\nu k-q^2}{2kq}\right)\theta\left(1+\frac{\nu^2+2\alpha\nu k-q^2}{2kq}\right)\\ &= \theta\left(k(q-\alpha\nu)-\frac{(\nu+q)(\nu-q)}{2}\right)\theta\left(k(q+\alpha\nu)+\frac{(\nu+q)(\nu-q)}{2}\right)\end{aligned}$$

and we study the different cases separately. In the following the reader has to keep in mind that by definition $k,\ q,\ \nu$ are positive quantities.

- $\alpha = 1$:

$$\begin{cases}\theta(\beta(\alpha\nu+k))\\ \theta\left(k(q-\alpha\nu)-\frac{(\nu+q)(\nu-q)}{2}\right)\\ \theta\left(k(q+\alpha\nu)+\frac{(\nu+q)(\nu-q)}{2}\right)\end{cases} \quad\rightarrow\quad \begin{cases}\theta(\beta)\\ \theta\left(q-\nu\right)\\ \theta\left(k-\frac{q-\nu}{2}\right)\end{cases}$$

  thus the full condition for $\alpha = 1$ reads

$$\theta(\beta)\theta\left(q-\nu\right)\theta\left(k-\frac{q-\nu}{2}\right)$$

- $\alpha = -1$:

$$\begin{cases}\theta(\beta(\alpha\nu+k))\\ \theta\left(k(q-\alpha\nu)-\frac{(\nu+q)(\nu-q)}{2}\right)\\ \theta\left(k(q+\alpha\nu)+\frac{(\nu+q)(\nu-q)}{2}\right)\end{cases} \quad\rightarrow\quad \begin{cases}\theta(\beta)\theta(k-\nu)+\theta(-\beta)\theta(\nu-k)\\ \theta\left(k-\frac{\nu-q}{2}\right)\\ \theta(q-\nu)\theta\left(k-\frac{q+\nu}{2}\right)+\theta(\nu-q)\theta\left(\frac{q+\nu}{2}-k\right)\end{cases}$$

  thus the full condition for $\alpha = -1$ reads

$$\left[\theta(\beta)\theta(k-\nu)+\theta(-\beta)\theta(\nu-k)\right]\theta\left(k-\frac{\nu-q}{2}\right)\left[\theta(q-\nu)\theta\left(k-\frac{q+\nu}{2}\right)+\theta(\nu-q)\theta\left(\frac{q+\nu}{2}-k\right)\right]$$

  Let's work out a bit further this latter term to make it simpler:

  - $\beta = 1$:

$$\theta(k-\nu)\theta\left(k-\frac{\nu-q}{2}\right)\left[\theta(q-\nu)\theta\left(k-\frac{q+\nu}{2}\right)+\theta(\nu-q)\theta\left(\frac{q+\nu}{2}-k\right)\right]$$

    The second term in the product is just zero since $k>\nu>q$ implies $2k>q+\nu$.

  - $\beta = -1$:

$$\theta(\nu-k)\theta\left(k-\frac{\nu-q}{2}\right)\left[\theta(q-\nu)\theta\left(k-\frac{q+\nu}{2}\right)+\theta(\nu-q)\theta\left(\frac{q+\nu}{2}-k\right)\right]$$

    The first term in the product is zero since $q>\nu>k$ and thus $2k<q+\nu$. The second term reads

$$\theta\left(k-\frac{\nu-q}{2}\right)\theta(\nu-q)\theta\left(\frac{q+\nu}{2}-k\right)$$

    where a redundant condition was dropped. We can rewrite it by exploiting the properties of the Heaviside function as

$$\theta(\nu-q)\left[\theta\left(\frac{q+\nu}{2}-k\right)-\theta\left(\frac{\nu-q}{2}-k\right)\theta\left(\frac{q+\nu}{2}-k\right)\right] = \theta(\nu-q)\left[\theta\left(\frac{q+\nu}{2}-k\right)-\theta\left(\frac{\nu-q}{2}-k\right)\right]$$

We found the final result to be

$$\theta(\alpha)\theta(\beta)\theta(q-\nu)\theta\left(k-\frac{q-\nu}{2}\right)+\theta(-\alpha)\left\{\theta(\beta)\theta(q-\nu)\theta\left(k-\frac{q+\nu}{2}\right)+\right.$$
$$\left.+\theta(-\beta)\theta(\nu-q)\left[\theta\left(\frac{q+\nu}{2}-k\right)-\theta\left(\frac{\nu-q}{2}-k\right)\right]\right\}$$

that we may rewrite as

$$\theta(\beta)\theta(q-\nu)\theta\left(k-\frac{q-\alpha\nu}{2}\right)+\theta(-\alpha)\theta(-\beta)\theta(\nu-q)\left[\theta\left(\frac{q+\nu}{2}-k\right)-\theta\left(\frac{\nu-q}{2}-k\right)\right] \tag{B.4}$$

Now that we have simplified the Heaviside functions we can proceed with the momentum integration. Summarizing the results so far we have simplified eq. (B.3) and obtained

$$I^{\alpha\beta}(\mathbf{k},\mathbf{q})=\alpha\sqrt{\frac{(2\alpha k+\nu)^2-q^2}{q^2-\nu^2}}\times\left\{\theta(\beta)\theta(q-\nu)\theta\left(k-\frac{q-\alpha\nu}{2}\right)+\right.$$
$$\left.+\theta(-\alpha)\theta(-\beta)\theta(\nu-q)\left[\theta\left(\frac{q+\nu}{2}-k\right)-\theta\left(\frac{\nu-q}{2}-k\right)\right]\right\}$$

Real part

$$\mathrm{Re}\left[\Delta\pi(\nu,\mathbf{q})\right]=-\frac{1}{4\pi^2}\int_0^{\mu}dk\sum_{\alpha=\pm}J^{\alpha}(\nu,\mathbf{k},\mathbf{q})$$

We switch to polar coordinates and perform the integration over the angle variable; we start by working out the RHS of eq. (3.13)

$$\begin{aligned}
\int_0^{2\pi}d\theta\,k\frac{\alpha\nu+2k+q\cos\theta}{(\nu+\alpha k+i\varepsilon)^2-k^2-q^2-2kq\cos\theta}&=\int_0^{2\pi}d\theta\,k\frac{\alpha\nu+2k+q\cos\theta}{(\nu^2+2\alpha\nu k-q^2)+i\varepsilon(\nu+\alpha k)-2kq\cos\theta}\\
&=\int_0^{2\pi}d\theta\,k\frac{q}{-2kq}\frac{\frac{\alpha\nu+2k}{q}+\cos\theta}{\frac{\nu^2+2\alpha\nu k-q^2+i\varepsilon(\nu+\alpha k)}{-2kq}+\cos\theta}\\
&=-\frac{1}{2}\int_0^{2\pi}d\theta\,\frac{\frac{\alpha\nu+2k}{q}+\cos\theta}{z+\cos\theta}\\
&=-\frac{1}{2}\int_0^{2\pi}d\theta\left(1+\frac{\frac{\alpha\nu+2k}{q}-z}{z+\cos\theta}\right)\\
&=-\pi-\frac{1}{2}\left(\frac{(2\alpha k+\nu)^2-q^2}{2kq}\right)\int_0^{2\pi}d\theta\,\frac{1}{z+\cos\theta}
\end{aligned}$$

where has been defined the parameter $z=\frac{\nu^2+2\alpha\nu k-q^2+i\varepsilon(\nu+\alpha k)}{-2kq}$. We now use the result given in eq. (3.12) to obtain:

$$\int_0^{2\pi}d\theta\,\frac{1}{z+\cos\theta}=2\pi\sqrt{\frac{4k^2q^2}{(\nu^2-q^2)((\nu+2\alpha k)^2-q^2)}}\left[\theta\left(\left(\frac{\nu^2+2\alpha\nu k-q^2}{-2kq}\right)^2-1\right)\mathrm{sgn}\left(\left(\frac{\nu^2+2\alpha\nu k-q^2}{-2kq}\right)\right)\right.$$
$$\left.\pm i\,\mathrm{sgn}(\nu+\alpha k)\theta\left(1-\left(\frac{\nu^2+2\alpha\nu k-q^2}{-2kq}\right)^2\right)\right]$$

Plugging the result in eq. (3.14) one gets

$$J^{\alpha}(\nu,\mathbf{k},\mathbf{q})=-\pi-\pi\sqrt{\frac{(2\alpha k+\nu)^2-q^2)}{\nu^2-q^2}}\theta\left(\left(\frac{\nu^2+2\alpha\nu k-q^2}{-2kq}\right)^2-1\right)\mathrm{sgn}\left(\left(\frac{\nu^2+2\alpha\nu k-q^2}{-2kq}\right)\right) \tag{B.5}$$

As done before, we rearrange the RHS of the equation by rewriting the Heaviside functions in a more convenient form

$$\theta\left(\left(\frac{\nu^2+2\alpha\nu k-q^2}{-2kq}\right)^2-1\right)=\theta\left(q^2-\nu^2-2\alpha\nu k-2kq\right)+\theta\left(\nu^2+2\alpha\nu k-q^2-2kq\right)$$

we proceed by splitting the analysis for the different values of α. Here is also important to keep an eye on the the sign function (we associate for each are delimited by the Heaviside function the respective value of the sign function):
Heaviside functions

- $\alpha = 1$:

$$\begin{cases} \theta\left(\frac{(q-\nu)(q+\nu)}{2} - k(\alpha\nu + q)\right) \\ \theta\left(\frac{(\nu-q)(\nu+q)}{2} + k(\alpha\nu - q)\right) \end{cases} \quad \rightarrow \quad \begin{cases} \theta\left(\frac{q-\nu}{2} - k\right) \\ \theta\left(\nu - q\right) \end{cases}$$

- $\alpha = -1$:

$$\begin{cases} \theta\left(\frac{(q-\nu)(q+\nu)}{2} - k(\alpha\nu + q)\right) \\ \theta\left(\frac{(\nu-q)(\nu+q)}{2} + k(\alpha\nu - q)\right) \end{cases} \quad \rightarrow \quad \begin{cases} \theta(q-\nu)\theta\left(\frac{q+\nu}{2} - k\right) + \theta(\nu - q)\theta\left(k - \frac{q+\nu}{2}\right) \\ \theta\left(\frac{\nu-q}{2} - k\right) \end{cases}$$

Sign function:

	$q > \nu$	$\nu > q$	
		$\frac{\nu-q}{2} > k$	$k > \frac{\nu+q}{2}$
$\alpha = 1$	$+1$	-1	
$\alpha = -1$	$+1$	-1	$+1$

Combining what found for the Heaviside function and for the sign function, we get the final expression for J^α,

$$J^\alpha(\mathbf{k}, \mathbf{q}) = -\pi + \pi\sqrt{\frac{(2\alpha k + \nu)^2 - q^2}{\nu^2 - q^2}} \left\{ \theta(q-\nu)\theta\left(\frac{q - \alpha\nu}{2} - k\right) + \right.$$
$$\left. + \theta(\nu - q)\left[\theta(\alpha) + \theta(-\alpha)\left(\theta\left(\frac{\nu - q}{2} - k\right) - \theta\left(k - \frac{\nu + q}{2}\right)\right)\right]\right\}$$

Appendix C

Self-energy diagram

$$\begin{aligned}\Sigma(i\omega,\mathbf{q}) &= \frac{e^2}{2\epsilon}\int\frac{d\nu}{2\pi}\int\frac{d^3k}{(2\pi)^3}\,\frac{i\omega_n+i\nu-w\mathbf{d}\cdot(\mathbf{k}+\mathbf{q})+v_F(\mathbf{k}+\mathbf{q})\cdot\sigma}{(i\omega_n+i\nu-w\mathbf{d}\cdot(\mathbf{k}+\mathbf{q}))^2-v_F^2|\mathbf{k}+\mathbf{q}|^2}\,\frac{1}{\mathbf{k}^2}\\ &= \frac{e^2}{2\epsilon}\int\frac{d\nu}{2\pi}\int\frac{d^3k}{(2\pi)^3}\,\frac{i\nu-w\mathbf{d}\cdot\mathbf{k}+v_F\mathbf{k}\cdot\sigma}{(i\nu-w\mathbf{d}\cdot\mathbf{k})^2-v_F^2|\mathbf{k}|^2}\,\frac{1}{|\mathbf{k}-\mathbf{q}|^2}\\ &= \frac{e^2}{2\epsilon}\int\frac{d^3k}{(2\pi)^3}\,\frac{1}{|\mathbf{k}-\mathbf{q}|^2}\int\frac{d\nu}{2\pi}\,\frac{i\nu-w\mathbf{d}\cdot\mathbf{k}+v_F\mathbf{k}\cdot\sigma}{(i\nu-w\mathbf{d}\cdot\mathbf{k})^2-v_F^2|\mathbf{k}|^2}\end{aligned}$$

we focus on the second integral:

$$\int_{-\infty}^{\infty}\frac{d\nu}{2\pi}\,\frac{i\nu-w\mathbf{d}\cdot\mathbf{k}+\mathbf{k}\cdot\sigma}{(i\nu-w\mathbf{d}\cdot\mathbf{k})^2-|\mathbf{k}|^2}=\int\limits_{-\infty+iw\mathbf{dk}}^{\infty+iw\mathbf{dk}}\frac{d\nu}{2\pi}\,-\frac{i\nu+\mathbf{k}\cdot\sigma}{\nu^2+|\mathbf{k}|^2}$$

We make use of the following identities:

$$\int dx\,\frac{x}{x^2+a^2}=\frac{1}{2}\log(x^2+a^2)$$
$$\int dx\,\frac{1}{x^2+a^2}=\frac{1}{2a}i\log\left(\frac{a-ix}{a+ix}\right)$$

Since the integral is divergent we introduce a hard cut-off Λ that will be removed later on:

$$\int\limits_{-\Lambda+iw\mathbf{dk}}^{\Lambda+iw\mathbf{dk}}\frac{d\nu}{2\pi}\,-\frac{i\nu+\mathbf{k}\cdot\sigma}{\nu^2+|\mathbf{k}|^2}=\frac{1}{2\pi}\left\{\frac{-i}{2}\log\left(\frac{(\Lambda+iw\mathbf{d}\cdot\mathbf{k})^2+|\mathbf{k}|^2}{(-\Lambda+iw\mathbf{d}\cdot\mathbf{k})^2+|\mathbf{k}|^2}\right)-i\frac{\mathbf{k}\cdot\sigma}{2|\mathbf{k}|}\left[\log\left(\frac{|\mathbf{k}|-i(\Lambda+iw\mathbf{d}\cdot\mathbf{k})}{|\mathbf{k}|+i(\Lambda+iw\mathbf{d}\cdot\mathbf{k})}\right)-\right.\right.$$
$$\left.\left.-\log\left(\frac{|\mathbf{k}|-i(-\Lambda+iw\mathbf{d}\cdot\mathbf{k})}{|\mathbf{k}|+i(-\Lambda+iw\mathbf{d}\cdot\mathbf{k})}\right)\right]\right\}$$

rearranging the arguments of the logarithms we get

$$\int\limits_{-\Lambda+iw\mathbf{dk}}^{\Lambda+iw\mathbf{dk}}\frac{d\nu}{2\pi}\,-\frac{i\nu+\mathbf{k}\cdot\sigma}{\nu^2+|\mathbf{k}|^2}=\frac{1}{2\pi}\left\{\frac{-i}{2}\log\left(\frac{\Lambda^2+|\mathbf{k}|^2-w^2(\mathbf{d}\cdot\mathbf{k})^2+2i\Lambda w\mathbf{d}\cdot\mathbf{k}}{\Lambda^2+|\mathbf{k}|^2-w^2(\mathbf{d}\cdot\mathbf{k})^2-2i\Lambda w\mathbf{d}\cdot\mathbf{k}}\right)-i\frac{\mathbf{k}\cdot\sigma}{2|\mathbf{k}|}\left[\log\left(\frac{|\mathbf{k}|+w\mathbf{d}\cdot\mathbf{k}-i\Lambda}{|\mathbf{k}|+w\mathbf{d}\cdot\mathbf{k}+i\Lambda}\right)-\right.\right.$$
$$\left.\left.-\log\left(\frac{|\mathbf{k}|-w\mathbf{d}\cdot\mathbf{k}+i\Lambda}{|\mathbf{k}|-w\mathbf{d}\cdot\mathbf{k}-i\Lambda}\right)\right]\right\}$$

the logarithms can be simplified further by expressing their arguments in polar coordinates:

$$\log\left(\frac{a+ib}{a-ib}\right)=\log\left(\frac{\sqrt{a^2+b^2}\,e^{i\mathrm{Atan}(b/a)}}{\sqrt{a^2+b^2}\,e^{-i\mathrm{Atan}(b/a)}}\right)=2i\mathrm{Atan}\left(\frac{b}{a}\right)$$

$$\int\limits_{-\Lambda+iw\mathbf{dk}}^{\Lambda+iw\mathbf{dk}}\frac{d\nu}{2\pi}\,-\frac{i\nu+\mathbf{k}\cdot\sigma}{\nu^2+|\mathbf{k}|^2}=\frac{1}{2\pi}\mathrm{Atan}\left(\frac{2\Lambda w\mathbf{d}\cdot\mathbf{k}}{\Lambda^2+|\mathbf{k}|^2-w^2(\mathbf{d}\cdot\mathbf{k})^2}\right)-\frac{\mathbf{k}\cdot\sigma}{2\pi|\mathbf{k}|}\left[\mathrm{Atan}\left(\frac{\Lambda}{|\mathbf{k}|+w\mathbf{d}\cdot\mathbf{k}}\right)+\mathrm{Atan}\left(\frac{\Lambda}{|\mathbf{k}|-w\mathbf{d}\cdot\mathbf{k}}\right)\right]$$

taking the limit for $\Lambda \to \infty$ we find the result

$$\int_{-\infty}^{\infty} \frac{d\nu}{2\pi} \frac{i\nu - w\mathbf{d}\cdot\mathbf{k} + \mathbf{k}\cdot\sigma}{(i\nu - w\mathbf{d}\cdot\mathbf{k})^2 - |\mathbf{k}|^2} = -\frac{\mathbf{k}\cdot\sigma}{2|\mathbf{k}|} \tag{C.1}$$

and the self-energy reads

$$\Sigma(\omega, \mathbf{q}) = -\frac{e^2}{4\epsilon v_F} \int \frac{d^3k}{(2\pi)^3} \frac{\mathbf{k}\cdot\sigma}{|\mathbf{k}||\mathbf{k}-\mathbf{q}|^2} \tag{C.2}$$

Integration within an ellipsoidal domain

We here compute the contribution that comes out from integrating an energy shell which has ellipsoidal boundaries.

$$\int_E \frac{d^3p}{(2\pi^3)} \frac{p^{N-3}}{(p^2+D^2)^{N/2}} \qquad , \quad D^2 > 0 \tag{C.3}$$

where E is a 3D ellipsoid solution of

$$\Lambda = \pm\sqrt{p_x^2 + p_y^2 + p_z^2} + wp_z$$

Depending on the sign of the cut-off Λ, we have two solutions, namely

$$\begin{cases} \Lambda & = \sqrt{p_x^2 + p_y^2 + p_z^2} + wp_z \\ -\Lambda & = -\sqrt{p_x^2 + p_y^2 + p_z^2} + wp_z \end{cases}$$

being $\Lambda > 0$. Luckily the two solutions are symmetric under the trasformation $w \to -w$, therefore we shall focus only on the first one. Notice that this implies that odd term in the integral can be dropped, since they give zero contribution, e.g. what assumed for the self-energy. We group the cut-off with the tilting term and square both sides,

$$(\Lambda - wp_z)^2 = p_x^2 + p_y^2 + p_z^2$$

$$\Lambda = p_x^2 + p_y^2 + (1-w^2)p_z^2 + 2\Lambda w p_z$$

we complete the square on the RHS and rearrange the equation to get

$$\frac{p_x^2 + p_y^2}{1-w^2} + \left(p_z + \frac{w\Lambda}{1-w^2}\right)^2 = \frac{\Lambda^2}{(1-w^2)^2}$$

Now rescale and shift momentum variables, $p_{x,y} \to \sqrt{1-w^2}\, p_{x,y}$ and $p_z \to p_z - \frac{w\Lambda}{1-w^2}$,

$$p_x^2 + p_y^2 + p_z^2 = \frac{\Lambda^2}{(1-w^2)^2}$$

which correspond to

$$\int_E \frac{d^3p}{(2\pi)^3} f(p_x, p_y, p_z) \quad \to \quad (1-w^2) \int_S \frac{d^3p}{(2\pi)^3} f\left(\sqrt{1-w^2}\, p_x, \sqrt{1-w^2}\, p_y, p_z - \frac{w\Lambda}{1-w^2}\right)$$

That is, the integration within an ellipsoid turned into an integration within a sphere S of radius $R = \frac{\Lambda}{1-w^2}$ and we can switch to spherical coordinates. Going back to eq. (C.3),

$$\int_E \frac{d^3p}{(2\pi^3)} \frac{(p_x^2+p_y^2+p_z^2)^{(N-3)/2}}{(p_x^2+p_y^2+p_z^2+D^2)^{N/2}} = \int_S \frac{d^3p}{(2\pi^3)} (1-w^2) \frac{\left((1-w^2)(p_x^2+p_y^2) + (p_z - \frac{w\Lambda}{1-w^2})^2\right)^{(N-3)/2}}{\left((1-w^2)(p_x^2+p_y^2) + (p_z - \frac{w\Lambda}{1-w^2})^2 + D^2\right)^{N/2}}$$

$$= \frac{1-w^2}{4\pi^2} \int_0^{\frac{\Lambda}{1-w^2}} dp \int_0^{\pi} d\theta\, p^2 \sin\theta \frac{\left((1-w^2)p^2\sin^2\theta + (p\cos\theta - \frac{w\Lambda}{1-w^2})^2\right)^{(N-3)/2}}{\left((1-w^2)p^2\sin^2\theta + (p\cos\theta - \frac{w\Lambda}{1-w^2})^2 + D^2\right)^{N/2}}$$

At this point we clean a bit the notation, scaling out D and defining $\tilde{\Lambda} = \frac{\Lambda}{(1-w^2)D}$,

$$= \frac{1-w^2}{4\pi^2} \int_0^{\tilde{\Lambda}} dp \int_0^{\pi} d\theta \, p^2 \sin\theta \frac{\left((1-w^2)p^2\sin^2\theta + (p\cos\theta - w\tilde{\Lambda})^2\right)^{(N-3)/2}}{\left((1-w^2)p^2\sin^2\theta + (p\cos\theta - w\tilde{\Lambda})^2 + 1\right)^{N/2}}$$

This derivation is pretty simple and gives us a general formula to transform an integral over a hard domain into an integral over a much simpler domain. The price to pay is that the integrand function becomes more complicated, however since we are doing on-shell integration we shall later see that we will approximate the integrand function, avoiding the problem.
The cases of interest for our diagrams are $N = 3$ and $N = 5$, therefore we focus on the two of them. For reasons that should be clear by now, our discussion is restricted to the region for which $|w| < 1$: we see that because of the square, $(1-w^2)^{-1}$ is much likely to give contribution of order 1.

- $N = 3$:

  $$\int_E \frac{d^3p}{(2\pi^3)} \frac{1}{(p^2+D^2)^{3/2}} = \frac{1-w^2}{4\pi^2} \int_{\tilde{\Lambda}'}^{\tilde{\Lambda}} dp \int_0^{\pi} d\theta \frac{p^2\sin\theta}{\left((1-w^2)p^2\sin^2\theta + (p\cos\theta - w\tilde{\Lambda})^2 + 1\right)^{3/2}}$$

  if we are interested in the on-shell contribution, it is useful to have a look at the integrand when $p = \tilde{\Lambda}$

  $$\frac{\tilde{\Lambda}^2\sin\theta}{\left((1-w^2)\tilde{\Lambda}^2\sin^2\theta + \tilde{\Lambda}^2(\cos\theta - w)^2 + 1\right)^{3/2}}$$

  If $\tilde{\Lambda} >> 1$, e.g. $\Lambda >> (1-w^2)D$, then we may drop the constant at the denominator. Performing the integration gives,

  $$\frac{1-w^2}{4\pi^2} \int_{\tilde{\Lambda}'}^{\tilde{\Lambda}} dp \int_0^{\pi} d\theta \frac{p^2\sin\theta}{\left((1-w^2)p^2\sin^2\theta + (p\cos\theta - w\tilde{\Lambda})^2\right)^{3/2}} = \frac{1}{2\pi^2}\frac{1}{1-w^2}\log\left(\frac{\Lambda}{\Lambda'}\right)$$

  we conclude that

  $$\int_{\delta E} \frac{d^3p}{(2\pi^3)} \frac{1}{(p^2+D^2)^{3/2}} = \frac{1}{2\pi^2}\frac{1}{1-w^2}\log\left(\frac{\Lambda}{\Lambda'}\right) + \mathcal{O}\left(\frac{1}{\Lambda}\right)$$

  where the integration region δE is the ellipsoidal shell.

- $N = 5$:

  $$\int_E \frac{d^3p}{(2\pi^3)} \frac{p^2}{(p^2+D^2)^{5/2}} = \left\{ \int_E \frac{d^3p}{(2\pi^3)} \frac{1}{(p^2+D^2)^{3/2}} - \int_E \frac{d^3p}{(2\pi^3)} \frac{D^2}{(p^2+D^2)^{5/2}} \right\}$$

  the first term is precisely the one computed above while the second gives finite contribution, naively by power counting. We conclude that the contribution is

  $$\int_{\delta E} \frac{d^3p}{(2\pi^3)} \frac{p^2}{(p^2+D^2)^{5/2}} = \frac{1}{2\pi^2}\frac{1}{1-w^2}\log\left(\frac{\Lambda}{\Lambda'}\right) + \mathcal{O}\left(\frac{1}{\Lambda}\right)$$

This are the results of the integration over **one** of the two ellipsoids; the contribution coming from the other is obtained by changing $w \to -w$, thus we see it is exactly the same. We shall keep it in mind later on, when computing the Feynman diagrams.

Bibliography

[1] *A decade of graphene research: production, applications and outlook*, Materials Today, 17 (2014), pp. 426 – 432.

[2] A. Altland and B. D. Simons, *Condensed matter field theory*, Cambridge University Press, 2010.

[3] T. Ando, *Screening effect and impurity scattering in monolayer graphene*, Journal of the Physical Society of Japan, 75 (2006), p. 074716.

[4] Y. Barlas, T. Pereg-Barnea, M. Polini, R. Asgari, and A. MacDonald, *Chirality and correlations in graphene*, Physical review letters, 98 (2007), p. 236601.

[5] B. A. Bernevig, *It's been a weyl coming*, Nature Physics, (2015).

[6] S. Borisenko, Q. Gibson, D. Evtushinsky, V. Zabolotnyy, B. Büchner, and R. J. Cava, *Experimental realization of a three-dimensional dirac semimetal*, Phys. Rev. Lett., 113 (2014), p. 027603.

[7] H. Bruus and K. Flensberg, *Many-body quantum theory in condensed matter physics: an introduction*, Oxford University Press, 2004.

[8] J. P. C. C. J. Talbert and E. J. Nicol, *Optical and transport properties in 3d dirac and weyl semimetals*, arXiv:1603.00866.

[9] A. H. Castro Neto, F. Guinea, N. M. R. Peres, K. S. Novoselov, and A. K. Geim, *The electronic properties of graphene*, Rev. Mod. Phys., 81 (2009), pp. 109–162.

[10] L. Fritz, J. Schmalian, M. Müller, and S. Sachdev, *Quantum critical transport in clean graphene*, Physical Review B, 78 (2008), p. 085416.

[11] J. González, F. Guinea, and M. Vozmediano, *Non-fermi liquid behavior of electrons in the half-filled honeycomb lattice (a renormalization group approach)*, Nuclear Physics B, 424 (1994), pp. 595–618.

[12] A. Grigorenko, M. Polini, and K. Novoselov, *Graphene plasmonics*, Nature photonics, 6 (2012), pp. 749–758.

[13] M. Z. Hasan and C. L. Kane, *Colloquium: topological insulators*, Reviews of Modern Physics, 82 (2010), p. 3045.

[14] P. Hosur, S. Parameswaran, and A. Vishwanath, *Charge transport in weyl semimetals*, Physical review letters, 108 (2012), p. 046602.

[15] E. H. Hwang and S. Das Sarma, *Dielectric function, screening, and plasmons in two-dimensional graphene*, Phys. Rev. B, 75 (2007), p. 205418.

[16] H. Isobe and N. Nagaosa, *Renormalization effects on quasi-two-dimensional organic conductor a-(bedt-ttf)2i3*, Journal of the Physical Society of Japan, 81 (2012), p. 113704.

[17] C. L. Kane and E. J. Mele, *Quantum spin hall effect in graphene*, Physical review letters, 95 (2005), p. 226801.

[18] C. Kittel, *Introduction to solid state*, John Wiley & Sons, 1966.

[19] V. N. Kotov, B. Uchoa, and A. C. Neto, *Electron-electron interactions in the vacuum polarization of graphene*, Physical Review B, 78 (2008), p. 035119.

[20] V. N. Kotov, B. Uchoa, V. M. Pereira, F. Guinea, and A. C. Neto, *Electron-electron interactions in graphene: Current status and perspectives*, Reviews of Modern Physics, 84 (2012), p. 1067.

[21] X. Luo, T. Qiu, W. Lu, and Z. Ni, *Plasmons in graphene: recent progress and applications*, Materials Science and Engineering: R: Reports, 74 (2013), pp. 351–376.

[22] G. D. Mahan, *Many-particle physics*, Springer Science & Business Media, 2013.

[23] M. Neupane, S. Xu, R. Sankar, N. Alidoust, G. Bian, C. Liu, I. Belopolski, T. Chang, H. Jeng, H. Lin, et al., *Observation of a three-dimensional topological dirac semimetal phase in high-mobility cd3as2.*, Nature communications, 5 (2013), pp. 3786–3786.

[24] K. S. Novoselov, A. K. Geim, S. V. Morozov, D. Jiang, Y. Zhang, S. V. Dubonos, I. V. Grigorieva, and A. A. Firsov, *Electric field effect in atomically thin carbon films*, science, 306 (2004), pp. 666–669.

[25] P. K. Pyatkovskiy, *Dynamical polarization, screening, and plasmons in gapped graphene*, Journal of Physics: Condensed Matter, 21 (2009), p. 025506.

[26] P. Rehberg and S. Klevansky, *One loop integrals at finite temperature and density*, Annals of physics, 252 (1996), pp. 422–457.

[27] G. W. Semenoff, *Condensed-matter simulation of a three-dimensional anomaly*, Physical Review Letters, 53 (1984), p. 2449.

[28] H. T. Stoof, K. B. Gubbels, and D. B. Dickerscheid, *Ultracold quantum fields*, vol. 1, Springer, 2009.

[29] C. Tabert and J. Carbotte, *Optical conductivity of weyl semimetals and signatures of the gapped semimetal phase transition*, Physical Review B, 93 (2016), p. 085442.

[30] R. E. Throckmorton, J. Hofmann, E. Barnes, and S. D. Sarma, *Many-body effects and ultraviolet renormalization in three-dimensional dirac materials*, Physical Review B, 92 (2015), p. 115101.

[31] M. Trescher, B. Sbierski, P. W. Brouwer, and E. J. Bergholtz, *Quantum transport in dirac materials: Signatures of tilted and anisotropic dirac and weyl cones*, Physical Review B, 91 (2015), p. 115135.

[32] P. R. Wallace, *The band theory of graphite*, Phys. Rev., 71 (1947), pp. 622–634.

[33] Wikipedia, *Plagiarism — Wikipedia, the free encyclopedia*, 2004.

[34] B. Wunsch, T. Stauber, F. Sols, and F. Guinea, *Dynamical polarization of graphene at finite doping*, New Journal of Physics, 8 (2006), p. 318.

[35] S. M. Young, S. Zaheer, J. C. Teo, C. L. Kane, E. J. Mele, and A. M. Rappe, *Dirac semimetal in three dimensions*, Physical review letters, 108 (2012), p. 140405.

[36] J. Zhou, H.-R. Chang, and D. Xiao, *Plasmon mode as a detection of the chiral anomaly in weyl semimetals*, Physical Review B, 91 (2015), p. 035114.

Bibliography]mybib